

Development and Testing of ENDF/B-VI.8 and ENDF/B-VII.0 Coupled Neutron-Gamma Libraries for SCALE 6

**AVAILABILITY OF REFERENCE MATERIALS
IN NRC PUBLICATIONS**

NRC Reference Material

As of November 1999, you may electronically access NUREG-series publications and other NRC records at NRC's Public Electronic Reading Room at <http://www.nrc.gov/reading-rm.html>. Publicly released records include, to name a few, NUREG-series publications; *Federal Register* notices; applicant, licensee, and vendor documents and correspondence; NRC correspondence and internal memoranda; bulletins and information notices; inspection and investigative reports; licensee event reports; and Commission papers and their attachments.

NRC publications in the NUREG series, NRC regulations, and *Title 10, Energy*, in the Code of *Federal Regulations*, may also be purchased from one of these two sources:

1. The Superintendent of Documents
U.S. Government Printing Office
P.O. Box SSOP
Washington, DC 20402-0001
Internet: bookstore.gpo.gov
Telephone: 202-512-1800
FAX: 202-512-2250
2. The National Technical Information Service
Springfield, VA 22161-0002
www.ntis.gov
1-800-553-6847 or, locally, 703-605-6000

A single copy of each NRC draft report for comment is available free, to the extent of supply, upon written request as follows:

Address: Office of the Chief Information Officer,
Reproduction and Distribution
Services Section
U.S. Nuclear Regulatory Commission
Washington, DC 20555-0001

E-mail: DISTRIBUTION@nrc.gov
Facsimile: 301-415-2289

Some publications in the NUREG series that are posted at NRC's Web site address <http://www.nrc.gov/reading-rm/doc-collections/nuregs> are updated periodically and may differ from the last printed version. Although references to material found on a Web site bear the date the material was accessed, the material available on the date cited may subsequently be removed from the site.

Non-NRC Reference Material

Documents available from public and special technical libraries include all open literature items, such as books, journal articles, and transactions, *Federal Register* notices, Federal and State legislation, and congressional reports. Such documents as theses, dissertations, foreign reports and translations, and non-NRC conference proceedings may be purchased from their sponsoring organization.

Copies of industry codes and standards used in a substantive manner in the NRC regulatory process are maintained at—

The NRC Technical Library
Two White Flint North
11545 Rockville Pike
Rockville, MD 20852-2738

These standards are available in the library for reference use by the public. Codes and standards are usually copyrighted and may be purchased from the originating organization or, if they are American National Standards, from—

American National Standards Institute
11 West 42nd Street
New York, NY 10036-8002
www.ansi.org
212-642-4900

Legally binding regulatory requirements are stated only in laws; NRC regulations; licenses, including technical specifications; or orders, not in NUREG-series publications. The views expressed in contractor-prepared publications in this series are not necessarily those of the NRC.

The NUREG series comprises (1) technical and administrative reports and books prepared by the staff (NUREG/XXXX) or agency contractors (NUREG/CR-XXXX), (2) proceedings of conferences (NUREG/CP-XXXX), (3) reports resulting from international agreements (NUREG/IA-XXXX), (4) brochures (NUREG/BR-XXXX), and (5) compilations of legal decisions and orders of the Commission and Atomic and Safety Licensing Boards and of Directors' decisions under Section 2.206 of NRC's regulations (NUREG-0750).

DISCLAIMER: This report was prepared as an account of work sponsored by an agency of the U.S. Government. Neither the U.S. Government nor any agency thereof, nor any employee, makes any warranty, expressed or implied, or assumes any legal liability or responsibility for any third party's use, or the results of such use, of any information, apparatus, product, or process disclosed in this publication, or represents that its use by such third party would not infringe privately owned rights.



United States Nuclear Regulatory Commission

Protecting People and the Environment

NUREG/CR-6990
ORNL/TM-2008/047

Development and Testing of ENDF/B-VI.8 and ENDF/B-VII.0 Coupled Neutron-Gamma Libraries for SCALE 6

Manuscript Completed: December 2008

Date Published: February 2009

Prepared by

D. Wiarda, M.E. Dunn, D.E. Peplow, T.M. Miller and H. Akkurt

Oak Ridge National Laboratory

Managed by UT-Battelle, LLC

Oak Ridge, TN 37831-6170

A.B. Barto, NRC Project Manager

NRC Job Code J5609

ABSTRACT

New coupled neutron-gamma shielding libraries have been developed for use with the SCALE (Standardized Computer Analyses for Licensing Evaluation) code system. Two libraries have been generated based on the Evaluated Nuclear Data File/B Version VI (ENDF/B-VI) Release 8 (ENDF/B-VI.8) and ENDF/B-VII Release 0 (ENDF/B-VII.0) cross-section evaluations. Both libraries were generated using 200 neutron and 47 gamma groups. The neutron group structure is identical to the 199-group VITAMIN-B6 structure except an additional neutron group has been added to extend the top energy boundary to 20 MeV. In addition to the “fine-group” libraries, a “broad-group” ENDF/B-VII.0 library has been generated using a 27 neutron and 19 gamma group structure. In addition to the coupled cross-section library development, new shielding codes Monaco and MAVRIC (**M**onaco with **A**utomated **V**ariance **R**eduction using **I**mportance **C**alculations) have been developed for SCALE. This report documents the ENDF/B-VI.8 and ENDF/B-VII.0 cross-section library development and the benchmark testing of the new libraries with the new SCALE shielding transport codes Monaco and MAVRIC.

TABLE OF CONTENTS

	<u>Page</u>
ABSTRACT.....	iii
LIST OF FIGURES	vii
LIST OF TABLES.....	xi
ACKNOWLEDGMENTS	xiii
ACRONYMS AND ABBREVIATIONS	xv
1 INTRODUCTION	1
2 LIBRARY GENERATION	3
2.1 AMPX Input File Generation.....	3
2.2 Processing.....	8
2.2.1 Group structure.....	8
2.2.2 AMPX execution sequences for neutron and gamma-ray yield processing.....	9
2.2.2.1 Point-wise cross-section data.....	13
2.2.2.2 Comparison with NJOY.....	15
2.2.2.3 Neutron and gamma yield processing.....	16
2.2.2.4 Thermal neutron processing.....	18
2.2.2.5 Generating full-range Bondarenko factors and thermal data.....	20
2.2.2.6 Gamma processing.....	22
2.2.2.7 Creating the master library.....	26
2.2.3 Adding dose data.....	28
3 BENCHMARK TESTING	37
3.1 SAS4 and MAVRIC Benchmark Comparison Calculations with ENDF/B-VI.8 Library	37
3.1.1 Cask descriptions.....	38
3.1.1.1 CASTOR-V/21	38
3.1.1.2 Westinghouse MC-10	39
3.1.1.3 TN-24P.....	40
3.1.2 Calculations.....	40
3.1.2.1 Computational results	41
3.1.2.2 Benchmark against experimental measurement.....	50
3.2 MAVRIC Benchmark Calculations Using ENDF/B-VI.8 and ENDF/B-VII.0 Libraries	53
3.2.1 Neutron fields in three-section concrete labyrinth from ²⁵² Cf source	53
3.2.1.1 Benchmark overview	53
3.2.1.2 Monaco/MAVRIC calculations	54
3.2.1.3 Detector response functions	55
3.2.1.4 Neutron transport through the labyrinth.....	60
3.2.2 Neutron and photon leakage spectra from ²⁵² Cf source at centers of six iron spheres of different diameters	68
3.2.2.1 Benchmark overview	68
3.2.2.2 Monaco calculations	69
3.2.3 Comparison of measured and calculated neutron transmission through heavy water for a ²⁵² Cf source placed in the center of a 30 cm diameter sphere	76
3.2.3.1 Experiment overview	76
3.2.3.2 Monaco calculations	76

TABLE OF CONTENTS (continued)

	<u>Page</u>
3.2.4 Comparison of measured and calculated neutron transmission through steel for a ²⁵² Cf source	80
3.2.4.1 Experiment overview	80
3.2.4.2 Monaco calculations	80
3.2.5 Systematic evaluation of neutron shielding effects for materials.....	82
3.2.5.1 Experimental overview	82
3.2.5.2 MCNP simulations.....	83
3.2.5.3 MAVRIC calculations	83
3.2.5.4 Results.....	84
4 SUMMARY	87
5 REFERENCES	89
APPENDIX A: XML INPUT TEMPLATES	A-1
APPENDIX B: EVALUATIONS INCLUDED IN ENDF/B-VI.8 LIBRARY	B-1
APPENDIX C: EVALUATIONS INCLUDED IN ENDF/B-VII.0 LIBRARY	C-1

LIST OF FIGURES

<u>Figure</u>	<u>Page</u>
2.1	Work flow for AMPX master library creation. 3
2.2	AMPX sequence for producing neutron multigroup data. 10
2.3	AMPX sequence to generate the coupled gamma-neutron multigroup data. 11
2.4	Weighting spectrum generated by JERGENS. 14
2.5	Point-wise capture cross section as processed with AMPX and NJOY for ¹⁴⁰ Ce. 16
2.6	AMPX and NJOY scattering data for MT=504 in hydrogen. 26
2.7	Interpolation for Claiborne-Trubey gamma dose function. 31
2.8	Interpolation for ICRU-57, Table A.21 (air) Kerma gamma dose function. 32
2.9	Interpolation for ambient dose equivalent. 33
2.10	Interpolation for effective dose. 34
3.1	Views of cask for storage and transport of radioactive material (CASTOR). 38
3.2	Views of MC-10 cask. 39
3.3	Views of TN-24P cask. 40
3.4	The ratio of the computed TN-24P cask tallies using the ENDF/B-VI.8 and ENDF/B-IV shielding cross sections. 43
3.5	The ratios of the computed TN-24P cask tallies using MAVRIC and SAS4. 44
3.6	The ratio of the computed MC-10 cask values using the ENDF/B-VI.8 and ENDF/B-IV shielding cross-section libraries with MAVRIC. 47
3.7	The ratio of the computed CASTOR cask values using the ENDF/B-VI.8 and ENDF/B-IV shielding cross-section libraries with MAVRIC. 50
3.8	The ratio of the computed to measured values using MAVRIC with the ENDF/B-VI.8 (new) and ENDF/B-IV (old) libraries for the neutron dose rates. 51
3.9	The ratio of the computed to measured values using MAVRIC with the ENDF/B-VI.8 (new) and ENDF/B-IV (old) shielding libraries for the gamma dose rates. 53
3.10	Cutaway view of labyrinth model. 54
3.11	⁶ Li(n,t) ⁴ He cross section from the ENDF/B VI.8 200n/47g shielding library. 55
3.12	Response (counts per unit flux) for the 2-inch diameter Bonner sphere (with cadmium cover). 57
3.13	Response (counts per unit flux) for the 3-inch diameter Bonner sphere (with cadmium cover). 57
3.14	Response (counts per unit flux) for the 5-inch diameter Bonner sphere (with cadmium cover). 58
3.15	Response (counts per unit flux) for the 5-inch diameter Bonner sphere (no cover). 58
3.16	Response (counts per unit flux) for the 8-inch diameter Bonner sphere (with cadmium cover). 59
3.17	Response (counts per unit flux) for the 10-inch diameter Bonner sphere (with cadmium cover). 59
3.18	Response (counts per unit flux) for the 12-inch diameter Bonner sphere (with cadmium cover). 60
3.19	Neutron count rate C/E for the 2-inch Bonner sphere (with cadmium) and the uncovered source. 61
3.20	Neutron count rate C/E for the 2-inch Bonner sphere (with cadmium) and the covered source. 61

LIST OF FIGURES (continued)

<u>Figure</u>		<u>Page</u>
3.21	Neutron count rate C/E for the 3-inch Bonner sphere (with cadmium) and the uncovered source.	62
3.22	Neutron count rate C/E for the 3-inch Bonner sphere (with cadmium) and the covered source.	62
3.23	Neutron count rate C/E for the 5-inch Bonner sphere (with cadmium) and the uncovered source.	63
3.24	Neutron count rate C/E for the 5-inch Bonner sphere (with cadmium) and the covered source.	63
3.25	Neutron count rate C/E for the 5-inch Bonner sphere (no cadmium) and the uncovered source.	64
3.26	Neutron count rate C/E for the 5-inch Bonner sphere (no cadmium) and the covered source.	64
3.27	Neutron count rate C/E for the 8-inch Bonner sphere (with cadmium) and the uncovered source.	65
3.28	Neutron count rate C/E for the 8-inch Bonner sphere (with cadmium) and the covered source.	65
3.29	Neutron count rate C/E for the 10-inch Bonner sphere (with cadmium) and the uncovered source.	66
3.30	Neutron count rate C/E for the 10-inch Bonner sphere (with cadmium) and the covered source.	66
3.31	Neutron count rate C/E for the 12-inch Bonner sphere (with cadmium) and the uncovered source.	67
3.32	Neutron count rate C/E for the 12-inch Bonner sphere (with cadmium) and the covered source.	67
3.33	Iron sphere experiments.	68
3.34	Comparison of the neutron calculation to the measurement of the bare source.	69
3.35	Comparison of the photon calculation to the measurement of the bare source.	70
3.36	Comparison of the neutron calculation to the measurement of the 20 cm shield.	70
3.37	Comparison of the neutron calculation to the measurement of the 30 cm shield.	71
3.38	Comparison of the neutron calculation to the measurement of the 40 cm shield.	71
3.39	Comparison of the neutron calculation to the measurement of the 50 cm shield.	72
3.40	Comparison of the neutron calculation to the measurement of the 60 cm shield.	72
3.41	Comparison of the neutron calculation to the measurement of the 70 cm shield.	73
3.42	Comparison of the photon calculation to the measurement of the 30 cm shield.	73
3.43	Comparison of the photon calculation to the measurement of the 40 cm shield.	74
3.44	Comparison of the photon calculation to the measurement of the 50 cm shield.	74
3.45	Comparison of the photon calculation to the measurement of the 60 cm shield.	75
3.46	Comparison of the photon calculation to the measurement of the 70 cm shield.	75
3.47	Photon flux through the 70 cm shield as calculated by Monaco and MCNP5.	76
3.48	Monaco model of ²⁵² Cf source in heavy water experiment.	77
3.49	Comparison of the Monaco (ENDF/B-VI.8) results and the measured data.	78
3.50	Ratios of the Monaco (ENDF/B-VI.8 fine-group library) results and the measured data.	78
3.51	Comparison of the Monaco (ENDF/B-VII.0) results and the measured data.	79
3.52	Ratios of the Monaco (ENDF/B-VII.0 fine-group library) results and the measured data.	79
3.53	Monaco output (ENDF/B-VI.8 fine-group library) for total flux at 10 cm using two different tallies compared to the two sets of measured data.	80

LIST OF FIGURES (continued)

<u>Figure</u>		<u>Page</u>
3.54	Ratios of the Monaco (ENDF/B-VI.8 fine-group library) point detector tally to the measured fluxes.	81
3.55	Monaco output (ENDF/B-VII.0 fine-group library) for total flux at 10 cm using two different tallies compared to the two sets of measured data.	81
3.56	Ratios of the Monaco (ENDF/B-VII.0 fine-group library) point detector tally to the measured fluxes.	82
3.57	Neutron shielding experiment example.....	83
3.58	Ratio of MAVRIC calculation of neutron detector dose rate to experimental measurement.....	84
3.59	Type 2a results—25 cm of stainless steel first, then polyethylene.....	85
3.60	Type 2b results—polyethylene, then 25 cm of stainless steel.	85
3.61	Type 3 results for polyethylene fixed at a thickness of 15 cm.	85

LIST OF TABLES

<u>Table</u>		<u>Page</u>
2.1	Substitution tags available for use in XML input templates	5
2.2	Template control elements that allow looping over the evaluations	7
2.3	Energy boundaries for the 200 neutron group structure	8
2.4	Energy boundaries for the 47 gamma group structure	9
2.5	Energy boundaries for the 27 neutron group structure	9
2.6	Energy boundaries for the 19 gamma group structure	9
2.7	Evaluations excluded from the ENDF/B-VI.8 library	12
2.8	Available dose functions on the coupled neutron-gamma libraries	28
3.1	TN-24P calculations input summary	41
3.2	The computational results for TN24P casks	42
3.3	Westinghouse MC-10 calculations input summary	45
3.4	The computational results for MC-10 casks	46
3.5	CASTOR-V/21 calculations input summary	48
3.6	The computational results for CASTOR casks	49
3.7	The measured and computed neutron dose rates and the ratio of computed to measured (C/M) dose rates for each cask model	51
3.8	The measured and computed gamma dose rates and the ratio of the computed to measured (C/M) dose rates for each cask model	52
B-1	Evaluations and IDs used for the ENDF/B-VII.8 library	B-1
C-1	Evaluations included in ENDF/B-VII.0 library	C-1

ACKNOWLEDGMENTS

Sincere appreciation is expressed to Andrew B. Barto of the U.S. Nuclear Regulatory Commission Office of Nuclear Material Safety and Safeguards for supporting the development and testing of ENDF/B-VI.8 and ENDF/B-VII.0 coupled neutron-gamma libraries for SCALE. In addition, the authors would like to thank Bryan Broadhead, Mark Williams, and Steve Bowman for their technical review of the report and guidance in the development and testing of the cross-section libraries. Also, special appreciation is expressed to Joyce B. Echols and Willena C. Carter for their efforts in preparing the final manuscript for publication.

ACRONYMS AND ABBREVIATIONS

1-D	one-dimensional
2-D	two-dimensional
3-D	three-dimensional
CADIS	Consistent Adjoint-Driven Importance Sampling
CENTRM	Continuous ENergy TRansport Module
ENDF/B-IV	Evaluated Nuclear Data File Version IV
ENDF/B-VI.8	Evaluated Nuclear Data File Version VI Release 8
ENDF/B-VII.0	Evaluated Nuclear Data File Version VII
ID	identifier
MAVRIC	Monaco with Automated Variance Reduction using Importance Calculations
MORSE	Multigroup Oak Ridge Stochastic Experiment
NNDC	National Nuclear Data Center
ORNL	Oak Ridge National Laboratory
SAS4	SCALE Shielding Analysis Sequence Number 4
SCALE	Standardized Computer Analyses for Licensing Evaluation
SGGP	SCALE Generalized Geometry Package
SLBW	Single-Level Breit-Wigner
XML	Extensible Markup Language

1 INTRODUCTION

Before development of Standardized Computer Analyses for Licensing Evaluation (SCALE) Version 6, coupled neutron-gamma cross-section libraries distributed with the code system were limited to U.S. Evaluated Nuclear Data File/B Version IV (ENDF/B-IV) data.¹ The latest version of the ENDF/B evaluation database that can be obtained from the National Nuclear Data Center (NNDC) at Brookhaven National Laboratory (BNL) is ENDF/B-VII.0 (Ref. 2). With the release of ENDF/B-VII in December 2006 (Ref. 3), the Oak Ridge National Laboratory (ORNL) initiated efforts to update the SCALE libraries for shielding applications to include both ENDF/B-VI Release 8 (ENDF/B-VI.8) and ENDF/B-VII.0 cross-section data. This report documents the cross-section library generation effort and the subsequent benchmark testing of the data libraries with SCALE.

In concert with the new cross-section library development activities, ORNL has developed new shielding capabilities for the SCALE code system. The Monaco shielding module is a new multigroup, fixed-source Monte Carlo transport code that can be used to perform shielding analyses for licensing applications. Monaco is the result of a modernization effort combining the multigroup neutron and photon physics of the well-known MORSE (Multigroup Oak Ridge Stochastic Experiment) Monte Carlo shielding code with the flexibility of the SCALE Generalized Geometry Package (SGGP) and cross-section processing. Monaco uses the same cross-section package as other SCALE modules. Available tallies in Monaco include point detectors, region-based flux tallies, and mesh tallies. Any Monaco tally can be folded with a response function, either user-entered or from a standard list available with each SCALE cross-section library. Mesh tally values and uncertainties can be viewed with a special Java viewer on all computer platforms that run SCALE. Monaco is implemented in SCALE through the MAVRIC (Monaco with Automated Variance Reduction using Importance Calculations) computational sequence. The MAVRIC sequence in SCALE combines the results of an adjoint calculation from the three-dimensional (3-D) deterministic code Denovo with Monaco. Both an importance map for weight windows and a biased source are automatically generated from the adjoint flux using the CADIS (Consistent Adjoint-Driven Importance Sampling) methodology. MAVRIC is completely automated— from a simple user input, it creates the cross sections (forward and adjoint), calculates the first collision source, computes the adjoint fluxes, creates the importance map and biased source, and executes Monaco. Users can start and stop the calculation at various points so that progress can be monitored and importance maps can be reused for similar problems. For simple problems that do not require the advanced variance reduction, the MAVRIC sequence is an easy way to compute problem-dependent cross sections and execute Monaco with a common user input. The MAVRIC/Monaco capability represents a significant radiation transport advancement for SCALE.

This report provides detailed computational results using the new shielding libraries and radiation transport capabilities of MAVRIC/Monaco.

2 LIBRARY GENERATION

2.1 AMPX Input File Generation

A flow diagram is presented in Fig. 2.1 to illustrate the automated procedure to generate the AMPX master library from ENDF/B evaluations.

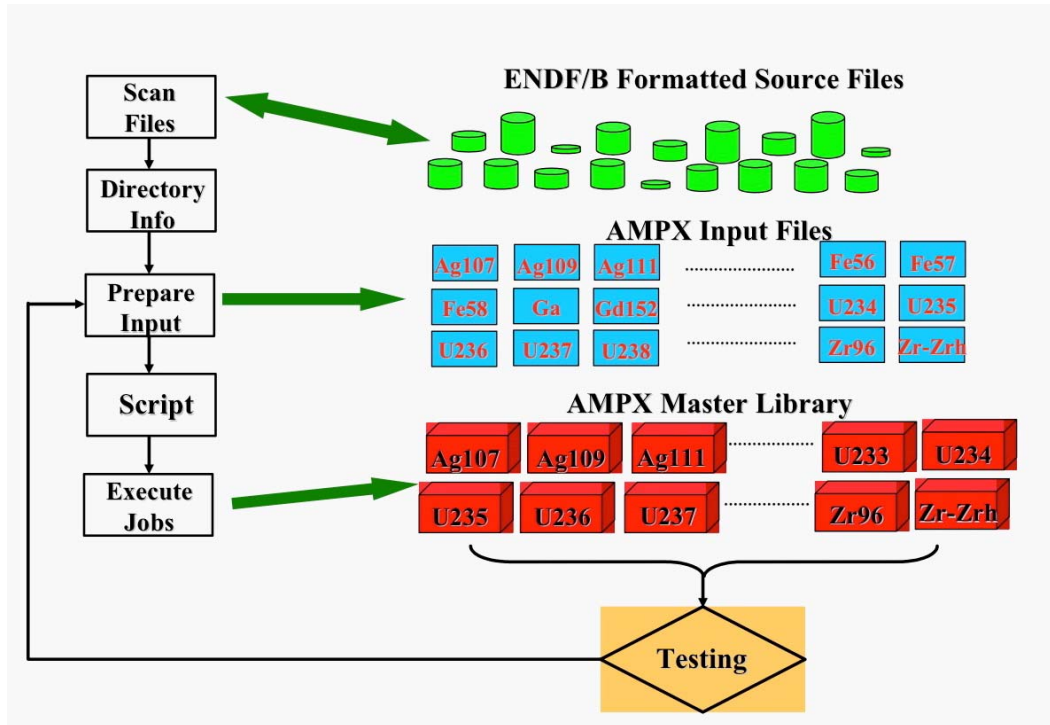


Fig. 2.1 Work flow for AMPX master library creation.

Input files are generated using an XML listing of the desired evaluations and XML templates. The XML listing of the desired evaluation is generated by a Java program that scans a directory tree of ENDF files and writes the relevant information to a file. A typical listing looks like the following.

```

<Material tag="al27"
  endf="1325"
  za="13027"
  tape="/home/dw8/ampx/running/endl6/rev8/First.endf"
  mod="4"
  rel="8"
  eval="EVAL-FEB97"
  neutron="yes"
  author="M.B.CHADWICK & P.G.YOUNG"
  lab="M.B.CHADWICK & P.G.YOUNG"
  dist="DIST-NOV 1"
  rdate="REV3-"
  rev="6"
  version="6"
  awr="26.74975"
  lis="0"
  nis="1"
  
```

```

        scattering="1.34799E+00"
        file2="yes"
        file3="yes"
        file4="yes"
        file6="yes"
        AWP0="yes"
        file12="yes"
    />
    <Material tag="graphite"
        endf="31"
        za="131"
        tape="/home/dw8/ampx/running/endl6/rev8/Thermal.endf"
        mod="1"
        rel="3"
        eval="EVAL-apr93"
        neutron="yes"
        author="MACFARLANE"
        lab="MACFARLANE"
        dist="DIST-DEC95"
        rdate=" "
        rev="6"
        version="6"
        awr="11.898"
        lis="0"
        scattering="0.0"
        nis="0"
        file7="yes"
        file7temps="296.0 400.0 500.0 600.0 700.0 800.0 1000.0 1200.0 1600.0 2000.0"
    />

```

XML templates used to create the AMPX input files are provided in Appendix A. The various templates can refer to the attribute values by name. For example *writeData(endf)* in the templates provided in Appendix A, will be substituted by the ENDF MAT number listed in the endf attribute. Table 2.1 lists some specialized additional values that can also be substituted.

In addition, the template reader reads a configuration file. The configuration file lists metastable isotopes, thermal moderator evaluations, and some special nuclei. In most cases the identifier (ID) used in SCALE is the ZA value; however, in the cases of metastable isotopes, thermal moderator evaluations, and some special nuclei, the SCALE ID is different. The configuration file allows supplying those special SCALE ID values. For the thermal moderators, one or more fast evaluations, identified by their endf numbers, are also supplied. The following is the configuration file used for the ENDF 6 data.

```

<ConfigFile>

    <!-- metastable nuclei for which the scale id is different from the real za value -->
    <metastable>
        <nuclei endf="9547" realza="95242" scaleza="95601"/> <!-- Am242m -->
        . . .
        <nuclei endf="5253" realza="52129" scaleza="52611"/> <!-- Te129m -->
        <nuclei endf="6153" realza="61148" scaleza="61601"/> <!-- Pm148m -->
    </metastable>

    <!-- nuclei for which the scale id is different from the real za value -->
    <specialNuclei>
        <nuclei endf="1001" realza="1001" scaleza="1801"/>
        <nuclei endf="1002" realza="1001" scaleza="1802"/>
    </specialNuclei>

    <!-- thermal nuclei - need to check the temperature stuff again - these are the
    temperatures listed in file 7 -->
    <thermal>
        <nuclei endf="1" realza="101" scaleza="1001"> <!-- H_H2O -->
            <fastMat endf="125"/> <!-- H -->
        </nuclei>

```

```

. . .
<nuclei endf="27" realza="127" scaleza="4509">    <!-- BEO -->
  <fastMat endf="425"/>    <!-- BE9 -->
  <fastMat endf="825"/>    <!-- 016 -->
</nuclei>

<nuclei endf="31" realza="131" scaleza="6312">    <!-- GRAPHITE -->
  <fastMat endf="600"/>    <!-- C -->
</nuclei>
</thermal>

</ConfigFile>

```

In addition to the attributes available directly from the above XML file, the tags listed in Table 2.1 can also be substituted.

Table 2.1 Substitution tags available for use in XML input templates

Attribute	Description
tag	The tag name of the material
version	The version of the evaluation
mod	The modification of the evaluation
rev	The revision of the evaluation
tape	The tape location of the evaluation
za	The ZA ID of the evaluation
a	The mass of the evaluation
z	The z value of the evaluation
scaleid or scaleidthermal1	The SCALE ZA ID. This is: $endf + 10000 * mod + 1000000 * version$. If this is a thermal material, the ENDF MAT ID of the first thermal evaluation is used. Similarly, the mod number of the first thermal evaluation is used. The version is always of the current material.
scaleidthermal2	The SCALE ZA ID. This is: $endf + 10000 * mod + 1000000 * version$. If this is a thermal material and a second thermal evaluation exists, the ENDF MAT ID of the second thermal evaluation is used. Similarly, the mod number of the first thermal evaluation is used. The version is always of the current material.
thermalscaleid	The same as scaleid but endf and mod value are from the current material, which is assumed to be a moderator.
changedza or changedzathermal1	For thermal, metastable, and some special material a changed ZA value is used in SCALE. This tag prints out the changed ZA value. If the ZA value does not need any changes, the original value is printed.
changedzatherml2	For thermal, metastable, and some special material a changed ZA value is used in SCALE. This tag prints out the changed ZA value for the second thermal evaluation.
Date	Prints the current date. The second argument optionally lists the date format.

The terms *fast1*, *fast2*, or *gamma* may be appended to all available attributes. If *fast1* is appended, the values of the attributes for the first fast thermal evaluation are printed. For example, in the case of graphite, appending *fast1* to the *writeData* attribute [*writeData(tagfast1)*] substitutes C, the tag for the first fast evaluation to be coupled with graphite. If *fast2* is appended, the values of the attributes for the second fast thermal evaluation are printed. For example, *writeData(endffast2)* for the case of BeO substitutes 825, the ENDF material for the second fast evaluation to be coupled with BeO. If *gamma* is appended, the value of the attribute pertaining to the coupled gamma evaluation is printed.

The *writeData(attribute)* function can optionally have two more parameters, the first of which gives the total length of the string to be printed and the second one the character to use for padding. Thus, in the case of graphite, the function *writeData(endf,10,*)* will print “*****600.”

The templates are XML files with several special elements that allow looping over the various evaluations. The tags listed in Table 2.2 control the behavior of the templates. Templates for the input files used for the library creation effort are given in Appendix A.

Each restriction can contain more than one value and those values can be preceded by a plus (+) or a minus (-). A plus indicates that the indicated condition must be met, whereas a minus negates the indicated condition. For example, *restrict=“+gamma +file2(yes)”* will only loop over evaluations that have a File 2 **and** have an associated gamma evaluation. However, *restrict=“gamma file2(yes)”* will only loop over evaluations that have a File 2 **or** have an associated gamma evaluation. The restriction *restrict=“-gamma +file2(yes)”* will only loop over evaluations that have a File 2 **and no** associated gamma evaluation.

The templates used to generate the various input files are given in Appendix A and should contain enough comments to serve as examples on how to use the input generator.

The template is parsed using a Java program where the program invocation is typically as follows.

```
java -jar ampx.jar -l Endf6.xml -c Config.xml -l template.xml
```

The argument for the *-t* option gives the file name of the template name, the argument for the *-l* option gives the file name containing the XML list of the ENDF evaluations, and the argument for the *-c* option lists the configuration file.

Table 2.2 Template control elements that allow looping over the evaluations

Tag	Description
loop	starts a loop over the various evaluations. It has the following optional attributes.
restrict	Restricts the loop to special cases. Available values are as follows.
thermal or thermal1	Only loops over materials that are moderators.
thermal2	Only loops over materials that are moderators and have second fast evaluations.
gamma or gammathermal1	Only loops over materials that have an associated gamma evaluation. In the case of moderators, the gamma evaluations need to exist for the first fast evaluation.
gammathermal2	Only loops over materials that are moderators and have at least two fast evaluations and the second fast evaluation has a gamma evaluation associated with it.
Metastable	Only loops over materials that are metastable.
	For any attribute listed in the XML file that has the associated value. For example <i>restrict="file2(yes),"</i> only loops over evaluations that contain a File 2.
start	The index at which to start. Before the value is used, any <i>writeData</i> functions are substituted.
stop	The index at which to stop. Before the value is used, any <i>writeData</i> functions are substituted.
step	The index at which to stop the loop. Before the value is used, any <i>writeData</i> functions are substituted
number	The number of times the loop should run. Before the value is used, any <i>writeData</i> functions are substituted.
openFile	With attribute name opens the indicated file for writing. The file name must be unique as it is used as the key.
closeFile	With attribute name closes a previously opened file.
writeFile	With attribute name writes data to the indicated file. Optionally it can contain an attribute <i>restrict</i> , which has the same function as for the loop element to restrict what gets written into the file. Any CDATA element and anything enclosed in a text element is written to the indicated file. Because a text element allows a <i>restrict</i> attribute with the same functionality as for the loop element, enclosure into this element allows writing different text depending on the particulars of the current evaluations.
noLast	Allows printing content if currently in a loop and if this is not the last time the loop will run.
first	Allows printing content if currently in a loop and if this is first time the loop will run.
noFirst	Allows printing content if currently in a loop and if this is not the first time the loop will run.

2.2 Processing

2.2.1 Group structure

The neutron group structure used is the 199-group VITAMIN-B6 structure with one extra group added to bring the upper group boundary to 20 MeV. The neutron group structure is listed in Table 2.3 and the gamma group structure in Table 2.4. For the broad-group library, 27 neutron groups and 19 gamma groups were used. The neutron group boundaries are listed in Table 2.5 and the gamma group boundaries in Table 2.6.

Table 2.3 Energy boundaries for the 200 neutron group structure

Energy boundaries for the 200 neutron groups used for the fine-group library									
1	2.0000E+07	42	2.7253E+06	83	3.3373E+05	124	2.3579E+04	165	5.0435E+00
2	1.9640E+07	43	2.5924E+06	84	3.0197E+05	125	2.1875E+04	166	3.9279E+00
3	1.7332E+07	44	2.4660E+06	85	2.9849E+05	126	1.9305E+04	167	3.0590E+00
4	1.6905E+07	45	2.3852E+06	86	2.9721E+05	127	1.5034E+04	168	2.3824E+00
5	1.6487E+07	46	2.3653E+06	87	2.9452E+05	128	1.1709E+04	169	1.8554E+00
6	1.5683E+07	47	2.3457E+06	88	2.8725E+05	129	1.0595E+04	170	1.4450E+00
7	1.4918E+07	48	2.3069E+06	89	2.7324E+05	130	9.1188E+03	171	1.3000E+00
8	1.4550E+07	49	2.2313E+06	90	2.4724E+05	131	7.1017E+03	172	1.1253E+00
9	1.4191E+07	50	2.1225E+06	91	2.3518E+05	132	5.5308E+03	173	1.0800E+00
10	1.3840E+07	51	2.0190E+06	92	2.2371E+05	133	4.3074E+03	174	1.0400E+00
11	1.3499E+07	52	1.9205E+06	93	2.1280E+05	134	3.7074E+03	175	1.0000E+00
12	1.2840E+07	53	1.8268E+06	94	2.0242E+05	135	3.3546E+03	176	8.7643E-01
13	1.2523E+07	54	1.7377E+06	95	1.9255E+05	136	3.0354E+03	177	8.0000E-01
14	1.2214E+07	55	1.6530E+06	96	1.8316E+05	137	2.7465E+03	178	6.8256E-01
15	1.1618E+07	56	1.5724E+06	97	1.7422E+05	138	2.6126E+03	179	6.2506E-01
16	1.1052E+07	57	1.4957E+06	98	1.6573E+05	139	2.4852E+03	180	5.3158E-01
17	1.0513E+07	58	1.4227E+06	99	1.5764E+05	140	2.2487E+03	181	5.0000E-01
18	1.0000E+07	59	1.3534E+06	100	1.4996E+05	141	2.0347E+03	182	4.1399E-01
19	9.5123E+06	60	1.2874E+06	101	1.4264E+05	142	1.5846E+03	183	3.6680E-01
20	9.0484E+06	61	1.2246E+06	102	1.3569E+05	143	1.2341E+03	184	3.2500E-01
21	8.6071E+06	62	1.1648E+06	103	1.2907E+05	144	9.6112E+02	185	2.7500E-01
22	8.1873E+06	63	1.1080E+06	104	1.2277E+05	145	7.4852E+02	186	2.2500E-01
23	7.7880E+06	64	1.0026E+06	105	1.1679E+05	146	5.8295E+02	187	1.8400E-01
24	7.4082E+06	65	9.6164E+05	106	1.1109E+05	147	4.5400E+02	188	1.5000E-01
25	7.0469E+06	66	9.0718E+05	107	9.8037E+04	148	3.5357E+02	189	1.2500E-01
26	6.7032E+06	67	8.6294E+05	108	8.6517E+04	149	2.7536E+02	190	1.0000E-01
27	6.5924E+06	68	8.2085E+05	109	8.2503E+04	150	2.1445E+02	191	7.0000E-02
28	6.3763E+06	69	7.8082E+05	110	7.9499E+04	151	1.6702E+02	192	5.0000E-02
29	6.0653E+06	70	7.4274E+05	111	7.1998E+04	152	1.3007E+02	193	4.0000E-02
30	5.7695E+06	71	7.0651E+05	112	6.7379E+04	153	1.0130E+02	194	3.0000E-02
31	5.4881E+06	72	6.7206E+05	113	5.6562E+04	154	7.8893E+01	195	2.1000E-02
32	5.2205E+06	73	6.3928E+05	114	5.2475E+04	155	6.1442E+01	196	1.4500E-02
33	4.9659E+06	74	6.0810E+05	115	4.6309E+04	156	4.7851E+01	197	1.0000E-02
34	4.7237E+06	75	5.7844E+05	116	4.0868E+04	157	3.7266E+01	198	5.0000E-03
35	4.4933E+06	76	5.5023E+05	117	3.4307E+04	158	2.9023E+01	199	2.0000E-03
36	4.0657E+06	77	5.2340E+05	118	3.1828E+04	159	2.2603E+01	200	5.0000E-04
37	3.6788E+06	78	4.9787E+05	119	2.8501E+04	160	1.7604E+01	201	1.0000E-05
38	3.3287E+06	79	4.5049E+05	120	2.7000E+04	161	1.3710E+01		
39	3.1664E+06	80	4.0762E+05	121	2.6058E+04	162	1.0677E+01		
40	3.0119E+06	81	3.8774E+05	122	2.4788E+04	163	8.3153E+00		
41	2.8651E+06	82	3.6883E+05	123	2.4176E+04	164	6.4760E+00		

Table 2.4 Energy boundaries for the 47 gamma group structure

Energy boundaries for the 47 gamma groups used for the fine-group library									
1	2.0000E+07	11	5.0000E+06	21	1.8000E+06	31	7.0000E+05	41	1.0000E+05
2	1.4000E+07	12	4.5000E+06	22	1.6600E+06	32	6.0000E+05	42	7.5000E+04
3	1.2000E+07	13	4.0000E+06	23	1.5700E+06	33	5.1200E+05	43	7.0000E+04
4	1.0000E+07	14	3.5000E+06	24	1.5000E+06	34	5.1000E+05	44	6.0000E+04
5	8.0000E+06	15	3.0000E+06	25	1.4400E+06	35	4.5000E+05	45	4.5000E+04
6	7.5000E+06	16	2.7500E+06	26	1.3300E+06	36	4.0000E+05	46	3.0000E+04
7	7.0000E+06	17	2.5000E+06	27	1.2000E+06	37	3.0000E+05	47	2.0000E+04
8	6.5000E+06	18	2.3500E+06	28	1.0000E+06	38	2.6000E+05	48	1.0000E+04
9	6.0000E+06	19	2.1500E+06	29	9.0000E+05	39	2.0000E+05		
10	5.5000E+06	20	2.0000E+06	30	8.0000E+05	40	1.5000E+05		

Table 2.5 Energy boundaries for the 27 neutron group structure

Energy boundaries for the 27 neutron groups used for the broad-group library									
1	2.0000E+07	7	4.0762E+05	13	2.9023E+01	19	1.0000E+00	25	5.0000E-02
2	6.3763E+06	8	1.1109E+05	14	1.0677E+01	20	8.0000E-01	26	3.0000E-02
3	3.0119E+06	9	1.5034E+04	15	3.0590E+00	21	4.1399E-01	27	1.0000E-02
4	1.8268E+06	10	3.0354E+03	16	1.8554E+00	22	3.2500E-01	28	1.0000E-05
5	1.4227E+06	11	5.8295E+02	17	1.3000E+00	23	2.2500E-01		
6	9.0718E+05	12	1.0130E+02	18	1.1253E+00	24	1.0000E-01		

Table 2.6 Energy boundaries for the 19 gamma group structure

Energy boundaries for the 19 gamma groups used for the broad-group library									
1	2.0000E+07	5	5.0000E+06	9	2.0000E+06	13	8.0000E+05	17	2.0000E+05
2	1.0000E+07	6	4.0000E+06	10	1.6600E+06	14	6.0000E+05	18	1.0000E+05
3	8.0000E+06	7	3.0000E+06	11	1.3300E+06	15	4.0000E+05	19	4.5000E+04
4	6.5000E+06	8	2.5000E+06	12	1.0000E+06	16	3.0000E+05	20	1.0000E+4

2.2.2 AMPX execution sequences for neutron and gamma-ray yield processing

The ORNL AMPX⁴ processing system contains more than 100 distinct modules that can be used to perform various nuclear data processing functions. For generating a cross-section library, the specific modules needed to process a cross-section evaluation depend upon the data specified in the nuclide evaluation. For example, if the nuclide is a resonance nuclide, it will require more modules to be executed relative to a nonresonance nuclide. If the evaluation is a thermal moderator material, the AMPX execution sequence will be different because the final cross-section data will be a mixture of data from one evaluation above the thermal range and from another evaluation in the thermal range.

The general procedure to generate groupwise neutron cross-section data is outlined in Fig. 2.2. The flow chart to produce the coupled part of the library is depicted in Fig. 2.3.

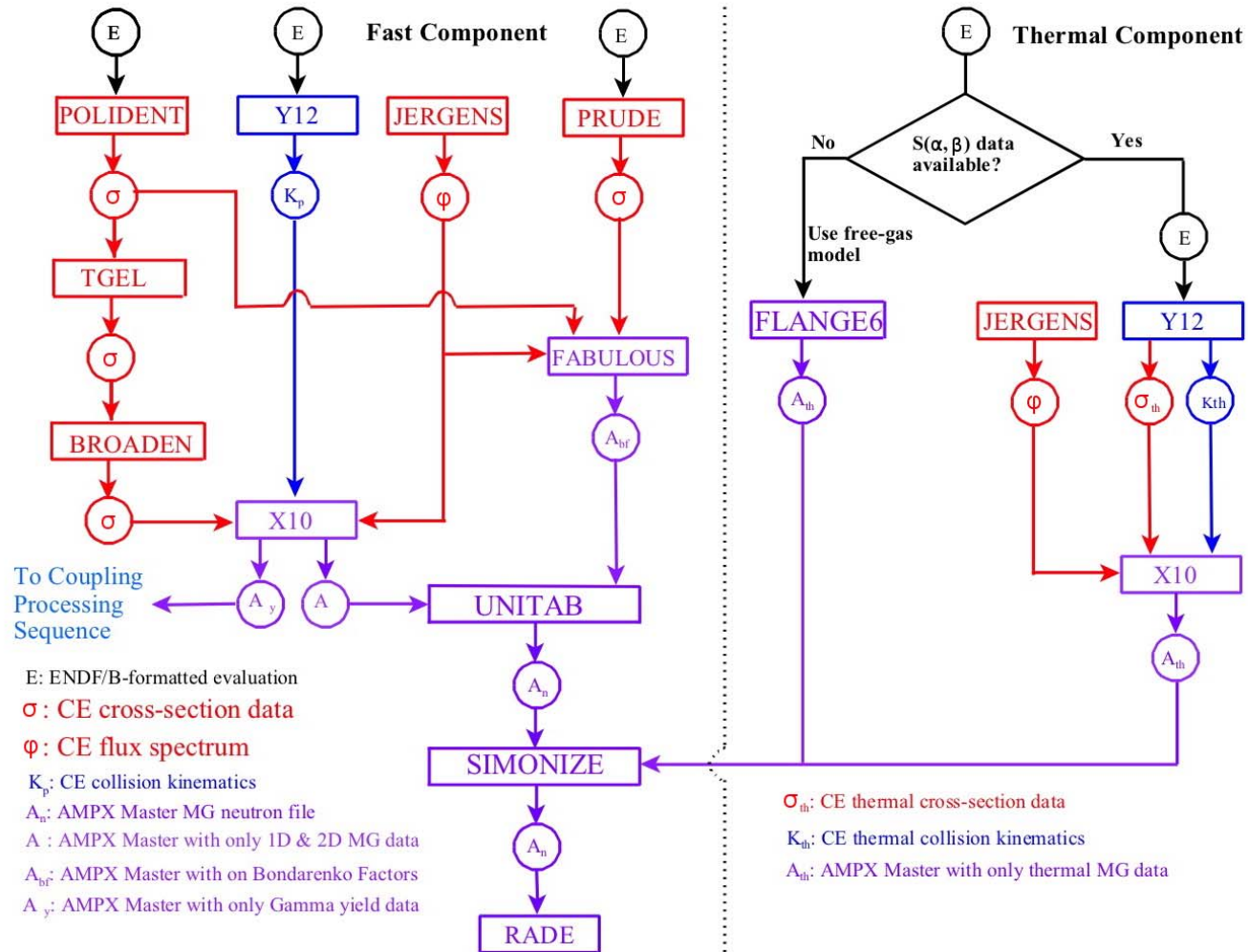


Fig. 2.2 AMPX sequence for producing neutron multigroup data.

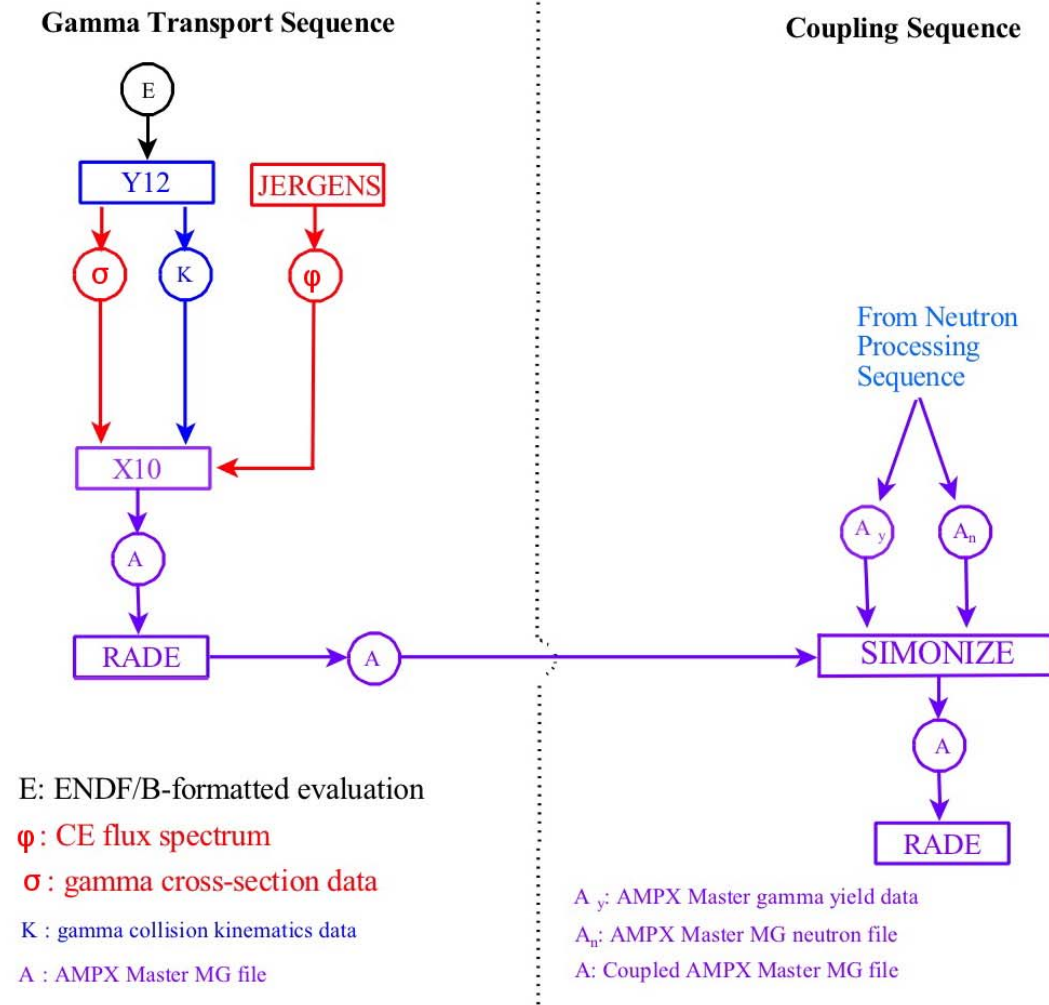


Fig. 2.3 AMPX sequence to generate the coupled gamma-neutron multigroup data.

The ENDF/B-VI.8 and ENDF/B-VII.0 cross-section evaluations were downloaded from the NNDC Web page.² Some of the ENDF/B-VI.8 evaluations contain incomplete evaluations preventing them from being used to generate a complete cross-section library for radiation transport calculations. These evaluations are excluded and are listed in Table 2.7. The ENDF/B-VI.8 evaluation for S (ENDF MAT 1600) does not list MT=18, fission, in File 3; therefore, the cross-section data for this reaction only extend from 1×10^{-5} eV to 1.0921×10^6 eV as derived from the resolved resonance data in File 2, which provides fission width data for some of the resonances. Clearly, the presence of fission width information for S in File 2 is not correct as S is not a fissionable nuclide.

Table 2.7 Evaluations excluded from the ENDF/B-VI.8 library

Evaluation	ENDF material	Reason for exclusion
⁴⁰ Ar	1837	Evaluation is missing a file 3 and thus does not yield energy data above 500000.0 eV (end of resolved resonance data).
¹¹⁵ In	4931	File 3 only gives cross-section data for MT=51 and 102, corresponding to (z,n ₁) and (z,γ).
⁴¹ K	1931	File 3 only gives cross-section data for MT=103, corresponding to (z,p).
²⁴ Mg	1225	File 3 only gives cross-section data for MT=102, corresponding to (z,γ).
¹⁰⁰ Mo	4249	File 3 only gives cross-section data for MT=102, corresponding to (z,γ).
⁹⁸ Mo	4243	File only gives cross-section data for MT=102, corresponding to (z,γ).
⁹² Mo	4225	File 3 only gives cross-section data for MT=102, corresponding to (z,γ).
⁵⁹ Ni	2828	File 3 only gives cross-section data for MT=102, 103, and 107, corresponding to (z,γ), (z,p), and (z,α).
⁴⁶ Ti	2225	File 3 only gives cross-section data for MT=103.
⁴⁷ Ti	2228	File 3 only gives cross-section data for MT=28 and 103, corresponding to (z,np) and (z,p).
⁴⁸ Ti	2231	File 3 only gives cross-section data for MT=28, 103, and 107, corresponding to (z,np), (z,p), and (z,α).
⁵⁰ Ti	2237	File 3 only gives data for MT=107 and (z,α).

In the case of the ENDF/B-VII.0 library, the thermal evaluations for U(UO₂) and O(UO₂) are excluded as there are some inconsistencies in the ENDF evaluations that prevent the AMPX module Y12 from processing the data.

2.2.2.1 Point-wise cross-section data

The following AMPX modules are used to create the point-wise neutron cross-section data.

POLIDENT

Whether cross sections are being prepared for continuous energy applications (CE-KENO or the CENTRM module in SCALE for resonance self-shielding) or for multigroup applications, the first module that will be executed is the POLIDENT module. For resonance nuclides, POLIDENT contains a procedure that determines a point energy mesh in the resolved resonance region and calculates the cross sections on the energy mesh. An analogous procedure is performed for nuclides having unresolved resonance data. For all nuclides, POLIDENT combines the resonance functions with the ENDF/B File 3 point data files to produce linearized cross-section functions. The combined data functions are written out in a standard AMPX tabular data format which is based on the ENDF/B TAB1 format.⁵

TGEL and DCON

One of the primary reasons to linearize the cross-section data is to produce internally consistent data sets. When all of the cross-section data are produced on a linear-linear grid, the sum of a group of linear functions is itself linear; however, simply linearizing the data that are given in an evaluation does not lead to this consistency. To ensure consistency, the total cross section and other “redundant” reactions (e.g., fission, inelastic) are formed by summing the partial values. The TGEL or DCON modules are used to ensure all redundant reactions are equal to the sum of the partial reactions. The output is written in the same tabular format that is used by POLIDENT.

BROADEN

Many applications, especially those dealing with reactors, need cross sections that vary as a function of temperature. The point cross sections can be Doppler broadened by a numerical treatment used in the BROADEN module. The output data from BROADEN are exported in an AMPX tabular format.

JERGENS

An energy-dependent weighting function is needed to produce multigroup cross sections. The JERGENS module provides a large variety of options for generating weighting spectra. JERGENS has options for calculating weighting spectra that may use point cross sections from POLIDENT. The output is written in an AMPX tabular format. To calculate the group-averaged infinite dilute cross sections, JERGENS was used to produce a “smooth” weighting spectrum that has the form of a Maxwellian—1/E—fission spectrum—1/E above 10 MeV. The weighting spectrum used for infinitely dilute group cross sections is shown in Fig. 2.4. The weighting spectrum is normalized with the factor $1/(\sigma_T + \sigma_0)$, where σ_T is the total cross section and σ_0 the background cross section.

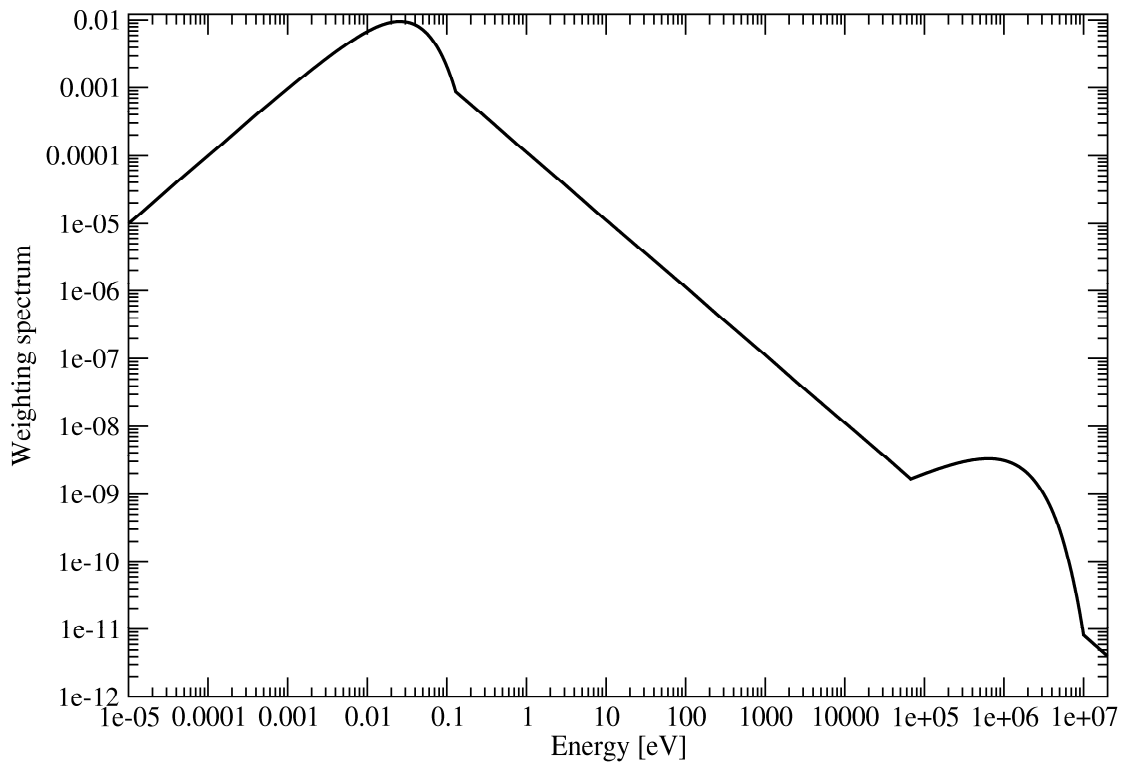


Fig. 2.4 Weighting spectrum generated by JERGENS.

Input template used

The input was generated using an XML template. The XML template used is given in Appendix A. The following is the generated AMPX input file for ^{235}U .

```
=shell
ln -sf /Users/dw8/ampx/running/endl7/rel0/n-092_U_235.endf ft11f001
end
=polident
-1$$ 20000
0$$ 31 32 e 1$$ 1 t
2$$ 9228 11 2 6 e
4** a5 0.001 e
6$$ a3 0 15000 t
end
=shell
cp ft31f001 ${RTNDR}/../neutron/u235_polident
cp ft32f001 ${RTNDR}/../neutron/u235_polident_ft32
end
=tgel
-1$$ 5000000
0$$ 31 33 e t
end
=broaden
limit=5000000
logpt=33 logdp=34
t= 0 300 600 900 1200 2400
end
=shell
cp ft34f001 ${RTNDR}/../neutron/u235_broaden
```

```

end
=pickeze
-1$$ 3000000
0$$ 34 35
1$$ 1 0 0 1 0 e t
2$$ 9228
5** 300.0 t
end
=jergens
-1$$ a11 3000000 e
0$$ 35 30 18 1$$ 2 t
3$$ 1 0 4 t
3$$ 1099 4 0 t
  2099 0 read 1.0 -1 0
  2099 0 save 0 0 0
  1099 2099 div 1.0 9228 1
  1099 0 save 0 0 0
end
=shell
cp ft30f001 ${RTNDIR}/../neutron/u235_weight
end

```

Input files have been processed on a DEC Alpha Tru64 machine, a 32-bit Linux machine, and a 64-bit Intel Mac. The differences, between the point-wise data from the different computing systems, are mostly smaller than 10^{-3} , the precision to which the energy grid was determined. In a few instances (^{148}Nd , ^{108}Cd , ^{239}Pu) larger differences are found due to rounding differences between the three platforms. For the final library, the data generated on the 64-bit Intel Mac were used.

The BROADEN module does not add additional points while performing Doppler broadening. This posed a problem at the boundary between the resolved and unresolved region and at the end of the unresolved range when generating Bondarenko factors. As the cross section in the unresolved region does not vary rapidly, normally relatively few energy points are needed to describe the point-wise cross-section data adequately. However, at the low energy end and the high energy range of the unresolved resonance region, the point-wise cross section may show discontinuities. This is an artifact of the evaluation. The ENDF formats and procedures⁵ do not define the procedure for treating discontinuities. The BROADEN module incorrectly interprets these discontinuities as sharp resonances unless there is a sufficient number of energy points on either site of the discontinuity. Therefore, the module POLIDENT has been updated to add 10 additional energy points at both ends of the unresolved resonance range to correct the problem for BROADEN.

2.2.2.2 Comparison with NJOY

For verification purposes, the AMPX-processed data were compared to NJOY-generated data.⁶ To investigate differences between the two programs that are relevant to the coupled library productions, we converted the point-wise data into group averaged data using a flux of Maxwellian 1/E fission spectrum—1/E above 10 MeV. Group averaged data were compared at 300 K because this temperature is used for the coupled library. Because AMPX leaves redundant reactions in the master library, whereas NJOY deletes them, these reactions are excluded from the comparison. Overall, the agreement with NJOY is good.

Differences are mostly due to the fact that the Doppler broadening module, BROADR, in NJOY adds additional data points whereas the AMPX BROADEN routine does not. As an example, we present the capture cross section in ^{140}Ce in Fig. 2.5.

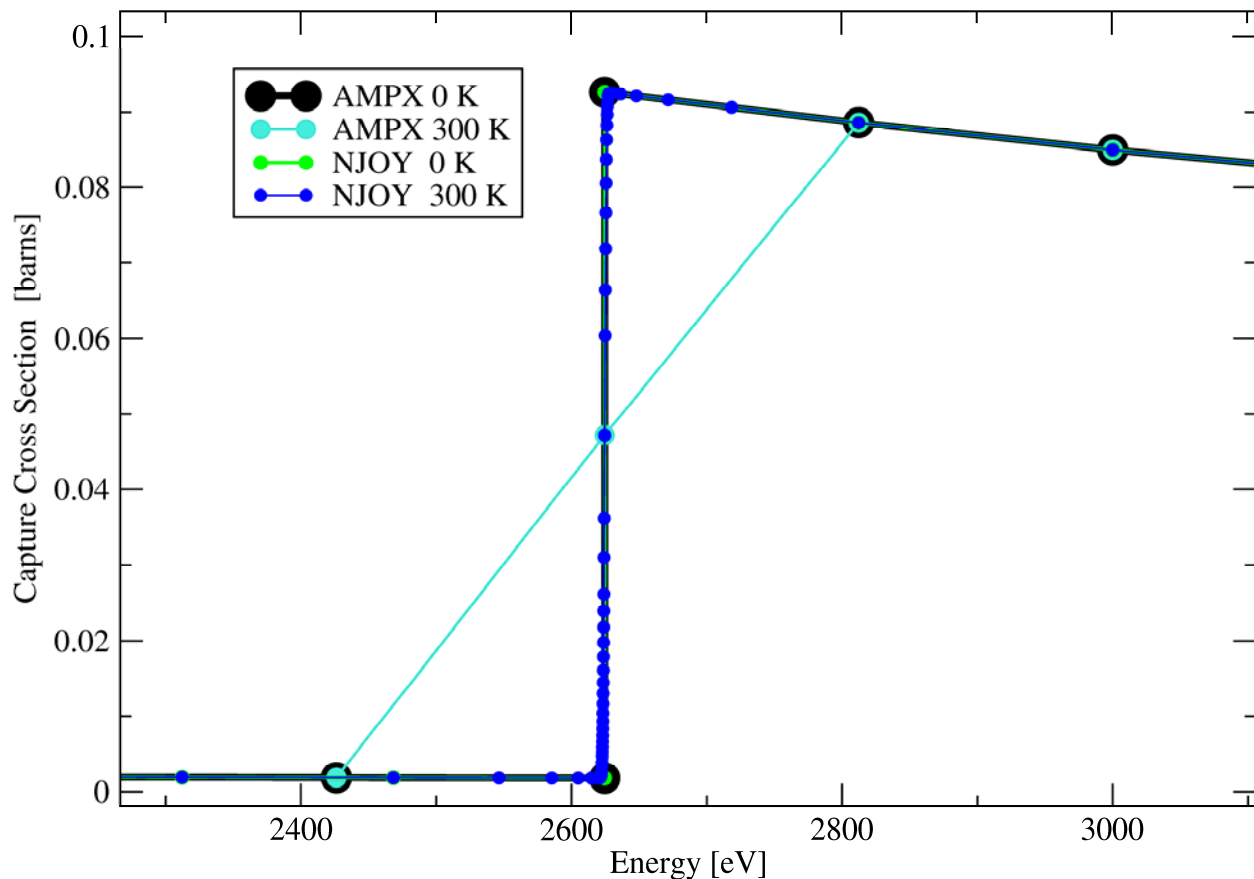


Fig. 2.5 Point-wise capture cross section as processed with AMPX and NJOY for ^{140}Ce .

2.2.2.3 Neutron and gamma yield processing

Fast neutron evaluation

Y12

A feature unique to the AMPX system is the Y12 module. This module reads an ENDF/B evaluation and produces tabular double-differential collision kinematics data for all reactions. The functions it produces tell what particles are produced and at what energies and directions when a reaction is encountered at some source energy point. The output from Y12 is an AMPX tabular kinematics file.

X10

The X10 module reads tabular point cross sections, a tabular weighting spectrum, and the tabular kinematics data file and uses these three files to produce group-averaged cross sections factors and group-to-group transfer matrices. This code contains no programming related to the physics of any reaction and is programmed in a manner that treats neutron data, gamma-ray data, or gamma-ray yield data. The output from X10 is a set of group cross sections that are written on a file in the AMPX master library format.

When a cross-section evaluation contains gamma-production data, either in ENDF File 6 or in the special Files 12, 13, 14, and 15, the kinematics data file produced by Y12, along with the point data files from POLIDENT and JERGENS are passed to X10 to produce gamma-ray yield transfer matrices. The gamma yield matrices tell where gamma rays are produced as a function of neutron reaction. The yield data are exported from X10 in an AMPX master library format. After the gamma transport data are processed in a separate AMPX sequence, the gamma yield data are coupled with the multigroup neutron and gamma-ray data.

Input template used

The input was generated using an XML template. The XML template used is given in Appendix A. The following is the generated AMPX input file for ^{235}U .

```
=shell
ln -sf /Users/dw8/ampx/running/endl7/relo/n-092_U_235.endf ft11f001
ln -sf ${RTNDR}/../neutron/u235_polident ft31f001
ln -sf ${RTNDR}/../neutron/u235_broaden ft34f001
ln -sf ${RTNDR}/../neutron/u235_weight ft30f001
end
=y12
0$$ 32 11 0 0
1$$ 9228
2$$ 2 6
3$$ 32 8 8 8 8 5 t
t
end
=pickeze
-1$$ 3000000
0$$ 34 35
1$$ 1 0 0 1 0 e t
2$$ 9228
5** 300.0 t
end
=x10
neutron
-1$$ 3000000
0$$ 1 30 35 32
1$$ 9228 238 90 0 5 0 0
2$$ 99 2099 9228 9228 3** 1.15860E+01 6$$ 99 2099 t
t
u235 9228 ENDFBV7 REL0 REV7 MOD7 AMPX 10/23/07
end
=rade
1$$ 1 e t
end
=shell
cp ft01f001 ${RTNDR}/../neutron/u235_fast
end
=x10
yield
-1$$ 9000000
0$$ 71 30 35 32
1$$ 9228 200 0 47 5 2 5
2$$ 99 2099 9228 9228 3** 1.15860E+01 6$$ 99 2099 t
t
u235 9228 ENDFBV7 REL0 REV7 MOD7 AMPX 02/11/08
end
=rade
1$$ 71 e t
end
=shell
cp ft71f001 ${RTNDR}/../neutron/u235_yield
end
```

Input files have been processed on a DEC Alpha Tru64 machine, a 32-bit Linux machine, and a 64-bit Intel Mac. For the final library, the data generated on the 64-bit Intel Mac were used.

2.2.2.4 Thermal neutron processing

FLANGE6

If the nuclide is a nonmoderator material, the FLANGE6 module is used to produce thermal scattering matrices at 300, 600, 900, 1200, and 2100 K based on the free-gas scattering model. The matrices are exported in the AMPX master library format.

JERGENS, Y12, and X10

If the nuclide is a moderator material with ENDF S(α,β) data (e.g., water-bound hydrogen, graphite), the thermal ENDF/B evaluations are processed by the Y12 module to produce thermal kinematics data as a function of temperatures provided in the ENDF/B evaluation. The thermal scatter kernel for other materials is represented as free gas. In addition, the Y12 module produces thermal point-wise cross-section data. The resulting thermal kinematics file and thermal point-wise cross-section file are passed to the X10 module, along with the JERGENS weighting spectrum, to produce a special thermal AMPX master library.

Special requirements for BeO

In all of the ENDF/B thermal scattering laws except BeO, the cross sections for the principal isotope in a compound can be isolated. For example, the thermal data for water gives the scattering law data for hydrogen in a manner that describes the specific binding effects for having hydrogen present in a water molecule. The file then specifies that oxygen should simply be treated by the free-gas model. This is very convenient because it allows one to produce a set of full-range cross sections for water-bound hydrogen by collecting together the thermal hydrogen values and combining them with the values from the fast neutron hydrogen evaluation. For BeO, it is not possible to separate the beryllium behavior (or oxygen) out of the data for the BeO molecule. The scattering law data are given for the molecule as a combined unit. There are several ways one can deal with this situation. The one that was chosen to be analogous to the water-bound hydrogen case was to couple the data from the fast neutron evaluation for Be with the thermal BeO data, and call this set “Be bound in BeO.” For the oxygen component, a special set is prepared and called “O bound in BeO.” For the O in BeO case, the oxygen data are prepared from the fast neutron evaluation without any thermal data (i.e., no thermal scattering data as would normally be present from a free-gas calculation by the FLANGE6 module).

Input for moderator data

The input was generated using an XML template. The XML template used is given in Appendix A. The following is the generated AMPX input file for hydrogen in H₂O.

```
=shell
ln -sf /Users/dw8/ampx/running/endl7/re10/ts1-HinH2O.endf ft11f001
ln -sf ${RTNDIR}/../groupStructure ft47f001
end
=y12
0$$ 37 11 38 0
1$$ 1
2$$ 2 6
3$$ 32 8 8 8 8 5 t
t
end
```

```

=shell
cp ft37f001 ${RTNDIR}/../thermal/h_h2o_kin
cp ft38f001 ${RTNDIR}/../thermal/h_h2o_point
end
=jergens
0$$ 11 30 18
1$$ 1 t
3$$ 1099 0 2 t
end
=x10
neutron
0$$ 4 30 38 37
1$$ 1 200 34
0
5 2 0
2$$ 99 1099 1 1
3** 0 t
t
h_h2o 1 ENDFB V6 RELO REV7 MOD0 AMPX 12/09/07
end
=shell
cp ft04f001 ${RTNDIR}/../thermal/h_h2o_master
end
=rade
1$$ 4 e t
end
=paleale
0$$ 4 e 2$$ 1 0 e 5$$ f 200 t
end

```

Input files have been processed on a DEC Alpha Tru64 machine, a 32-bit Linux machine, and a 64-bit Intel Mac. For the final library, the data generated on the 64-bit Intel Mac were used. Differences between the results on the three platforms were within expected ranges.

Input for nonmoderator data

The input was generated using an XML template. The XML template used is given in Appendix A. The following is the generated AMPX input file for ^{235}U .

```

=shell
ln -sf ${RTNDIR}/../neutron/u235_weight ft30f001
ln -sf ${RTNDIR}/../groupStructure ft47f001
=flange6
nl=3 za=92235 awr=233.0248 free=1.15860E+01
mat=0 master=41 igm=200 neg=34
t=300 t=600 t=900 t=1200 t=2100
end
=shell
cp ft41f001 ${RTNDIR}/../neutron/u235_flange6
end

```

Input files have been processed on a DEC Alpha Tru64 machine, a 32-bit Linux machine, and a 64-bit Intel Mac. The cross-section data produced on the 64-bit Intel Mac are used in the final coupled library.

Differences between the results on the three platforms exist, even if the Legendre coefficients are expanded and the real scattering matrices are compared. This is most likely due to rounding effects because mostly small scattering values are affected. The differences do not have significant impact on the library data.

2.2.2.5 *Generating full-range Bondarenko factors and thermal data*

To facilitate self-shielding calculations, full-range Bondarenko factors for several temperatures and background cross sections are supplied on the coupled library. The Bondarenko method is basically a self-shielding method that parameterizes cross sections for a nuclide as a function of temperature, T , and the “background” cross section, σ_0 , of all the other nuclides mixed with the nuclide. Simplistically, given the temperature and background cross-section values, one determines self-shielded cross sections by interpolating in tables. Since self-shielding causes the “background” values that a nuclide sees to change, an iterative procedure involving all nuclides is used.

PRUDE

For nuclides with unresolved resonance data, the PRUDE module must be run to produce point “averaged” cross sections that are a function of temperature and “background” cross section. The background cross section is simply defined as the cross section per unit atom of a nuclide of the mixture (other than the nuclide itself) in which the nuclide is mixed. In the sequences that were prepared, temperatures of 300, 900, and 2100 K were chosen, along with background values of 10^{-6} , 1, 10, 100, 1000, 10^4 , 10^5 , 10^6 , and 10^8 . The cross sections are written out in an AMPX tabular file. This module can only be run for mono-isotopic evaluations.

FABULOUS

For all nuclides, the point data from PRUDE (if applicable) and POLIDENT are passed to the FABULOUS module with the weighting spectrum file from JERGENS. FABULOUS uses the same temperatures and background cross sections described for PRUDE to numerically Doppler broaden the functions exterior to the unresolved region, after which the functions are spliced together with the appropriate unresolved functions. These spliced functions are then used in a numerical scheme that calculates Bondarenko factors for all nuclides for elastic scattering, capture, fission, and total cross sections. The Bondarenko factors can be used in resonance self-shielding calculations.

Input files

The input was generated using an XML template. The XML template used is given in Appendix A. The following is the generated AMPX input file for ^{235}U .

```
=shell
ln -sf /Users/dw8/ampx/running/endl7/re10/n-092_U_235.endf ft11f001
ln -sf ${RTNDR}/../../neutron/u235_polident ft31f001
ln -sf ${RTNDR}/../../neutron/u235_weight ft30f001
ln -sf ${RTNDR}/../../groupStructure ft47f001

ln -sf ${RTNDR}/../../bon_test/neutron/u235_polident ft31f001
ln -sf ${RTNDR}/../../bon_test/neutron/u235_weight ft30f001
end
=prude
0$$ 36
1$$ 1 t
2$$ 9228 9 3 11 2 t
3** 1+8 1+6 1+5 1+4 1000 100 10 1 1-6
4** 300.0 900.0 2000.0 e
5** 0 1 e t
end
=shell
cp ft36f001 ${RTNDR}/../../neutron/u235_prude
end
```

```

=tgel
-1$$ 9000000
0$$ 31 32 e t
end
=fabulous
Title Card for FABULOUS case
-1$$ 2500000
0$$ 2 32 30 36
1$$ 9228 9228 3 9 200
2$$ 99 2099
5** 233.0248 0.0001 t
8** 300.0 900.0 2000.0
9** 1+8 1+6 1+5 1+4 1000 100 10 1 1-6
t
end
=shell
cp ft02f001 ${RTNDIR}/../neutron/u235_fabulous
end

```

Input files have been processed on a DEC Alpha Tru64 machine, a 32-bit Linux machine, and a 64-bit Intel Mac. The data generated on the 64-bit Intel Mac were used for the final library.

During the course of the library generation, several issues were discovered and corrected in PRUDE and FABULOUS. The PRUDE module calculates the point-wise cross sections for the unresolved resonance range for different values of σ_0 , combining File 2 and File 3 data if necessary. The same calculation is done in the POLIDENT module for infinite dilution. The two modules produced inconsistent results because the combining was done in two different ways. The PRUDE module was updated to use the same methods as POLIDENT. The infinite diluted cross-section data are now consistent between the two modules.

Initially the FABULOUS module could not process all evaluations because some of the unresolved cross-section data are negative for lower values of σ_0 (i.e., highly self-shielded). This is most likely due to Single-Level Breit-Wigner (SLBW) approximation. Calculation of the “total” Bondarenko factor is given by

$$\frac{\int \frac{\phi \sigma_T}{(\sigma_T + \sigma_0)^2}}{\int \frac{\phi}{(\sigma_T + \sigma_0)^2}} \quad (2.1)$$

The value for $(\sigma_T + \sigma_0)$ can become negative. The NJOY⁶ manual describes how the calculation in the UNRES function is done, which is similar to the PRUDE calculation. The manual states that for the higher actinides the approximation used in calculating this quantity can produce negative shielded cross-section data for lower values of σ_0 . This should not be a problem as the higher actinides are rarely present in these quantities in a reactor. The affected evaluations are ²³⁸Np, ^{242m}Am, ²⁴²Am, and ²⁵³Cf. In addition, an infinite loop was discovered in FABULOUS for ²³⁸Np because the code tried to use a step-size smaller than the available computer precision. This problem and some overstepped bounds issues have been fixed.

Greater than expected differences were found between the Bondarenko factors calculated in Linux and on Tru64. These differences occurred because the Doppler broadening routine in FABULOUS converts the energy into velocity-like terms for the Bondarenko calculation. These terms are converted back to energy afterwards. On occasion, the end points of the unresolved resonance range may not be included in the

final point-wise cross-section data due to this conversion. The code has been updated to always include these end points. After these changes, good agreement is obtained for the Bondarenko factors calculated on the three platforms.

2.2.2.6 *Gamma processing*

The processing for gamma-ray interactions is much simpler in contrast to neutron interactions. Most of the important gamma-ray scattering reactions are due to interactions of the gamma ray with the electrons in a nucleus. Since the number of electrons in a nucleus is just the Z -value, the cross sections are calculated on a per electron basis and simply multiplied by Z to get the value for a nuclide. Since Z is the same for all isotopes of an element, one only has to calculate values for the elements. Furthermore, there are only two processes—incoherent (Klein-Nishina) and coherent (Rutherford) scattering—to be treated. There is only one exception to the number of processes, and this exception is the pair-production of two 0.511 MeV photons.

JERGENS

The JERGENS module is used to produce a weighting spectrum. For gamma-ray processing, the spectrum is typically a $1/E$ spectrum with “roll-offs” that account for significant absorption of the gamma rays because of photoelectric absorption. As before, the weighting spectrum is written out in a point-wise AMPX tabular file based on the ENDF/B TAB1 format.

Y12

The Y12 module produces a tabular kinematics file that describes coherent and incoherent scattering and pair production. In addition, Y12 produces a point-wise data file for all of these processes, and the point-wise file is exported in an AMPX tabular format.

X10

The tabular files from JERGENS and Y12 are passed to X10 with the tabular kinematics file. X10 produces a group-averaged AMPX master library for gamma-ray interactions.

RADE and PALEALE

The RADE module is used to perform internal consistency checks on the AMPX master library containing the gamma-ray interaction data. The PALEALE module is used to print the content of the library and allows data checking.

Gamma interaction data used

The Photo-Atomic interaction sublibrary of ENDF/B-VI.8 and ENDF/B-VII.0 were used in the library generation effort. In both cases data exist for the following 100 elements:

H He Li Be B C N O F Ne Na Mg Al Si P S Cl Ar K Ca Sc Ti V Cr Mn Fe Co Ni Cu Zn Ga Ge
As Se Br Kr Rb Sr Y Zr Nb Mo Tc Ru Rh Ce Pr Nd Pm Sm Eu Gd Tb Dy Ho Er Tm Yb Lu Hf
Ta W Re Os Ir Pt Au Hg Tl Pb Bi Po At Rn Fr Ra Ac Th Pa U Np Pu Am Cm Bk Cf Es Fm

Input used to process gamma cross-section data

The input was generated using an XML template. The XML template used is given in Appendix A. The following is the generated AMPX input file for uranium.

```
=shell
ln -sf /Users/dw8/ampx/running/endl7/re10/photoat-092_U_000.endf ft11f001
end
=y12
0$$ 32 11 31 0
1$$ 9200
2$$ 2 6
3$$ 32 8 8 8 5 t
t
end
=shell
cp ft32f001 ${RTNDR}/../gamma/u_kin
cp ft31f001 ${RTNDR}/../gamma/u_point
end
=jergens
0$$ 0 30 18
1$$ 1
2** 1.0e3 3.0e7 t
3$$ 1599 0 11 t
end
=x10
gamma
0$$ 1 30 31 32
1$$ 9200 0 0
47
0 0 5
2$$ 99 1599 9200 9200
3** 0.0 t
7** 2.0E+7      1.4E+7      1.2E+7      1.E+7      8.E+6
    7.5E+6      7.E+6      6.5E+6      6.E+6      5.5E+6
    5.0E+6      4.5E+6      4.E+6      3.5E+6      3.E+6
    2.75E+6     2.5E+6     2.35E+6     2.15E+6     2.E+6
    1.8E+6      1.66E+6    1.57E+6    1.5E+6     1.44E+6
    1.33E+6     1.2E+6     1.E+6      9.0E+5     8.0E+5
    7.0E+5      6.0E+5     5.12E+5    5.1E+5     4.5E+5
    4.0E+5      3.0E+5     2.6E+5     2.0E+5     1.5E+5
    1.0E+5      7.5E+4     7.0E+4     6.0E+4     4.5E+4
    3.0E+4      2.0E+4     1.0E+4 e
t
u 9200 ENDFB V6 REL8 REV7 MOD1 AMPX 12/09/07
end
=shell
cp ft01f001 ${RTNDR}/../gamma/u_master
end
=rade
1$$ 1 e t
end
=paleale
0$$ 1 e 2$$ 0 1 e 4$$ 502 504 e 5$$ f 47 t
end
```

Input files have been processed on a DEC Alpha Tru64 machine, a 32-bit Linux machine, and a 64-bit Intel Mac. While the data processed on all three platforms were compared, no significant differences were found, and the final library uses the data generated on the 64-bit Intel Mac.

Processing of gamma data

File 23 containing “smooth” photon interaction cross sections gives the data for MT=502, photon coherent scattering in the range from 1.0 eV to 1.0×10^{11} eV. These data need to be combined with form factors from File 27, MT=502 (form factor), MT=505 (imaginary scattering factor), and MT=506 (real scattering factor), which are given over the ranges 0.0 eV to 1.0×10^9 eV, 1.0 eV to 1.0×10^7 eV, and 1.0 eV to 1.0×10^7 eV, respectively. The program then tries to interpolate for energies listed for MT=502 and warns that the interpolation is outside the range. In the case of tungsten, the two values bracketing the 1.0×10^7 eV in MT=502 are 7.070513×10^6 eV and 2.135261×10^7 eV. The program gives a warning and assumes that the desired value is 0.0.

While the number of energy points in File 23 for MT=502 change for the various elements, the data for MT=505 and MT=506 in File 27 come in the range from 1.0 eV to 1.0×10^7 eV for all elements. Thus, the above problem is present for all elements used in the coupled library.

On Tru64, Y12 fails for hydrogen as the last two interpolation points for File 27 and MT=502 are given as $(1.0 \times 10^6; 8.18290 \times 10^{-27})$ and $(1.0 \times 10^9; 8.18290 \times 10^{-39})$. After the last two values are changed to 0.0 in the ENDF file, the calculation succeeds.

Data generated on Linux and on Tru64 show greater than expected differences in the scattering matrix for MT=504 for the lower energy groups. This is due to rounding effects in the calculations of the grid for the Klein-Nishina scattering, where Y12 reconstructs the point-wise scattering in terms of the scatter-cosine, which is given as a function of incident energy E and scattered energy E' as

$$\frac{e'}{e} = \frac{1}{1 + e(1 - \mu)}, \quad (2.2)$$

where e and e' are the energy in terms of the electron mass unit $e = E/0.5110034$. A function then calculates the cosine of the scattering angle from the above formula as

$$\mu = 1 + \frac{1}{e} - \frac{1}{e'} = 1 + \frac{5.110034 \times 10^5 \times (E' - E)}{E \times E'}, \quad (2.3)$$

using the first approach after first calculating e and e' , all in single precision. In single precision, the two forms of the equation can have two difference values. An example is $E = 1.0$ eV and $E' = 0.99999607$. In this case, the first form yields $\mu = -1.0186844$ and the second form $\mu = -1.0102476$. The later is consistent with the value calculated for both forms of the equation if calculation is done in double precision. This can lead to large differences. An example is silicon, where the largest difference is found scattering from group 41 to 41 in the fourth Legendre coefficient: single precision $4.0716E-02$, double precision $-1.6598E-01$. For the final library, all calculations in the Y12 klein_nishina function were done internally in double precision and returned as single precision values.

After these changes, good agreement is obtained for gamma cross-section data generated on the three platforms.

Comparison with NJOY

For independent verification purposes, the AMPX-processed data were compared to NJOY-generated data.⁶ The NJOY code was used to process the gamma evaluations. The groupwise ENDF files generated by GAMINR were converted to AMPX master files using SMILER. This module converts MT=522 to MT=527 and MT=525 to MT=1527—this feature is temporarily disabled to allow direct comparison. All NJOY files have the following one-dimensional (1-D) MT values: 501, 502, 504, 516, 522, 525, and 1599. The MT=1599 gives the flux and MT=525 is not defined in the ENDF-VI or ENDF-V reaction list. The NJOY manual states that this is the heating cross section defined in ENDF-V as 621.

AMPX writes out more reaction values because it keeps the redundant reactions.

The flux written by GAMINR is not normalized to the sum of the flux over all energy groups as is done for gamma processes in X10. SMILER has been changed to write out the normalized flux to allow a direct comparison between the results from AMPX and NJOY.

Summation over total and redundant reactions

X10 first calculates the group averages for all reactions listed in the ENDF file as translated by Y12. The following reactions are then treated in a special manner.

If MT=515 (pair production, electron field) or MT=517 (pair production, nuclear field) exists, the redundant reaction MT=516 (pair production) is created as the sum of the two, erasing all previous data in the reaction that might have been set by the ENDF evaluation. If MT=516 does not previously exist, it is **NOT** created, even if MT=515 or MT=517 exists.

If any MT in the range MT=534–572 (subshell photoelectric or electro-atomic cross section for various atomic levels) exist, then calculate

$$\begin{aligned} \text{MT}=522 &= \sum x_{MT} && \text{Photoelectric absorption. (In version 5, this was MT=602.)} \\ \text{MT}=602 &= \sum x_{MT} && \text{Photoelectric absorption.} \\ \text{MT}=527 &= \sum x_{MT} + x_{\text{MT}=602}, \end{aligned}$$

where x_{MT} is the group averaged cross section for the indicated reaction and the sum extends over reaction numbers MT=534–572. The total cross section is then recalculated as

$$\text{MT} = 501 = x_{\text{MT}=502} + x_{\text{MT}=504} + x_{\text{MT}=516} + x_{\text{MT}=522} .$$

(These calculations are done in the subroutine fixsums_g of X10).

Not all evaluations considered for the coupled library include MT=527 or MT=602, which are added by X10 as outlined above. All evaluations include MT=515, 516, and 517, and X10 will recalculate MT=516. All evaluations include MT=522, which will be erased by X10 and recalculated as outlined above. All evaluations include MT=501, which will be erased by X10 and recalculated as outlined above.

AMPX defines some special MT values. MT=527 is the sum of all gamma-ray absorption processes (in contrast to the ENDF defined value where it is defined as electro-atomic bremsstrahlung). MT=602 is still assumed to be photoelectric absorption, and the group-averaged cross-section data for MT=602 and

MT=522 are identical in the final library. MT=1527 is the gamma energy absorption coefficient or kerma factor. NJOY writes this into MT=527 in GAMINR.

One-dimensional processes

AMPX and NJOY results are compared for MT=501, 502, 504, 516, and 522 because these cross sections are directly comparable between the two programs. No significant differences were found.

Two-dimensional processes

To compare the two-dimensional (2-D) processes, we first compared the Legendre coefficients. If there was a big difference between NJOY and AMPX for these, we expanded the Legendre series and compared the scattering matrices directly. An example of the observed differences can be seen in Fig. 2.6 for MT=504 in hydrogen. Scattering is from group 1 to group 38.

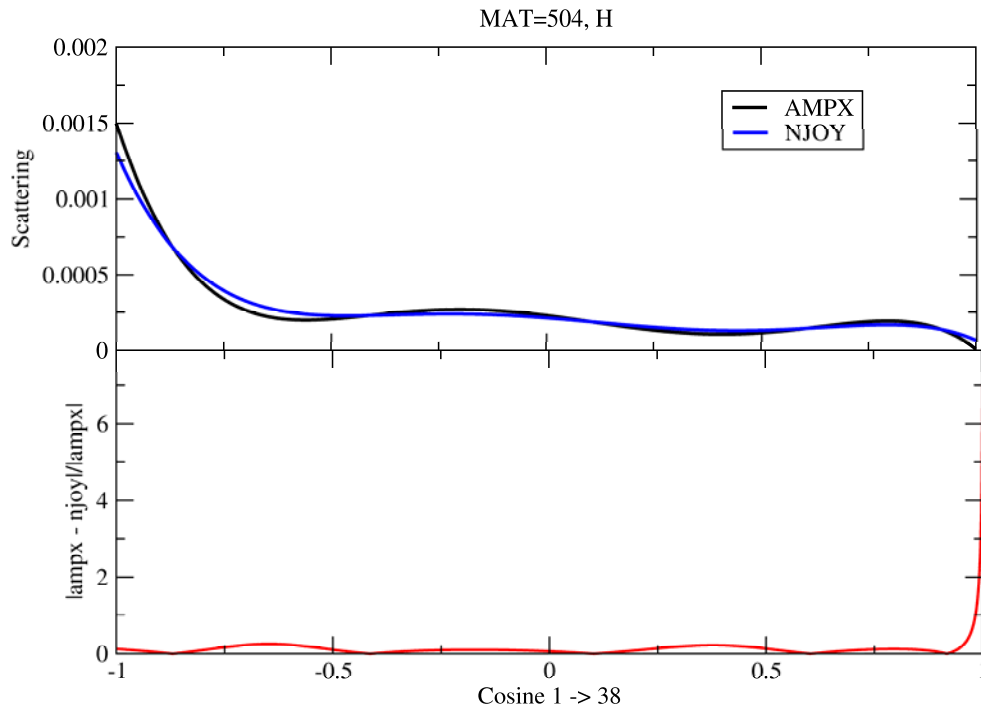


Fig. 2.6 AMPX and NJOY scattering data for MT=504 in hydrogen. Scattering is from group 1 to group 38.

2.2.2.7 Creating the master library

Three steps are needed to create the final master library.

1. Create a master library for each evaluation containing the neutron data, Bondarenko shielding factors, and gamma data. In the case of moderator data, the fast evaluation also needs to be combined into this master library. The ENDF material ID needs to be changed to the SCALE ID.
2. Combine the master libraries for various evaluations into one master library.

3. Add dose data to the master library.

The steps are outlined in more detail below.

Create master library for each evaluation

The master library for nonmoderator data needs to contain gamma data, fast neutron data, neutron yield data, and Bondarenko data. In addition, several SCALE specific identifiers need to be set. Input files are generated from XML templates which are given in Appendix A. The following is the generated AMPX input for ^{235}U .

```
=shell
ln -sf ${RTNDIR}/../neutron/u235_fast ft01f001
ln -sf ${RTNDIR}/../neutron/u235_yield ft02f001
ln -sf ${RTNDIR}/../neutron/u235_fabulous ft03f001
ln -sf ${RTNDIR}/../neutron/u235_flange6 ft04f001
ln -sf ${RTNDIR}/../gamma/u_master ft05f001
end
=simonize
Identifier=92235 master=20 source=endf
title= u235 9228 ENDFB7 REL0 REV7 MOD7 AMPX 02/11/08
id45=7079228 id46=0 id47=7019200 id48=7079228
neutron=1 id19=9228
yield=2 id19=9228
BONDARENKO=3 id19=9228
2dn=4 id19=92235
gamma=5 id19=9200
end
=rade
l$$ 20 e t
end
=shell
cp ft20f001 ${RTNDIR}/../master/u235_neutron
end
```

In the case of thermal moderators, the fast evaluations need to be added to the master. The full template used to generate the input files is given in Appendix A. The following is the generated AMPX input for hydrogen in H_2O .

```
=shell
ln -sf ${RTNDIR}/../neutron/h1_fast ft01f001
ln -sf ${RTNDIR}/../neutron/h1_yield ft02f001
ln -sf ${RTNDIR}/../neutron/h1_fabulous ft03f001
ln -sf ${RTNDIR}/../thermal/h_h2o_master ft04f001
ln -sf ${RTNDIR}/../gamma/h_master ft05f001
end
=simonize
Identifier=1001 master=20 source=endf
title= Fast: h1 Thermal: h_h2o 1 ENDFB7 REL0 REV7 MOD0 AMPX 02/11/08
id45=7050125 id46=7000001 id47=7010100 id48=0
neutron=1 id19=125
yield=2 id19=125
BONDARENKO=3 id19=125
2dn=4 id19=1 MT=0 MODERATOR
gamma=5 id19=100
end
=shell
cp ft20f001 ${RTNDIR}/../master/h_h2o_thermal
end
```

2.2.3 Adding dose data

The SCALE master library contains dose factor data as listed in Table 2.8. The same dose data are used for all three libraries (i.e., the ENDF/B-VI.8 fine-group library and the ENDF/B-VII.0 fine-group and broad-group libraries).

Table 2.8 Available dose functions on the coupled neutron-gamma libraries

MAT	MT	Description
999	1	1/V absorber
	27	1/v function (normalized to 1.0 at 2200 m/s \iff 0.0253 eV)
	101	All reaction values contain the same data
	102	
900	9032	International Commission on Radiation Units and Measurements, Report 44 (ICRU-44), Table B.3 (air) Kerma (Gy/h)/(neutron/cm ² /s)
	9033	ICRU-44, Table B.3 (air) Kerma (rad/h)/(neutron/cm ² /s)
	9034	Ambient dose equivalent (ICRU-57, Table A.42) (Sv/h)/(neutron/cm ² /s)
	9035	Ambient dose equivalent (ICRU-57, Table A.42) (rem/h)/(neutron/cm ² /s)
	9036	Effective dose (ICRU-57, Table A.41) (Sv/h)/(neutron/cm ² /s)
	9037	Effective dose (ICRU-57, Table A.41) (rem/h)/(neutron/cm ² /s)
	9029	American National Standards Institute (ANSI) standard (1977) neutron flux-to-dose-rate factors (rem/h)/(neutron/cm ² /s)
	9031	ANSI standard (1991) neutron flux-to-dose-rate factors (rem/h)/(neutron/cm ² /s)
	9503	Claiborne-Trubey conversion factors (rad/h)/(photons/cm ² /s)
	9504	ANSI standard (1977) gamma flux-to-dose-rate factors (rem/h)/(photons/cm ² /s)
	9505	ANSI standard (1991) gamma flux-to-dose-rate factors (rem/h)/(photons/cm ² /s)
	9506	ICRU-57 Table A.21 (air) Kerma (Gy/h)/(photons/cm ² /s)
	9507	ICRU-57 Table A.21 (air) Kerma (rad/h)/(photons/cm ² /s)
	9508	Ambient dose equivalent (ICRU-57 Table A.21) (Sv/h)/(photons/cm ² /s)
	9509	Ambient dose equivalent (ICRU-57 Table A.21) (rem/h)/(photons/cm ² /s)
9510	Effective dose (ICRU-57 Table A.17) (Sv/h)/(photons/cm ² /s)	
9511	Effective dose (ICRU-57 Table A.17) (rem/h)/(photons/cm ² /s)	

Source: Table S1.4.8 in Ref. 1.

The JERGENS module is used to generate the point-wise data, and the VEL module is used to create the group averages.

Input is as follows for the MAT=900 input.

```

=jergens
-1$$ 2 2 100 900 3 e
0$$ 0 1 19 1$$ 18 t
3$$ 9032 0 9032 e t
3$$ 9033 0 9033 e t
3$$ 9034 0 9034 e t
3$$ 9035 0 9035 e t
3$$ 9036 0 9036 e t
3$$ 9037 0 9037 e t
3$$ 9029 0 9029 e t
3$$ 9031 0 9031 e t
3$$ 9503 0 9503 e t
3$$ 9504 0 9504 e t
3$$ 9505 0 9505 e t
3$$ 9506 0 9506 e t
3$$ 9507 0 9507 e t
3$$ 9508 0 9508 e t
3$$ 9509 0 9509 e t
3$$ 9510 0 9510 e t
3$$ 9511 0 9511 e t
3$$ 9502 0 9027 e t
end
=jergens
0$$ 0 4 18
1$$ 2 t
3$$ 1099 0 4 e t
3$$ 1599 0 11 e t
end
=shell
ln -sf ${RTNDIR}/groupStructure ft47f001
end
=vel Do the 238 Group Neutron Case
0$$ 2 1 4 1$$ 14 200 47 t
t
10$$ 900 9032 0 11$$ 900 9032 3 99 1099 3 t
10$$ 900 9033 0 11$$ 900 9033 3 99 1099 3 t
10$$ 900 9034 0 11$$ 900 9034 3 99 1099 3 t
10$$ 900 9035 0 11$$ 900 9035 3 99 1099 3 t
10$$ 900 9036 0 11$$ 900 9036 3 99 1099 3 t
10$$ 900 9037 0 11$$ 900 9037 3 99 1099 3 t
10$$ 900 9029 0 11$$ 900 9029 3 99 1099 3 t
10$$ 900 9031 0 11$$ 900 9031 3 99 1099 3 t
10$$ 900 9734 0 11$$ 900 9034 3 99 1099 3 t
10$$ 900 9735 0 11$$ 900 9035 3 99 1099 3 t
10$$ 900 9736 0 11$$ 900 9036 3 99 1099 3 t
10$$ 900 9737 0 11$$ 900 9037 3 99 1099 3 t
10$$ 900 9729 0 11$$ 900 9029 3 99 1099 3 t
10$$ 900 9731 0 11$$ 900 9031 3 99 1099 3 t
          900Dose Factors from ICRU Report 44 and 57
end
=vel Do the 238 Group Neutron Case
0$$ 9 1 4 1$$ 16 200 47 2 t
t
10$$ 900 9502 1 11$$ 900 9502 3 99 1599 3 t
10$$ 900 9503 1 11$$ 900 9503 3 99 1599 3 t
10$$ 900 9504 1 11$$ 900 9504 3 99 1599 3 t
10$$ 900 9505 1 11$$ 900 9505 3 99 1599 3 t
10$$ 900 9506 1 11$$ 900 9506 3 99 1599 3 t
10$$ 900 9507 1 11$$ 900 9507 3 99 1599 3 t
10$$ 900 9508 1 11$$ 900 9508 3 99 1599 3 t
10$$ 900 9509 1 11$$ 900 9509 3 99 1599 3 t
10$$ 900 9510 1 11$$ 900 9510 3 99 1599 3 t
10$$ 900 9511 1 11$$ 900 9511 3 99 1599 3 t
10$$ 900 9734 1 11$$ 900 9505 3 99 1599 3 t

```

```

10$$$ 900 9735 1 11$$$ 900 9506 3 99 1599 3 t
10$$$ 900 9736 1 11$$$ 900 9510 3 99 1599 3 t
10$$$ 900 9737 1 11$$$ 900 9511 3 99 1599 3 t
10$$$ 900 9729 1 11$$$ 900 9504 3 99 1599 3 t
10$$$ 900 9731 1 11$$$ 900 9505 3 99 1599 3 t
          900Dose Factors from ICRU Report 44 and 57
end
=simonize
Identifier=900 master=3 source=endf
id45=900 id46=0 id47=0 id48=0
ldn= 2 idl9=900
IDG= 9 IDL9=900
title= Dose factors from ansl/ans 6.1.1 - 1977
end
=rade
0$$$ 3 e t
end
=paleale
0$$$ 3 0 2$$$ 1 1 e t
end
=shell
cp ft03f001 ${RTNDIR}/dose_900_master
end

```

Input is as follows for the MAT=999 input.

```

=jergens
-1$$$ 2 2 100 999 3 e
0$$$ 0 1 18 1$$$ 4 t
3$$$ 1 0 7 e t
3$$$ 27 0 7 e t
3$$$ 101 0 7 e t
3$$$ 102 0 7 e t
end
=jergens
0$$$ 0 4 18
1$$$ 1 t
3$$$ 1099 0 4 e t
end
=shell
ln -sf ${RTNDIR}/groupStructure ft47f001
end
=prilosec
tabl= 1
logwt= 4
matwt= 99 mtwt= 1099 IGM= 200
master= 2
end
=simonize
Identifier=999 master=3 source=endf
id45=999 id46=0 id47=0 id48=0 iftg=0
ldn= 2 idl9=999
title= 1/v function (normalized to 1.0 at 2200m/s<==>0.0253eV)
end
=rade
0$$$ 3 e t
end
=shell
cp ft03f001 ${RTNDIR}/dose_999_master
end

```

Some gamma dose factors did not extend to higher energies and the JERGENS module needed to be changed to extend the dose factors. In these cases an extrapolation to higher energies was used as follows.

9503: Claiborne-Trubey conversion factors (rad/h)/(photons/cm²/s)

We used an interpolation with five coefficients and interpolated from 6×10^6 eV to 1.48×10^7 eV. The interpolation was used for energies above 15 MeV. The following formula was used.

$$y = C_0 * \exp(C_1 + C_2X + C_3X^2 + C_4X^3 + C_5X^4)$$

$$X = \ln(E), E \text{ in eV}$$

$$C_0 = 6.65922 \times 10^{-11}$$

$$C_1 = 2.91298$$

$$C_2 = 0.622646$$

$$C_3 = -0.00467212$$

$$C_4 = -0.00105295$$

$$C_5 = 6.73012 \times 10^{-5}$$

The interpolation is shown in Fig. 2.7.

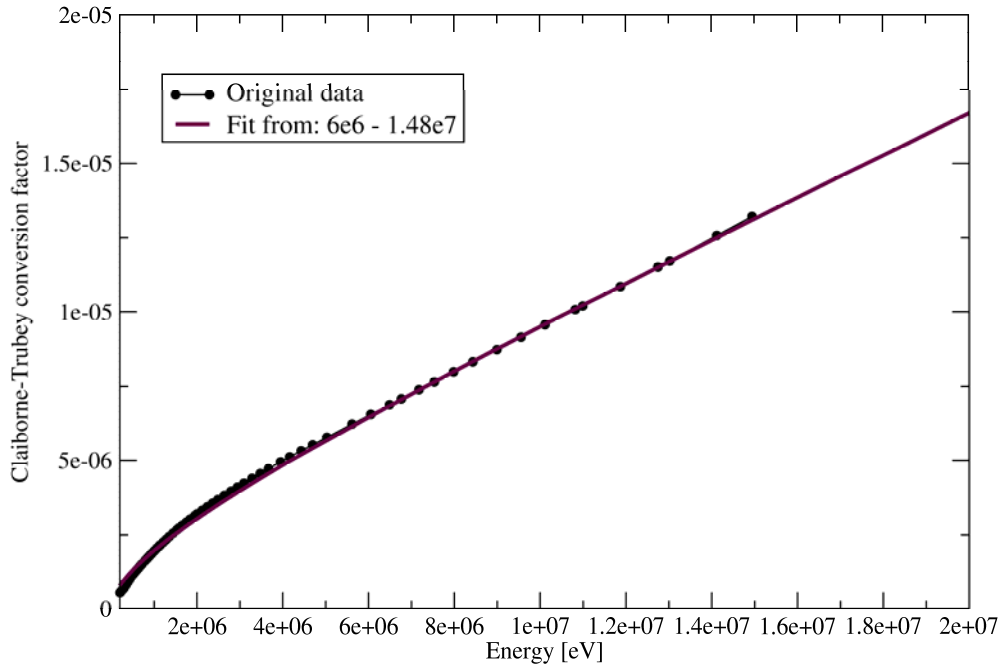


Fig. 2.7 Interpolation for Claiborne-Trubey gamma dose function.

9506 and 9507: International Commission on Radiation Units and Measurements, Report 57 (ICRU-57), Table A.21 (air) Kerma

We used an interpolation with five coefficients and interpolated from 4×10^6 eV to 1.0×10^7 eV. The interpolation was used for energies above 10 MeV. The formula is as follows.

$$y = C_0 * \exp(C_1 + C_2X + C_3X^2 + C_4X^3 + C_5X^4)$$

$$X = \ln(E), E \text{ in eV}$$

$$C_0 = 4.422278 \times 10^{-6}$$

$$C_1 = -0.898794$$

$$C_2 = 1.4646$$

$$C_3 = -0.0209916$$

$$C_4 = -0.00152315$$

$$C_5 = 6.80427 \times 10^{-5}$$

(The factor C_0 takes into account that the JERGENS module scales the internal results to obtain the results in (Gy/h)/(photons/cm²/s) or (rad/h)/(photons/cm²/s). The interpolation is shown in Fig. 2.8.

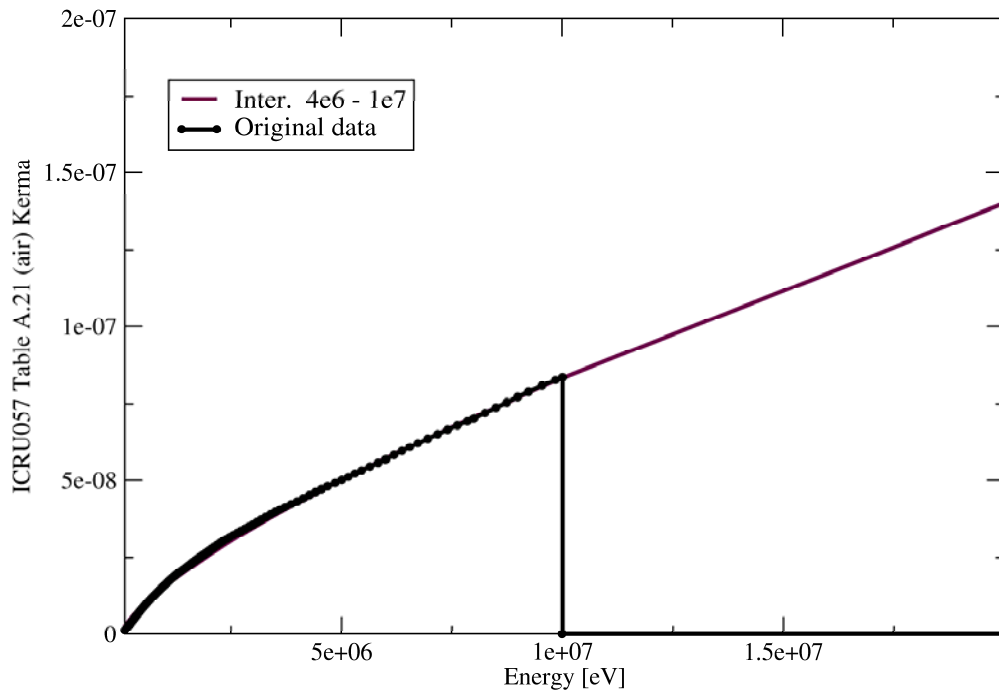


Fig. 2.8 Interpolation for ICRU-57, Table A.21 (air) Kerma gamma dose function.

9508 and 9509: Ambient dose equivalent (ICRU-57, Table A.21)

We used an interpolation with five coefficients and interpolated from 4×10^6 eV to 1.0×10^7 eV. The interpolation was used for energies above 10 MeV. The formula is as follows.

$$y = C_0 * \exp(C_1 + C_2X + C_3X^2 + C_4X^3 + C_5X^4)$$

$$X = \ln(E), E \text{ in eV}$$

$$C_0 = 8.043111 \times 10^{-10}$$

$$C_1 = -11.8556$$

$$C_2 = 4.52715$$

$$C_3 = -0.0788323$$

$$C_4 = -0.0110208$$

$$C_5 = 0.000440013$$

(The factor C_0 takes into account that the JERGENS module scales the internal result to obtain the results in (Sv/h)/(photons/cm²/s) or (rem/h)/(photons/cm²/s). The interpolation is shown in Fig. 2.9.

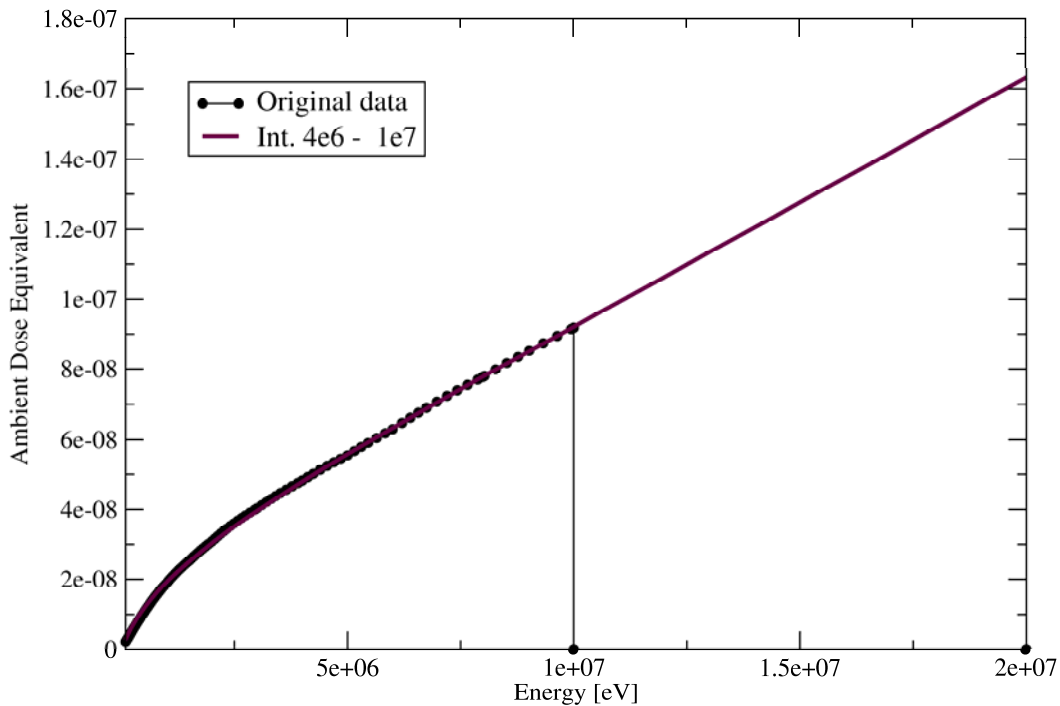


Fig. 2.9 Interpolation for ambient dose equivalent (ICRU-57, Table A.21).

9510 and 9511 Effective dose (ICRU-57, Table A.17) (Sv/h)/(photons/cm²/s)

We used an interpolation with five coefficients and interpolated from 4×10^6 eV to 1.0×10^7 eV. The interpolation was used for energies above 10 MeV. The formula is as follows.

$$y = C_0 * \exp(C_1 + C_2 X + C_3 X^2 + C_4 X^3 + C_5 X^4)$$

$$X = \ln(E), E \text{ in eV}$$

$$C_0 = 2.154528e-5$$

$$C_1 = 4.74445$$

$$C_2 = 1.12057$$

$$C_3 = -0.0487202$$

$$C_4 = -0.00119816$$

$$C_5 = 0.000129643$$

(The factor C_0 takes into account that the JERGENS module scales the internal result to obtain the results in (Sv/h)/(photons/cm²/s) or (rem/h)/(photons/cm²/s). The interpolation is depicted in Fig. 2.10.

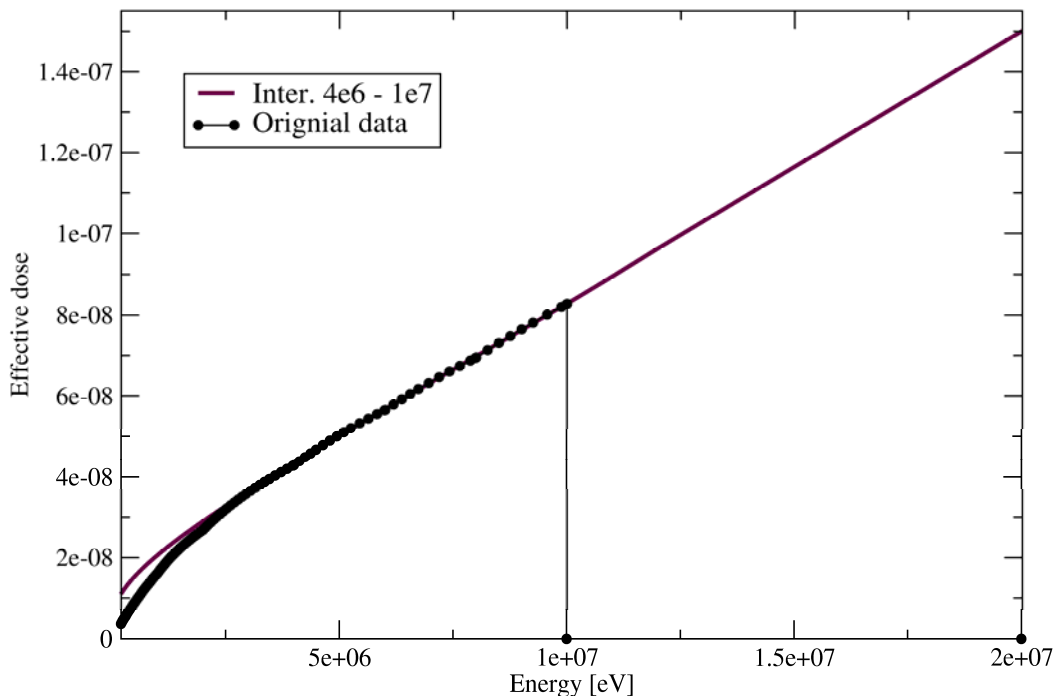


Fig. 2.10 Interpolation for effective dose (ICRU-57, Table A.17) .

Using AMPX, coupled neutron-gamma libraries were generated for ENDF/B-VI.8 and ENDF/B-VII.0. Complete listings of the ENDF/B-VI.8 and ENDF/B-VII.0 libraries are provided in Appendixes B and C, respectively.

3 BENCHMARK TESTING

As noted in the Introduction, new shielding capabilities have been developed for SCALE along with the ENDF/B-VI.8 and ENDF/B-VII.0 coupled library development. To this end, benchmark testing was performed to test both the new shielding transport capabilities and the new data libraries. As a result, the initial series of benchmark calculations have been used to compare the previous SCALE 5.1 Shielding Analysis Sequence Number 4 (SAS4) shielding sequence with the new MAVRIC sequence in SCALE 6. The SAS4-MAVRIC comparisons are used to verify the new transport capability relative to the previous SAS4 capability. These comparison calculations were performed using the ENDF/B-VI.8 coupled library. Because of this, the SAS4-MAVRIC calculations serve to verify the new shielding capability with the ENDF/B-VI.8 library. After the SAS4-MAVRIC comparisons, the ENDF/B-VI.8 and ENDF/B-VII.0 libraries are used with MAVRIC for benchmark calculations to validate the performance of MAVRIC and the ENDF/B-VI.8 and ENDF/B-VII.0 libraries.

3.1 SAS4 and MAVRIC Benchmark Comparison Calculations with ENDF/B-VI.8 Library

The new ENDF/B-VI.8 200 neutron group and 47 gamma group shielding library was tested by benchmarking the computational results against the results obtained with the previous SCALE shielding library, which was ENDF/B-IV with 27 neutron and 18 gamma groups. The computational results with the new library were also benchmarked against experimental measurements. The computations were performed using both the SAS4 and MAVRIC sequences of SCALE. SAS4 uses MORSE to perform Monte Carlo radiation transport along with XSDRN to create 1-D biasing parameters. MAVRIC uses Monaco to perform the Monte Carlo radiation transport and Denovo to create 3-D biasing parameters. Three sets of experimental measurements were selected for comparison purposes. All three consist of dose measurements on the outer surface of fully loaded spent nuclear fuel storage casks. Where feasible, SAS4 in the SCALE 5.1 release was used to model these storage casks with the new ENDF/B-VI.8 and the old ENDF/B-IV shielding libraries. MAVRIC, which is to be released as part of the SCALE 6 package, was also used to model each of these casks with the ENDF/B-VI.8 and ENDF/B-IV shielding libraries. Details about the storage casks, measurements, and previous validation calculations with SCALE 4.3 can be found in EPRI report TR-104329 (Ref. 7). A brief summary of the current verification and validation calculations for each cask and the computational results are presented in the following sections.

3.1.1 Cask descriptions

3.1.1.1 CASTOR-V/21

The CASTOR (CAsk for Storage and Transport Of Radioactive material) cask was developed by Gesellschaft für Nuklear Service. This cask consists of a cast-iron body, and is 4.9 m tall and 2.4 m in diameter. Two concentric rows of polyethylene rods are incorporated in the cask wall to provide neutron shielding. The external surface consists of heat transfer fins oriented circumferentially around the cask surface. The fuel basket is configured to hold 21 pressurized water reactor (PWR) spent fuel assemblies and is constructed of stainless steel and borated stainless steel. The vertical and horizontal 2-D slices of the CASTOR geometry, as represented in Monaco using the SCALE Generalized Geometry Package (SGGP) are shown in Fig. 3.1. The green and pink rectangles and squares in Fig. 3.1 represent the homogenized fuel assemblies. The red regions in Fig. 3.1 above and below the fuel assemblies represents the end fittings where the ^{60}Co activation sources are located.

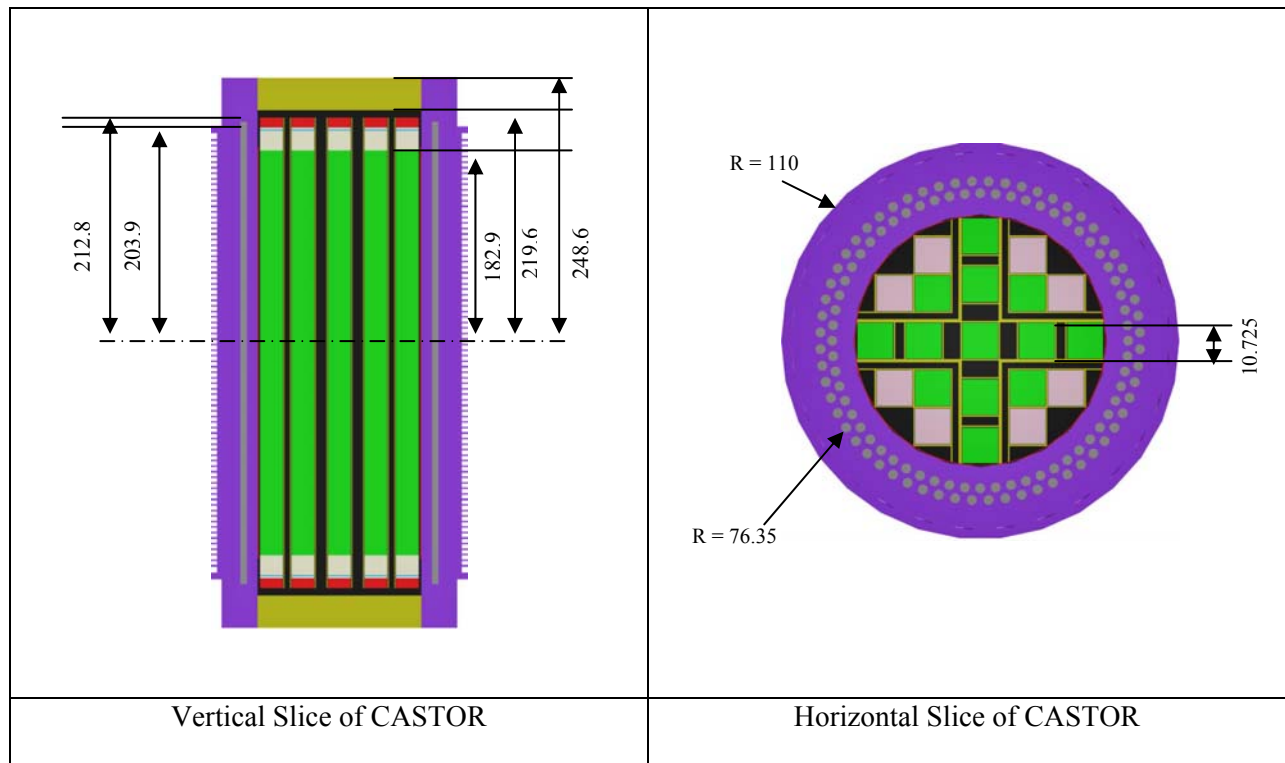


Fig. 3.1 Views of cask for storage and transport of radioactive material (CASTOR). (Dimensions in centimeters.)

3.1.1.2 Westinghouse MC-10

The Westinghouse MC-10 PWR spent fuel cask consists of a forged steel body. The cask is 4.8 m tall and 2.7 m in diameter. Neutron shielding is provided by a layer of BISCO NS-3 on the outside of the cask. The fuel basket is configured to hold 24 PWR spent fuel assemblies and is constructed of aluminum. Each of the 24 basket locations contains a removable stainless steel enclosure and neutron poison material for criticality control. Figure 3.2 shows 2-D slices of the MC-10 geometry as represented in Monaco using SGGP. The green and magenta rectangles and squares in Fig. 3.2 represent the homogenized fuel assemblies. The red regions above and below the fuel assemblies in Fig. 3.2 represents the end fittings where the ^{60}Co activation sources are located.

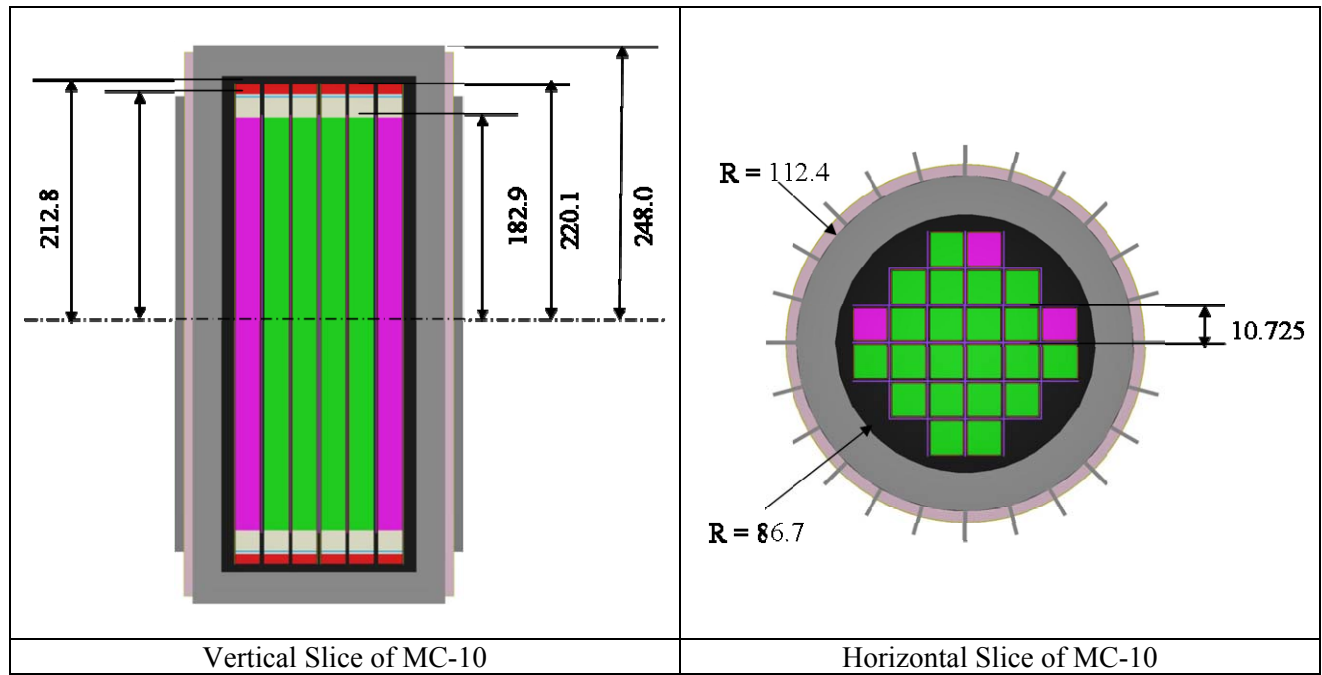


Fig. 3.2 Views of MC-10 cask. (Dimensions in centimeters.)

3.1.1.3 TN-24P

The TN-24P cask was developed by Transnuclear, Inc. The TN-24P cask also has a forged steel body, but is surrounded by a thin layer of resin enclosed in a steel outer shell. The resin is for neutron shielding. The TN-24P cask is 5 m tall and 2.3 m in diameter. The fuel basket will also hold 24 PWR spent fuel assemblies and is constructed of aluminum and boron plates. The vertical and horizontal 2-D slices of the TN-24P geometry, as represented in Monaco using the standard KENO-VI geometry package, are shown in Fig. 3.3. The dark blue and aquamarine rectangles and squares in Fig. 3.3 represent the homogenized fuel assemblies. The light blue above and below the fuel assemblies in Fig. 3.3 represents the end fittings where the ^{60}Co activation sources are located.

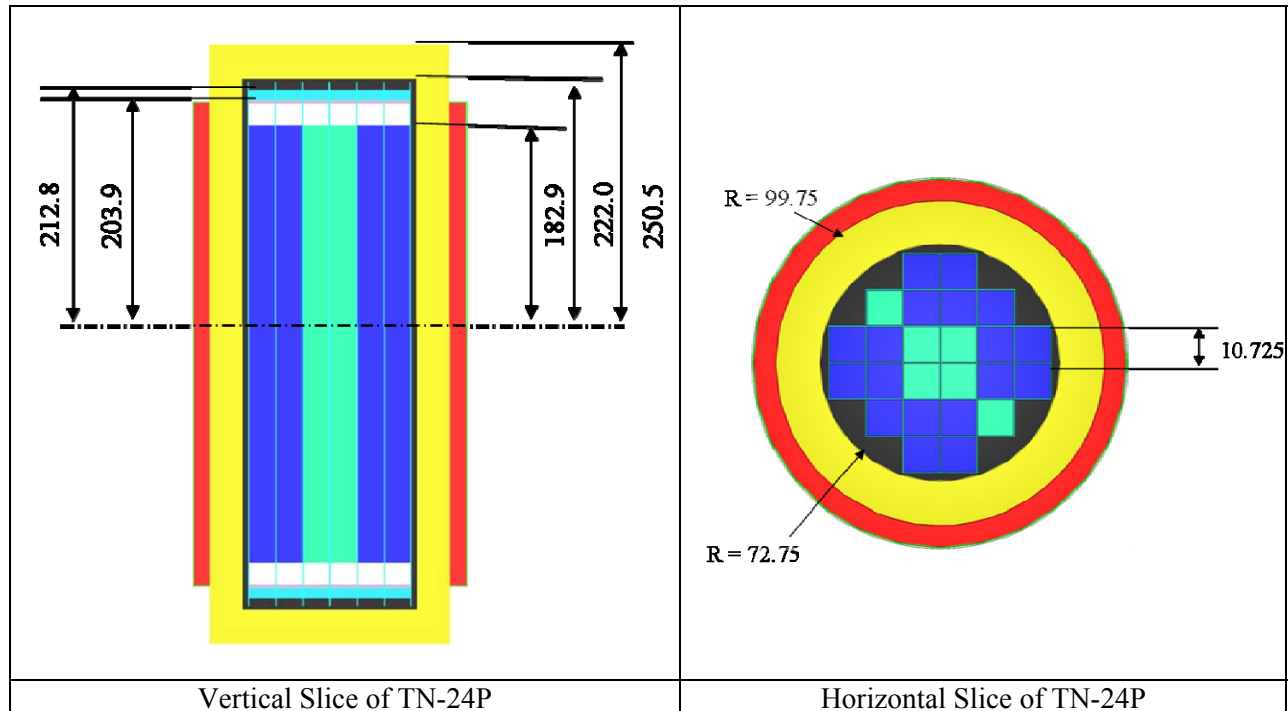


Fig. 3.3 Views of TN-24P cask. (Dimensions in centimeters.)

3.1.2 Calculations

Each cask was loaded with spent Westinghouse 15×15 fuel assemblies. The initial enrichment, burnup, and cooling times for all the fuel assemblies are described in Ref. 7. For the calculations with the ENDF/B-IV shielding library, the neutron and gamma sources from the spent fuel in the previous SCALE 4.3 SAS4 calculations were used. For the ENDF/B-VI.8 library, the data from Ref. 7, which described the life of the spent fuel assemblies, were entered into OrigenArp, and the neutron and photon sources from the spent fuel were calculated using the ENDF/B-VI.8 shielding library group structure. The version of OrigenArp that was used in this process is the version that was released with SCALE 5.1. The previous SCALE 4.3 SAS4 calculations most likely used the version of ORIGEN-S that was released with SCALE 4.3 to create the spent fuel sources, so this could be one source of differences in comparison of old and new calculated results. Similarly, the ^{60}Co sources previously used in the SCALE 4.3 SAS4 calculations were used again with the ENDF/B-IV library. For the ENDF/B-VI.8 shielding library, the 27 neutron-18 gamma group structure was converted to the new 200 neutron-47 gamma group structure. In this conversion, energy was conserved rather than number of particles.

Dose measurements were made at several different points on the top, bottom, and radial (near the fuel midplane) surfaces of each cask. SAS4 calculates dose averaged over a surface that represents the average of the measurements made at the different points on the surfaces of each cask. However, in the current version, Monaco does not yet have the capability of tallying on a surface. Therefore, very thin (1 mm thick) volume tallies were used instead of surface tallies. For the side or radial doses, the averaging surface is an outside cask surface (either the fin tips or the cask body) with an extent corresponding to the middle half of the fuel height. This is similar to the measurements made in Ref. 7. The top and bottom doses are on the top and bottom surfaces respectively, with radii also similar to those used in Ref. 7. These similarities allow for a more direct comparison between the calculations and experimental measurements.

SAS4 requires that the cask model be symmetric around the fuel midplane, so the geometries for the top and bottom doses vary slightly above and below the active fuel region. Since this variation is very small, either the top or bottom geometry could be used to calculate the radial doses. Therefore, the Monaco geometries were also modeled symmetric about the fuel midplane, instead of using the actual geometries, to be consistent with the SAS4 simulations. The source types referred to in Table 3.1, Table 3.3, and Table 3.5 are all spent fuel assemblies, except for Co source type, which is a ^{60}Co activation source. The same nomenclature as in Ref. 7 is used in this report to designate source or spent fuel assembly types. The full details about each spent fuel assembly and ^{60}Co source are given in Ref. 7, Section 3.

3.1.2.1 Computational results

The input summary for each cask and the computed results using MAVRIC and SAS4, where available, with the ENDF/B-VI.8 and ENDF/B-IV shielding cross sections are presented in the following tables. The computational results were benchmarked against measurements as well, and the results are presented at the end of this section.

Table 3.1 summarizes the geometry, source type, tally location, and particle type tallied for all the different TN-24P cask calculations.

Table 3.1 TN-24P calculations input summary

Case number	Filename	Geometry	Source type	Tally location	Particle tallied
1	out22.t24	Bottom	W	Bottom	Gamma
2	out24.t24	Bottom	V	Bottom	Gamma
3	out12.t24	Bottom	W	Radial	Gamma
4	out14.t24	Bottom	V	Radial	Gamma
5	out5.t24	Bottom	Co	Bottom	Gamma
6	out7.t24	Top	Co	Top	Gamma
7	out8.t24	Top	Co	Top	Gamma
8	out16.t24	Top	W	Top	Gamma
9	out18.t24	Top	V	Top	Gamma
10	out21.t24	Bottom	W	Bottom	Neutron
11	out23.t24	Bottom	V	Bottom	Neutron
12	out11.t24	Bottom	W	Radial	Neutron
13	out13.t24	Bottom	V	Radial	Neutron
14	out15.t24	Top	W	Top	Neutron
15	out17.t24	Top	V	Top	Neutron

The computational results for TN-24P casks, using SAS4 in SCALE 5.1 and MAVRIC, with the ENDF/B-VI.8 and ENDF/B-IV libraries are presented in Table 3.2.

Table 3.2 The computational results for TN24P casks

Case no.	SAS4 SCALE 5.1 (ENDF/B-IV)		MAVRIC (ENDF/B-IV)		SAS4 SCALE 5.1 (ENDF/B-VI.8)		MAVRIC (ENDF/B-VI.8)	
	Dose rate (rem/h)	1 σ	Dose rate (rem/h)	1 σ	Dose rate (rem/h)	1 σ	Dose rate (rem/h)	1 σ
1	9.200E-03	0.017	9.800E-03	0.034	4.600E-03	0.017	4.900E-03	0.015
2	3.900E-03	0.016	4.000E-03	0.034	1.900E-03	0.017	2.000E-03	0.025
3	2.880E-02	0.017	2.840E-02	0.029	1.560E-02	0.020	1.420E-02	0.035
4	6.400E-03	0.025	5.700E-03	0.027	3.000E-03	0.023	2.900E-03	0.031
5	9.880E-02	0.007	9.690E-02	0.022	7.230E-02	0.008	7.180E-02	0.023
6	3.140E-02	0.006	3.120E-02	0.019	2.240E-02	0.007	2.200E-02	0.024
7	5.100E-03	0.009	5.100E-03	0.020	3.500E-03	0.010	3.500E-03	0.042
8	1.400E-03	0.020	1.300E-03	0.028	7.000E-04	0.015	7.000E-04	0.017
9	6.000E-04	0.039	5.000E-04	0.022	3.000E-04	0.018	3.000E-04	0.026
10	4.520E-02	0.012	4.920E-02	0.005	5.410E-02	0.011	5.800E-02	0.007
11	2.320E-02	0.012	2.490E-02	0.004	2.720E-02	0.012	2.950E-02	0.005
12	1.100E-03	0.008	1.100E-03	0.007	1.400E-03	0.009	1.300E-03	0.007
13	4.000E-04	0.008	4.000E-04	0.008	4.000E-04	0.008	4.000E-04	0.006
14	2.020E-02	0.012	1.850E-02	0.008	2.230E-02	0.015	2.040E-02	0.017
15	9.900E-03	0.013	8.900E-03	0.009	1.040E-02	0.015	9.500E-03	0.008

The ratio of the computed values using the new (ENDF/B-VI.8, 200 neutron and 47 gamma groups) and old (ENDF/B-IV, 27 neutron and 18 gamma groups) shielding libraries for all the TN-24P cask calculations are shown in Fig. 3.4. The corresponding geometries and source types for the case numbers were described in Table 3.1. In these figures red and blue points represent the computed ratios using SAS4 in SCALE 5.1 and MAVRIC, respectively. The error bars represent two sigma values.

As can be seen from the figures, the computed ratios using SAS4 in SCALE 5.1 and MAVRIC are in good agreement, within statistical fluctuations, for all tallies. Therefore, both codes show similar behavior when the same libraries are used. Furthermore, the ratios are above 1 (from a few percent up to 30%) for all the neutron tallies and below 1 (20% to 50%) for all the gamma tallies for both codes in a very consistent way. However, there are substantial differences in the response values computed with the two different versions of ENDF data.

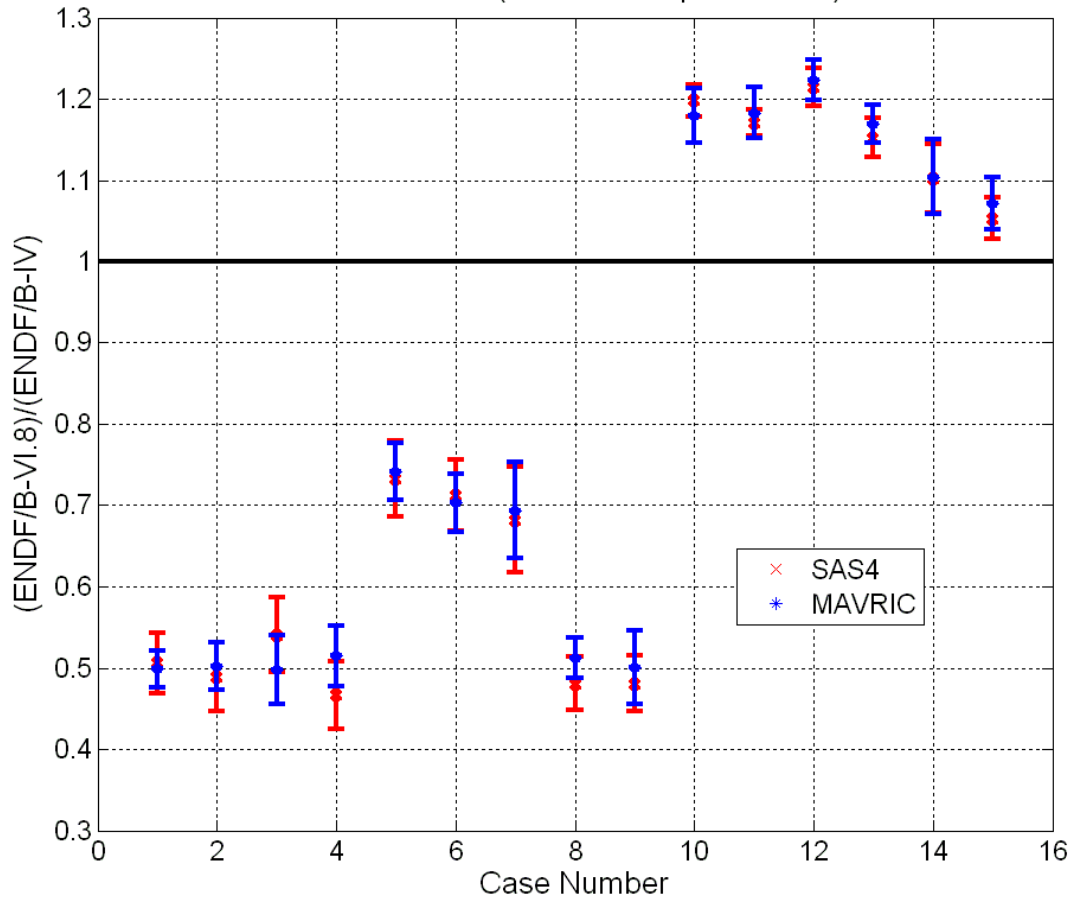


Fig. 3.4 The ratio of the computed TN-24P cask tallies using the ENDF/B-VI.8 and ENDF/B-IV shielding cross sections. The red and blue points represent the computed ratios using SAS4 in SCALE 5.1 and MAVRIC, respectively. The error bars represent two standard deviations.

For code comparison, the ratios of the computed values using MAVRIC and SAS4 in SCALE 5.1 with both the ENDF/B-VI.8 and ENDF/B-IV shielding libraries, for the results in Table 3.2, are shown in Fig. 3.5. As can be seen from the figures, the two codes are in agreement within $\pm 20\%$.

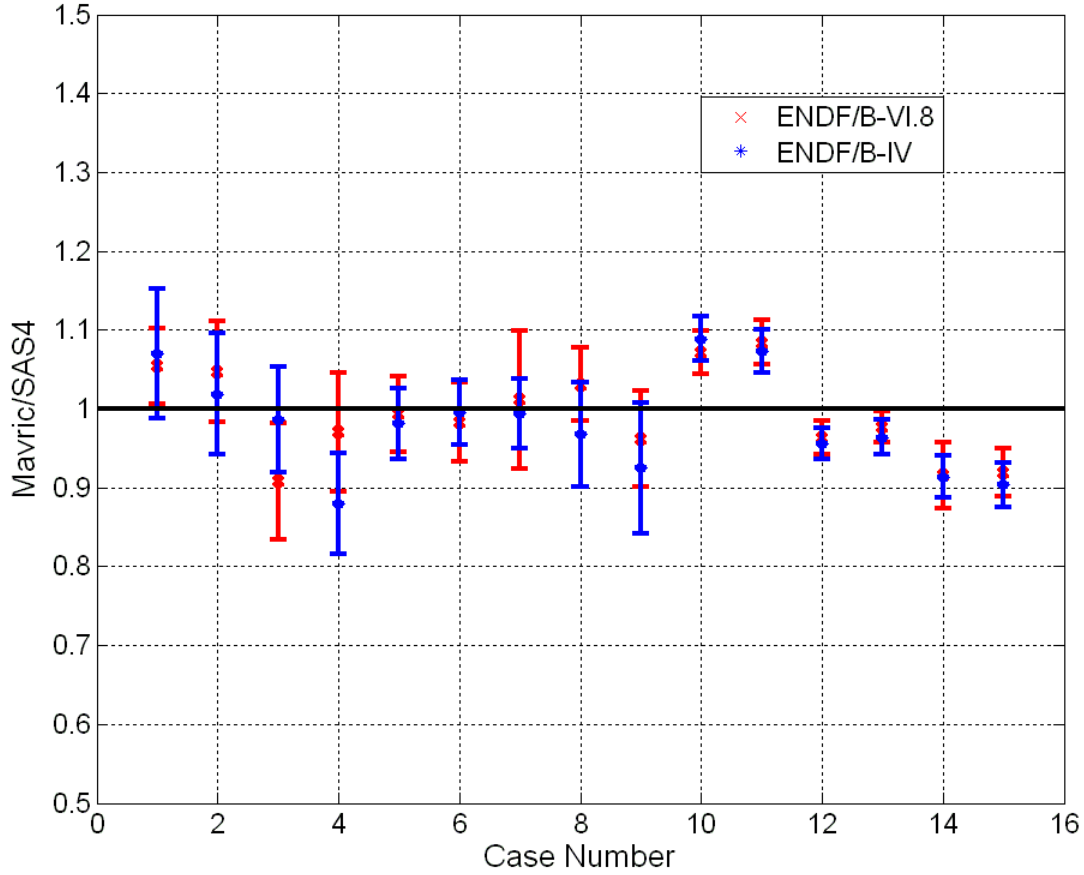


Fig. 3.5 The ratios of the computed TN-24P cask tallies using MAVRIC and SAS4. In this figure, the red and blue points represent the computed ratios using the ENDF/B-VI.8 (new) and ENDF/B-IV (old) cross sections, respectively. The error bars represent two standard deviations.

The geometry, source type, tally location, and particle type tallied for all the different MC-10 cask calculations are summarized in Table 3.3.

Table 3.3 Westinghouse MC-10 calculations input summary

Case number	Filename	Geometry	Source type	Tally location	Particle tallied
1	mcbtmg1	Bottom	W	Bottom	Gamma
2	mcbtmg2	Bottom	R	Bottom	Gamma
3	mcbtmg3	Bottom	N	Bottom	Gamma
4	mcradg1	Top	W	Radial	Gamma
5	mcradg2	Top	R	Radial	Gamma
6	mcradg3	Top	N	Radial	Gamma
7	mctopg1	Top	W	Top	Gamma
8	mctopg2	Top	R	Top	Gamma
9	mctopg3	Top	N	Top	Gamma
10	mcbtmc1	Bottom	Co	Bottom	Gamma
11	mcbtmc2	Bottom	Co	Bottom	Gamma
12	mcbtmc3	Bottom	Co	Bottom	Gamma
13	mctopc1	Top	Co	Top	Gamma
14	mctopc2	Top	Co	Top	Gamma
15	mcbtmn1	Bottom	R	Bottom	Neutron
16	mcbtmn2	Bottom	N	Bottom	Neutron
17	mcradn1	Top	R	Radial	Neutron
18	mcradn2	Top	N	Radial	Neutron
19	mctopn1	Top	R	Top	Neutron
20	mctopn2	Top	N	Top	Neutron

The computational results for MC-10 casks using MAVRIC with the ENDF/B-IV and ENDF/B-VI.8 shielding libraries and their ratios are presented in Table 3.4.

Table 3.4 The computational results for MC-10 casks

Case no.	MAVRIC (ENDF/B-IV)		MAVRIC (ENDF/B-VI.8)		Ratio
	Dose rate (rem/h)	1 σ	Dose rate (rem/h)	1 σ	
1	2.278E-04	0.034	1.971E-04	0.04	0.865
2	7.194E-04	0.031	4.689E-04	0.04	0.652
3	2.076E-03	0.029	1.188E-03	0.02	0.572
4	1.129E-02	0.063	1.008E-02	0.07	0.894
5	2.038E-02	0.044	1.522E-02	0.07	0.747
6	2.638E-03	0.059	1.537E-03	0.08	0.582
7	8.393E-05	0.034	7.022E-05	0.03	0.837
8	1.964E-04	0.024	1.281E-04	0.04	0.652
9	3.448E-04	0.055	2.229E-04	0.03	0.647
10	4.468E-02	0.013	3.249E-02	0.01	0.727
11	7.308E-03	0.023	4.830E-03	0.03	0.661
12	4.001E-02	0.009	2.854E-02	0.01	0.713
13	3.675E-03	0.018	2.451E-03	0.02	0.667
14	1.584E-02	0.021	1.177E-02	0.02	0.743
15	1.732E-03	0.040	1.485E-03	0.01	0.857
16	1.716E-03	0.034	1.558E-03	0.01	0.908
17	1.507E-02	0.023	1.608E-02	0.01	1.067
18	6.390E-03	0.019	6.308E-03	0.01	0.987
19	1.766E-02	0.007	1.535E-02	0.01	0.869
20	1.257E-02	0.008	1.084E-02	0.01	0.862

The ratio of the computed values using MAVRIC with the ENDF/B-VI.8 and ENDF/B-IV shielding libraries for all the MC-10 cask tallies are shown in Fig. 3.6. The corresponding geometries and source types for the case numbers were described in Table 3.3. In these figures, the error bars represent two sigma values.

As can be seen from the figures, the ratios are below 1 (20% to 60%) for all the gamma tallies, as they were for the TN-24P casks.

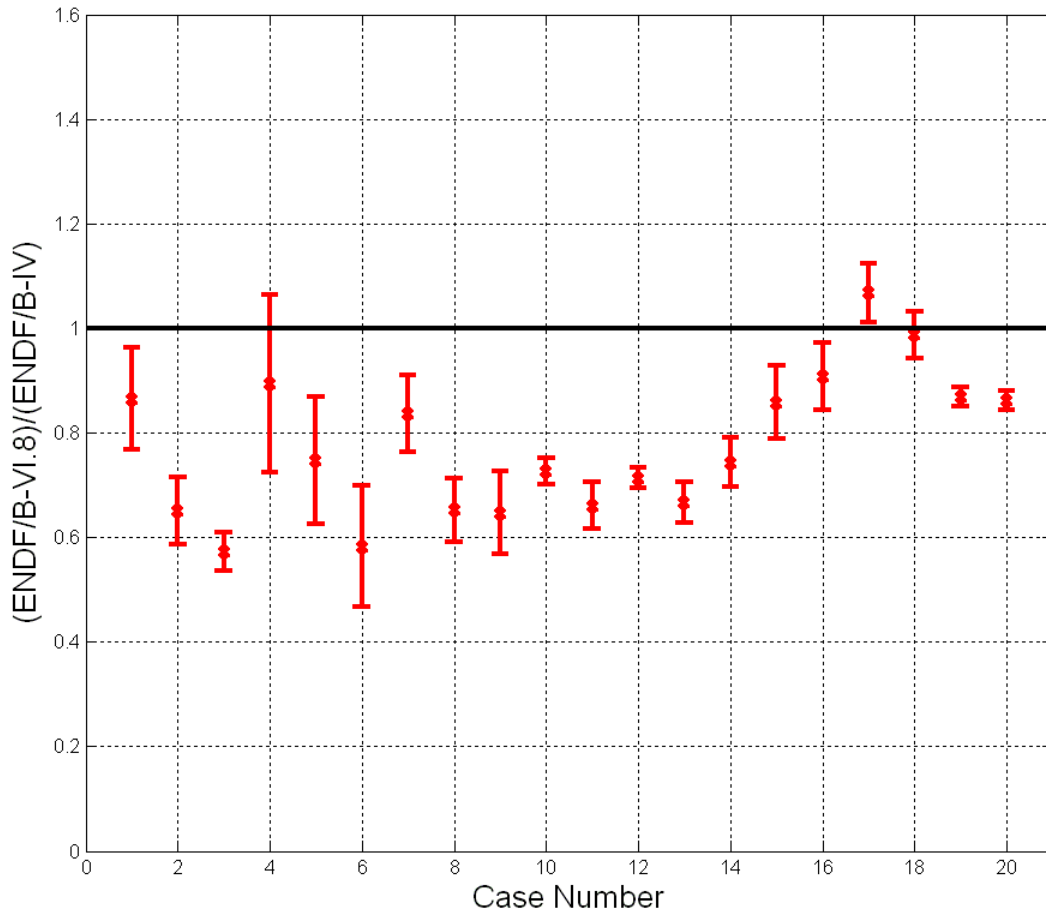


Fig. 3.6 The ratio of the computed MC-10 cask values using the ENDF/B-VI.8 and ENDF/B-IV shielding cross-section libraries with MAVRIC.

The geometry, source type, tally location, and particle type tallied for all the different CASTOR cask calculations are summarized in Table 3.5.

Table 3.5 CASTOR-V/21 calculations input summary

Case number	Filename	Geometry	Source type	Tally location	Particle tallied
1	c21bg1	Bottom	V-15	Bottom	Gamma
2	c21bg2	Bottom	T	Bottom	Gamma
3	c21rg1	Top	V-15	Radial	Gamma
4	c21rg2	Top	T	Radial	Gamma
5	c21tg1	Top	V-15	Top	Gamma
6	c21tg2	Top	T	Top	Gamma
7	c21bc1	Bottom	Co	Bottom	Gamma
8	c21tc1	Top	Co	Top	Gamma
9	c21tc2	Top	Co	Top	Gamma
10	c21bn2	Bottom	T	Bottom	Neutron
11	c21rn1	Top	V-15	Radial	Neutron
12	c21rn2	Top	T	Radial	Neutron
13	c21tn1	Top	V-15	Top	Neutron
14	c21tn2	Top	T	Top	Neutron

The computational results for CASTOR casks using MAVRIC with the ENDF/B-VI.8 and ENDF/B-IV shielding libraries and their ratios are presented in Table 3.6.

Table 3.6 The computational results for CASTOR casks

Case no.	MAVRIC (ENDF/B-IV)		MAVRIC (ENDF/B-VI.8)		Ratio
	Dose rate (rem/h)	1 σ	Dose rate (rem/h)	1 σ	
1	1.368E-03	0.038	8.309E-04	0.024	0.607
2	4.309E-03	0.026	2.399E-03	0.016	0.557
3	5.710E-02	0.041	3.528E-02	0.026	0.618
4	1.350E-02	0.035	6.941E-03	0.020	0.514
5	6.306E-04	0.050	3.931E-04	0.032	0.623
6	1.839E-03	0.043	1.058E-03	0.026	0.575
7	1.738E-02	0.024	1.164E-02	0.026	0.669
8	2.951E-03	0.049	2.022E-03	0.057	0.685
9	1.654E-02	0.039	1.230E-02	0.047	0.744
10	2.964E-02	0.020	3.402E-02	0.027	1.148
11	3.744E-03	0.012	6.763E-03	0.010	1.807
12	4.020E-03	0.012	5.985E-03	0.011	1.489
13	2.065E-02	0.045	3.009E-02	0.029	1.457
14	2.396E-02	0.024	3.027E-02	0.030	1.263

The ratio of the computed values using MAVRIC with the ENDF/B-VI.8 and ENDF/B-IV shielding libraries for all the CASTOR cask tallies are shown in Fig. 3.7. The corresponding geometries and source types for the case numbers were described in Table 3.5. In these figures, the error bars represent two sigma values.

As can be seen from the figures, the ratios are above 1 (up to 80%) for all the neutron tallies and below 1 (up to 50%) for all the gamma tallies.

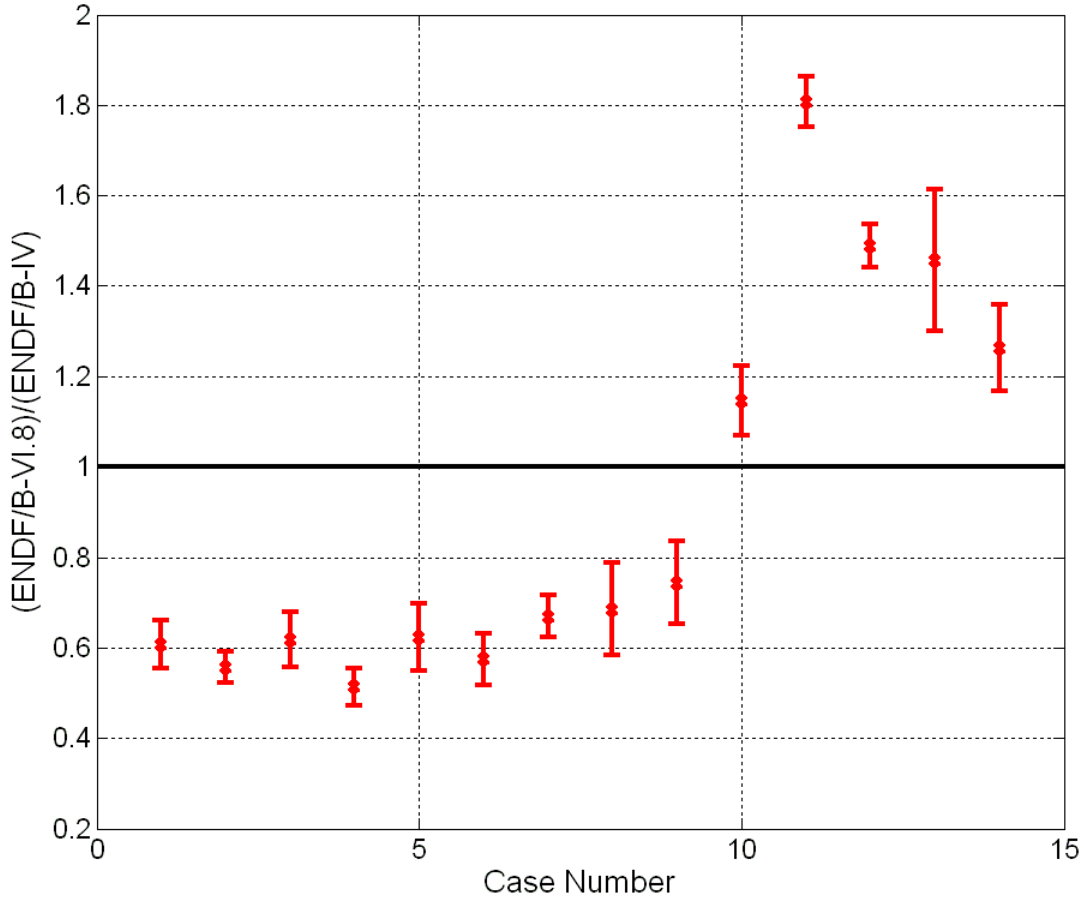


Fig. 3.7 The ratio of the computed CASTOR cask values using the ENDF/B-VI.8 and ENDF/B-IV shielding cross-section libraries with MAVRIC.

3.1.2.2 Benchmark against experimental measurement

The computational results using MAVRIC with both shielding libraries were benchmarked against the measured data points. The measured, computed (using both the ENDF/B-VI.8 and ENDF/B-IV libraries), and the ratio of computed to measured (C/M) data for neutron cases are presented in Table 3.7. The C/M ratios for the neutron cases for both the ENDF/B-VI.8 and ENDF/B-IV shielding libraries are plotted in Fig. 3.8.

As shown in Table 3.7 and Fig. 3.8, overall the computed values using the ENDF/B-VI.8 shielding library are higher than the values computed using the ENDF/B-IV shielding library. There is better agreement with the measured values using the ENDF/B-VI.8 library for cases 8 and 9. Since the uncertainties in the measured values are not available, it is not clear whether the change in the ratios is within the statistical uncertainty.

Table 3.7 The measured and computed neutron dose rates and the ratio of computed to measured (C/M) dose rates for each cask model

Case no.	Cask type	Geometry	Meas. (mrem/h)	ENDF/B-IV (mrem/h)	ENDF/B-VI.8 (mrem/h)	C/M ENDF/B-IV	C/M ENDF/B-VI.8
1	TN24	Bottom	57.90	74.09	87.48	1.28	1.51
2		Side	2.80	1.45	1.76	0.52	0.63
3		Top	28.50	27.37	29.93	0.96	1.05
4	MC10	Bottom	4.60	3.45	3.04	0.75	0.66
5		Side	19.60	21.46	22.39	1.09	1.14
6		Top	56.70	40.22	46.18	0.71	0.81
7	CASTOR	Bottom	51.30	56.65	68.70	1.10	1.34
8		Side	11.40	7.76	12.75	0.68	1.12
9		Top	51.50	44.61	60.35	0.87	1.17

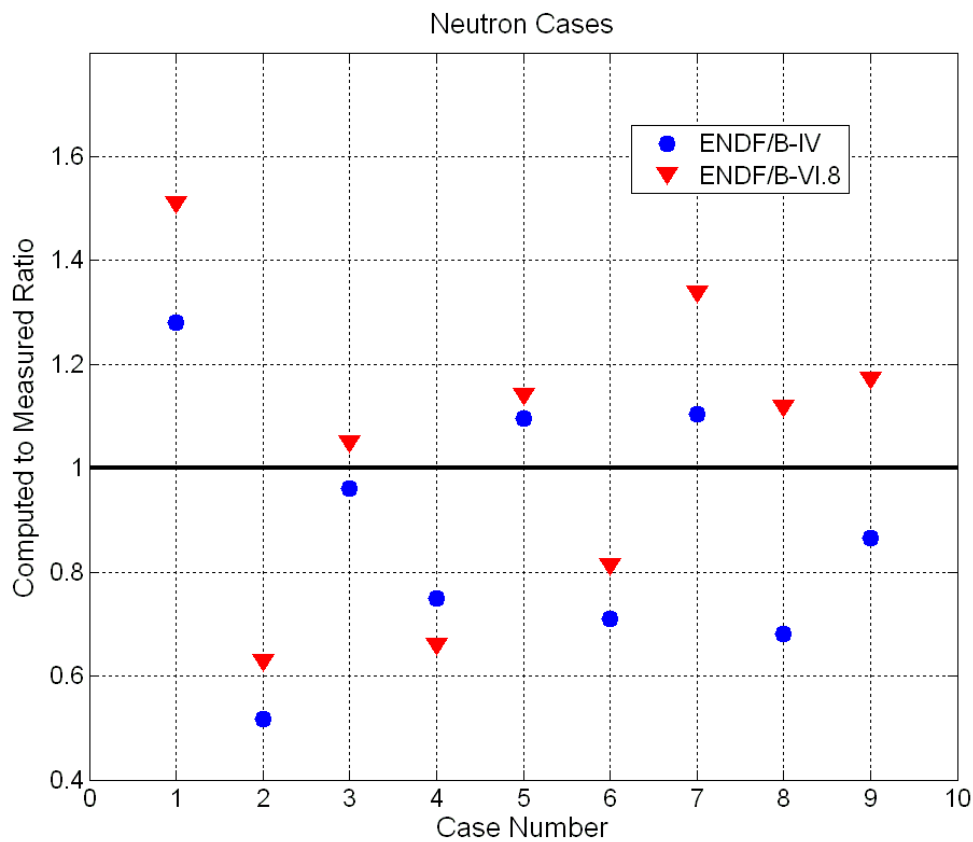


Fig. 3.8 The ratio of the computed to measured values using MAVRIC with the ENDF/B-VI.8 (new) and ENDF/B-IV (old) libraries for the neutron dose rates.

The measured, computed (using both the ENDF/B-VI.8 and ENDF/B-IV shielding libraries), and C/M ratio data for the gamma cases are presented in Table 3.8. The C/M ratios for these cases for both the ENDF/B-VI.8 and ENDF/B-IV shielding libraries are plotted in Fig. 3.9. As presented in the table and figure, for the gamma cases, the computed values using the ENDF/B-VI.8 shielding library are lower than the values computed using the ENDF/B-IV shielding library. This trend was investigated further and found to be consistent with a neglect of coherent scattering at relatively low photon energies in the older library. Indeed it appears that the older library used gamma data that preceded ENDF/B-IV. The newer library has a much stronger theoretical basis. There is better agreement with the measured values using the ENDF/B-VI.8 library for case 6, and for cases 2, 5, and 8 even though the discrepancies for these cases are still between 40 and 50%. However for cases 1, 3, 4, 7, and 9, the agreement with the measured data was better with the ENDF/B-IV shielding library. Since the uncertainties in the measured values are not available, it is not clear whether the change in the ratios is within the experimental uncertainty.

Table 3.8 The measured and computed gamma dose rates and the ratio of the computed to measured (C/M) dose rates for each cask model

Case no.	Cask type	Geometry	Meas. (mrem/h)	ENDF/B-IV (mrem/h)	ENDF/B-VI.8 (mrem/h)	C/M ENDF/B-IV	C/M ENDF/B-VI.8
1	TN24	Bottom	117.0	110.68	88.73	0.95	0.76
2		Side	12.3	34.11	17.08	2.77	1.39
3		Top	37.9	38.17	26.44	1.01	0.70
4	MC10	Bottom	62.0	55.03	67.70	0.89	1.09
5		Side	21.4	34.30	26.85	1.60	1.25
6		Top	14.6	20.14	14.64	1.38	1.00
7	CASTOR	Bottom	24.5	23.06	14.86	0.94	0.61
8		Side	30.2	70.60	42.22	2.34	1.40
9		Top	38.4	21.96	15.77	0.57	0.41

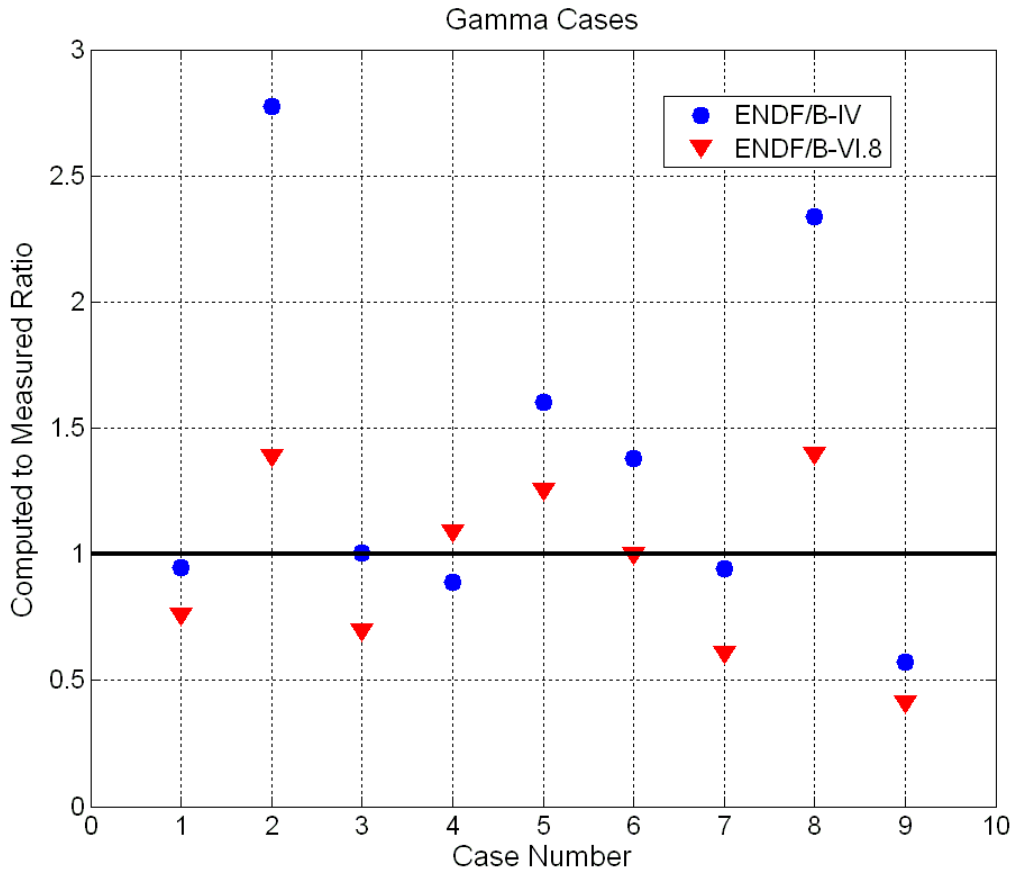


Fig. 3.9 The ratio of the computed to measured values using MAVRIC with the ENDF/B-VI.8 (new) and ENDF/B-IV (old) shielding libraries for the gamma dose rates.

3.2 MAVRIC Benchmark Calculations Using ENDF/B-VI.8 and ENDF/B-VII.0 Libraries

3.2.1 Neutron fields in three-section concrete labyrinth from ^{252}Cf source

3.2.1.1 Benchmark overview

Experimental measurements of the neutron flux from a ^{252}Cf source through an 18 m concrete labyrinth were made in Russia in 1982 to obtain benchmark data for code validation.⁸

Two sources were used: (1) a bare ^{252}Cf neutron source and (2) a ^{252}Cf neutron source encased in a polyethylene sphere.

Six labyrinths were constructed.

1. Empty, three-section labyrinth.
2. First corner is lined with polyethylene plates covered with cadmium.
3. First corner is lined with polyethylene plates without cadmium.
4. Two corners are lined with borated concrete.
5. Two polyethylene plates are installed in the second leg of the labyrinth (bare source only).

6. Dead end at the end of the first leg of the labyrinth.

Seven Bonner sphere detectors [with ${}^6\text{Li}(\text{Eu})$ crystal] were used.

1. 2 in. diameter, cadmium covered
2. 3 in. diameter, cadmium covered
3. 5 in. diameter, cadmium covered
4. 5 in. diameter, not covered
5. 8 in. diameter, cadmium covered
6. 10 in. diameter, cadmium covered
7. 12 in. diameter, cadmium covered.

The geometry of the labyrinth is shown in Fig. 3.10.

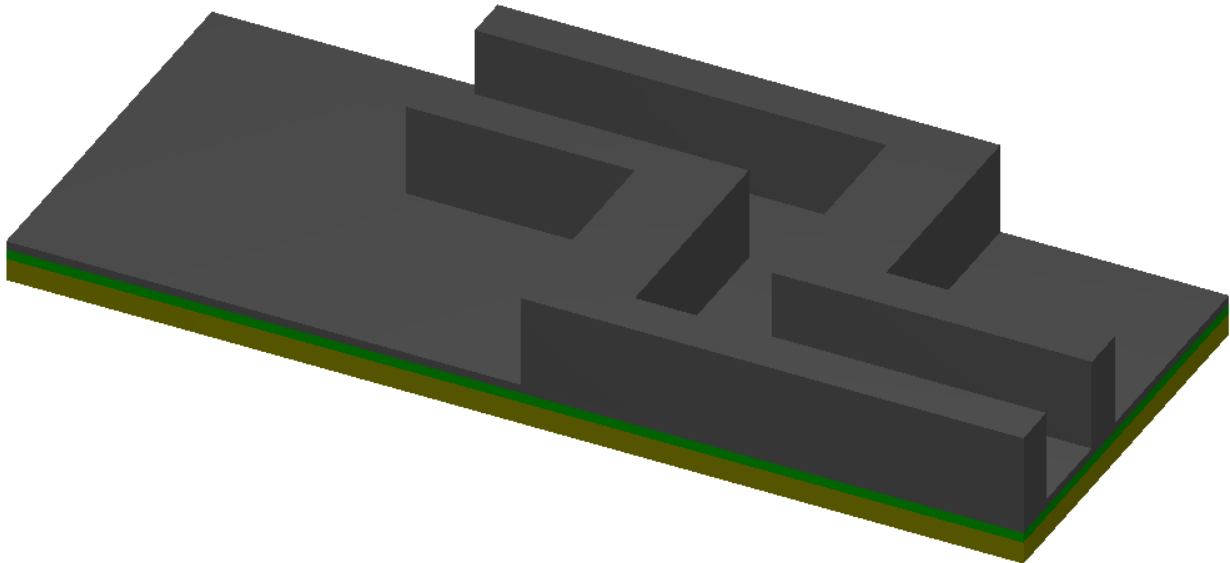


Fig. 3.10 Cutaway view of labyrinth model (ceiling removed).

As part of the study in Ref. 8, benchmark calculations were performed with Monte Carlo N-particle (MCNP) code. Calculations were done in two steps: (1) the determination of the detector response in a free-field and (2) the transport of neutrons through the labyrinth, where computed fluxes were convolved with the response functions.

3.2.1.2 Monaco/MAVRIC calculations

Monaco and MAVRIC and the new ENDF/B-VI.8 200 neutron-47 gamma shielding library were used to compute the detector count rates measured by the various detectors for the first labyrinth design (empty, three section) using both the covered and uncovered californium (${}^{252}\text{Cf}$) source. Calculations followed the benchmark instructions and were done in two steps.

1. Determination of the detector response function using Monaco—for each energy group, a Monaco calculation was done to find the integrated product of the ${}^6\text{Li}(n,t){}^4\text{He}$ cross section and neutron flux

inside the crystal of the detector (Fig. 3.11). Monaco calculations were done for each energy group (200) incident on each detector (7).

- MAVRIC, using the FW-CADIS method, was used to calculate neutron fluxes along the path through the labyrinth. FW-CADIS performs a quick forward discrete ordinates calculation and a quick adjoint discrete ordinates calculation to create an importance map and biased source distribution that, when used with Monaco, will give results for multiple tallies with nearly uniform statistical uncertainty. Each FW-CADIS calculation is optimized for a specific source and response, so calculations had to be done for each source (2) using each detector size (7).

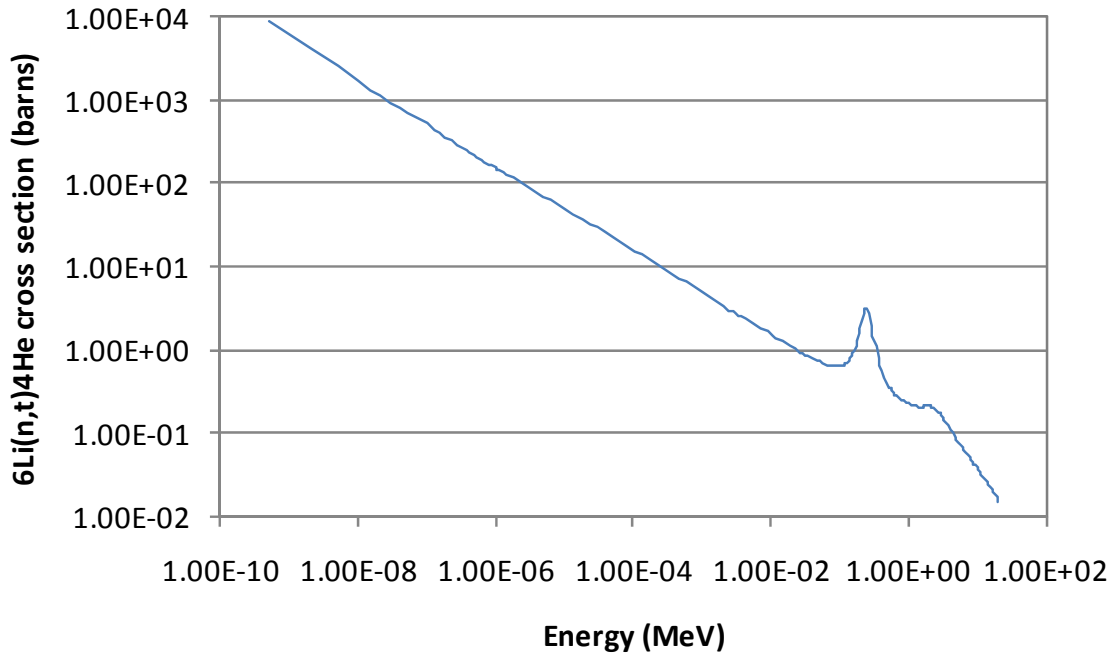


Fig. 3.11 ${}^6\text{Li}(n,t){}^4\text{He}$ cross section from the ENDF/B VI.8 200n/47g shielding library.

3.2.1.3 Detector response functions

Seven Bonner spheres were used to measure the neutron flux through the labyrinths. Sizes were 2-, 3-, 5-, 8-, 10- and 12-inch diameters. Each was made of polyethylene ($\rho=0.92\pm 0.03 \text{ g/cm}^3$) with an 0.08-cm-thick cadmium layer ($\rho= 8.648 \text{ g/cm}^3$). One other detector, 5 inches in diameter, had no cadmium cover. The crystal was a ${}^6\text{LiI}(\text{Eu})$ cylinder, 1 cm in diameter and 1 cm high ($\rho=4.08 \text{ g/cm}^3$), with a lithium enrichment of 90 at. %.

The benchmark model used by the experimental team for making detector response functions left out the europium content (since it was less than 0.3 wt %). Source particles were started on the surface of a sphere with radius=160 cm, pointed inward striking the outer sphere of the detector model. The model of the detector is shown in Figure 20 of Ref. 8.

The Monaco model of the detector was a spherically symmetric model and included the following layers (outward, from center):

- 0.57235712 cm of LiI (to maintain volume of 0.7853982 cm³),
- 0.05 cm of TiO₂,
- 0.03 cm of aluminum D16,
- 0.07 cm of void,
- 0.10 cm of aluminum D16,
- 0.05 cm of void, and
- polyethylene of the detector and its optional 0.08 cm cadmium cover.

For a detector response function, what is needed is the total number of ⁶Li(n,t)⁴He reactions occurring in the crystal (radius R_c) per unit flux for monoenergetic source neutrons. The count rate $C(E)$ for incident neutrons of energy E is

$$C(E) = N_{6Li} V \int \sigma_{n,t}(E') \phi(E') dE' , \quad (3.1)$$

for a source strength S scaled such that the flux in an empty sphere the same size as the Bonner sphere (radius R_D) is unity. (This gives $S = \pi R_D^2$.)

$$C(E) = \left(\frac{1.66072 \times 10^{-2}}{b \text{ cm}} \right) \left(\frac{4\pi}{3} R_c^3 \right) \int \sigma_{n,t}(E') \phi(E') dE' . \quad (3.2)$$

The volume of the crystal is $\frac{4\pi}{3} R_c^3 = 0.7853982 \text{ cm}^3$.

For each detector (7), a series of 200 Monaco calculations were done (about 18 minutes each), and the responses for each incident neutron energy were determined as described above. As can be seen in Figs. 3.12–3.18, the computed detector response functions were similar to the response functions computed by MCNP in the benchmark report.

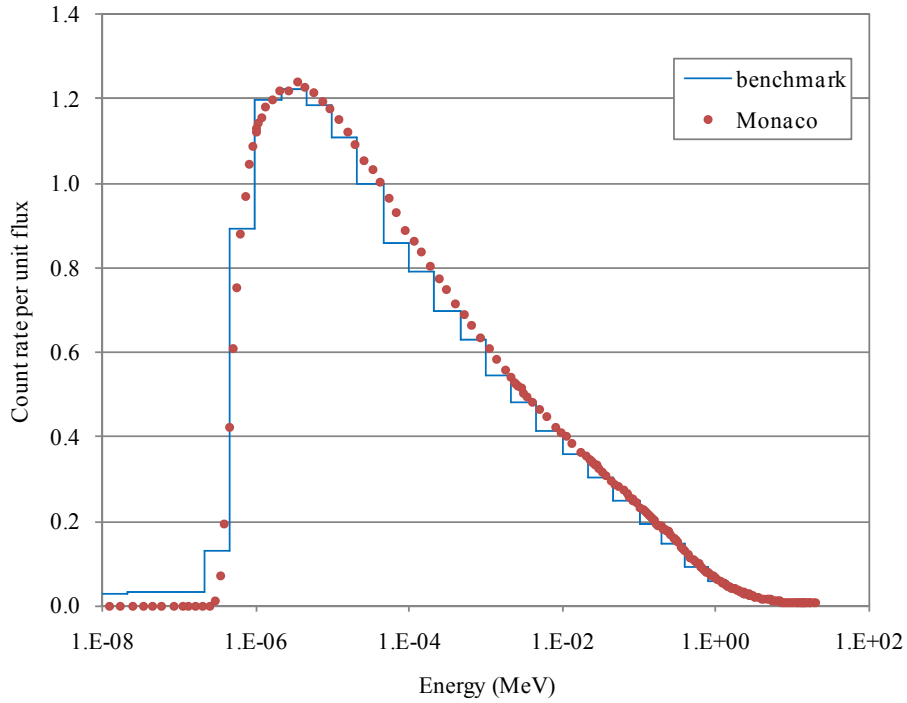


Fig. 3.12 Response (counts per unit flux) for the 2-inch diameter Bonner sphere (with cadmium cover). (Benchmark is computed function from Ref. 8.)

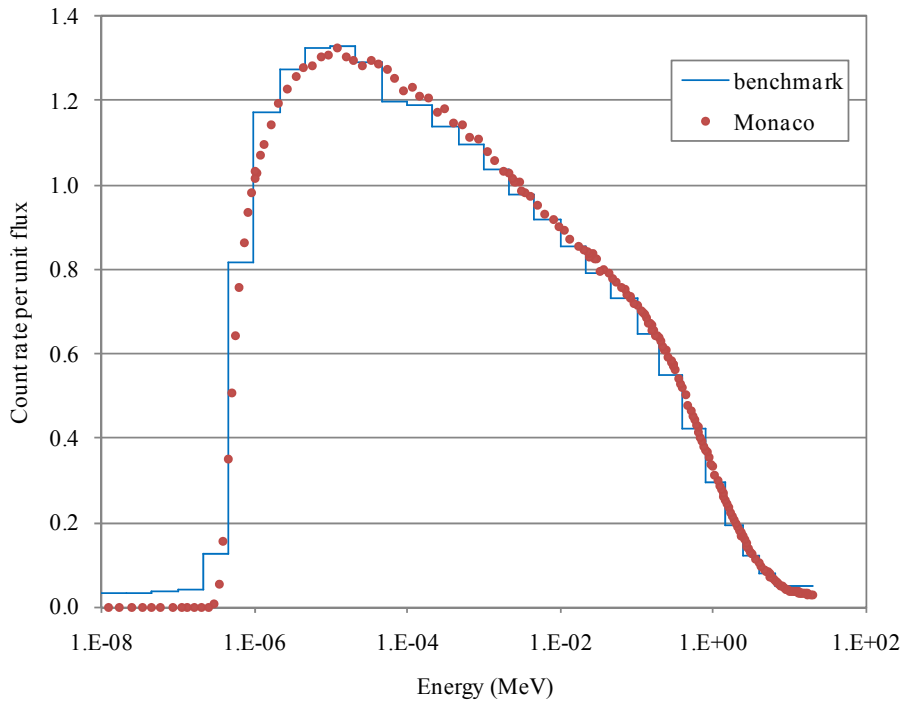


Fig. 3.13 Response (counts per unit flux) for the 3-inch diameter Bonner sphere (with cadmium cover). (Benchmark is computed function from Ref. 8.)

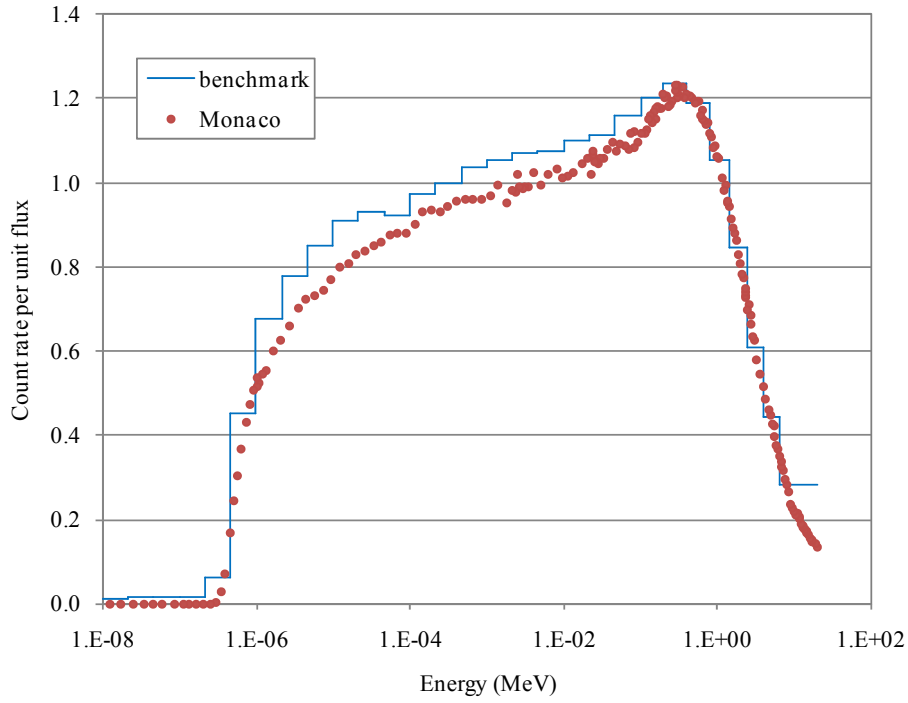


Fig. 3.14 Response (counts per unit flux) for the 5-inch diameter Bonner sphere (with cadmium cover). (Benchmark is computed function from Ref. 8.)

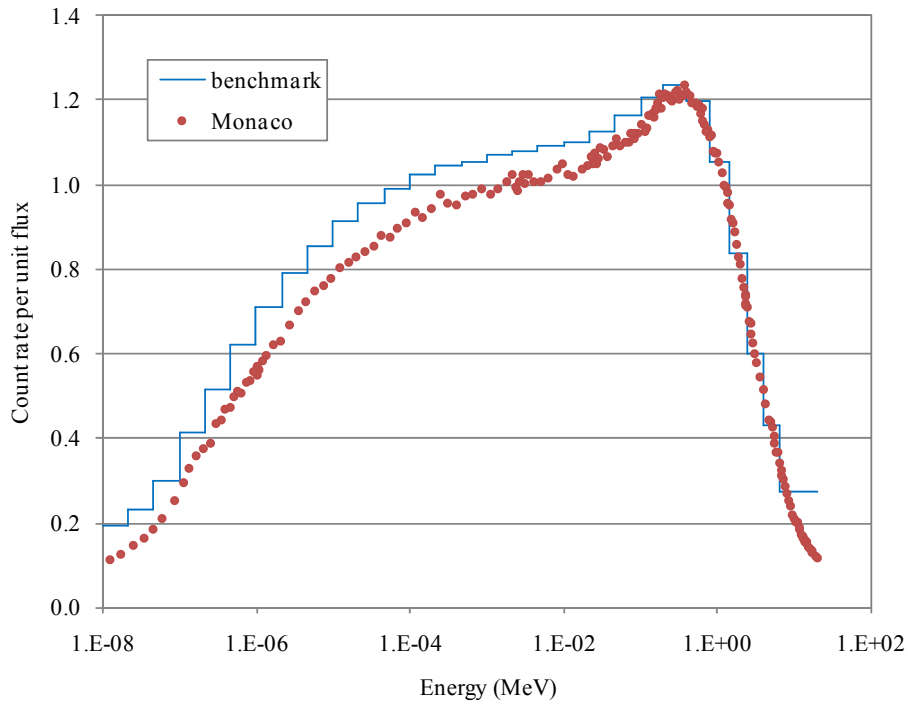


Fig. 3.15 Response (counts per unit flux) for the 5-inch diameter Bonner sphere (no cover). (Benchmark is computed function from Ref. 8.)

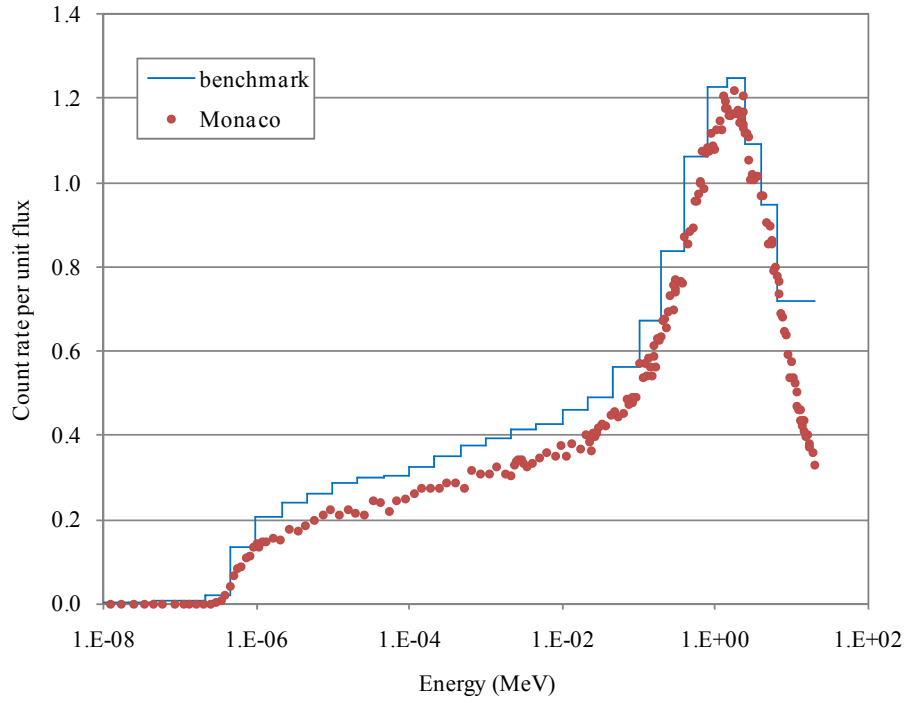


Fig. 3.16 Response (counts per unit flux) for the 8-inch diameter Bonner sphere (with cadmium cover). (Benchmark is computed function from Ref. 8.)

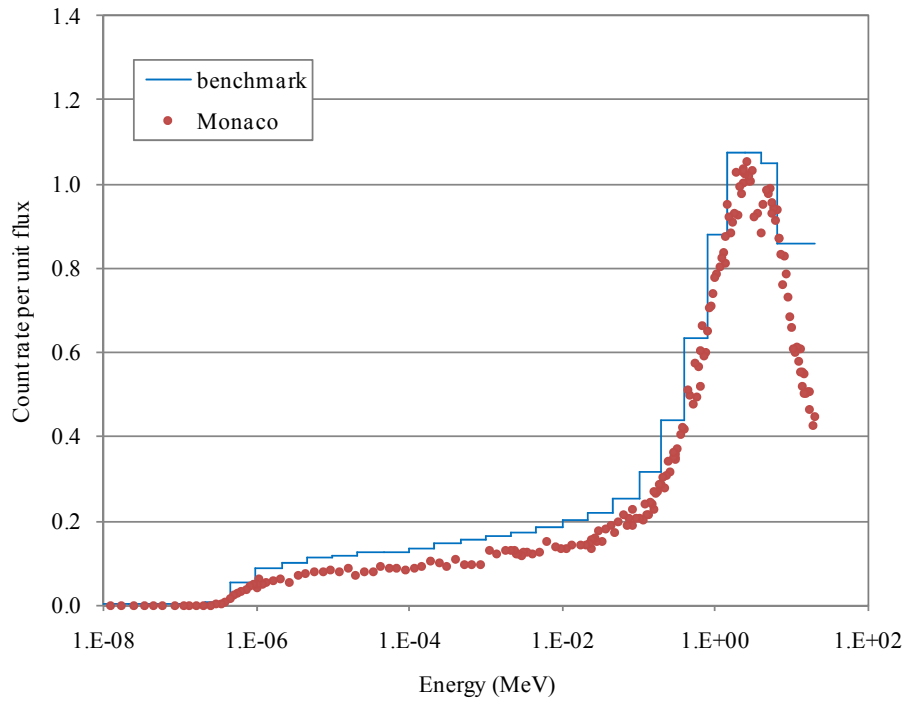


Fig. 3.17 Response (counts per unit flux) for the 10-inch diameter Bonner sphere (with cadmium cover). (Benchmark is computed function from Ref. 8.)

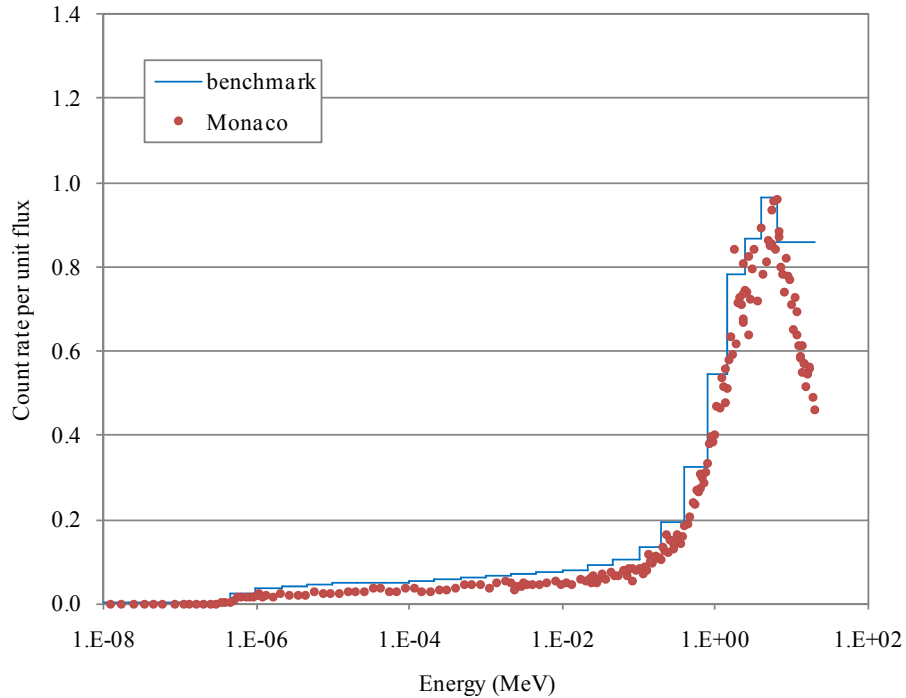


Fig. 3.18 Response (counts per unit flux) for the 12-inch diameter Bonner sphere (with cadmium cover). (Benchmark is computed function from Ref. 8.)

The Monaco-computed detector response functions compared well to the response functions computed by the benchmark team using MCNP. The results for the larger Bonner spheres show statistical noise in the Monaco results and could be reduced by longer run times. For these detectors, the Monaco responses are also a bit lower than the MCNP responses and could give lower total detector count rates.

3.2.1.4 Neutron transport through the labyrinth

The materials and labyrinth dimensions were taken from the benchmark report.⁸ For each size detector (7) and for each type of source (2), MAVRIC and the FW-CADIS method were used to compute the detector count rates at all 10 detector locations for the first labyrinth design (empty, three-section labyrinth). Neutron flux spectra were computed at each location and then folded with the different detector response functions.

In the benchmark report, the authors computed the detector count rates with MCNP. For the 12-inch detector, the stated relative uncertainties ranged from 0.5% for the closest detector location to 2% for the furthest detector location.

The ratios of the calculated count rates to the experimentally measured count rates are shown for both the benchmark team using MCNP and MAVRIC in Figs. 3.19–3.32. The error bars in the C/E ratio are due almost entirely to the uncertainty in the experimental measurements. MAVRIC relative uncertainties were in the 1–2% range for the bare source and in the 2–3% range for the covered source.

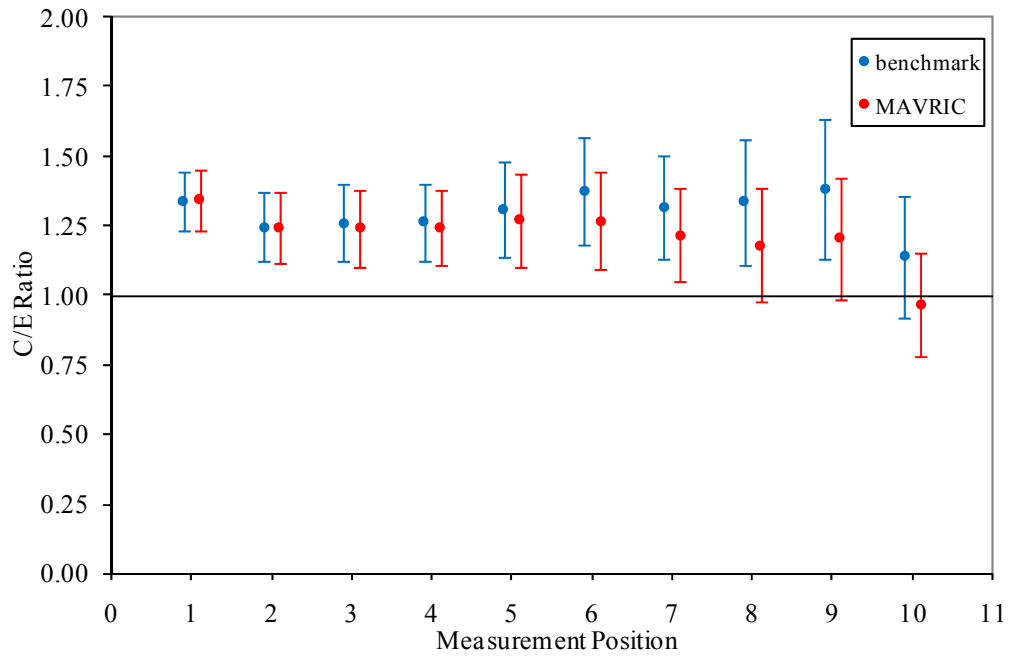


Fig. 3.19 Neutron count rate C/E for the 2-inch Bonner sphere (with cadmium) and the uncovered source. (Benchmark is computed function from Ref. 8.)

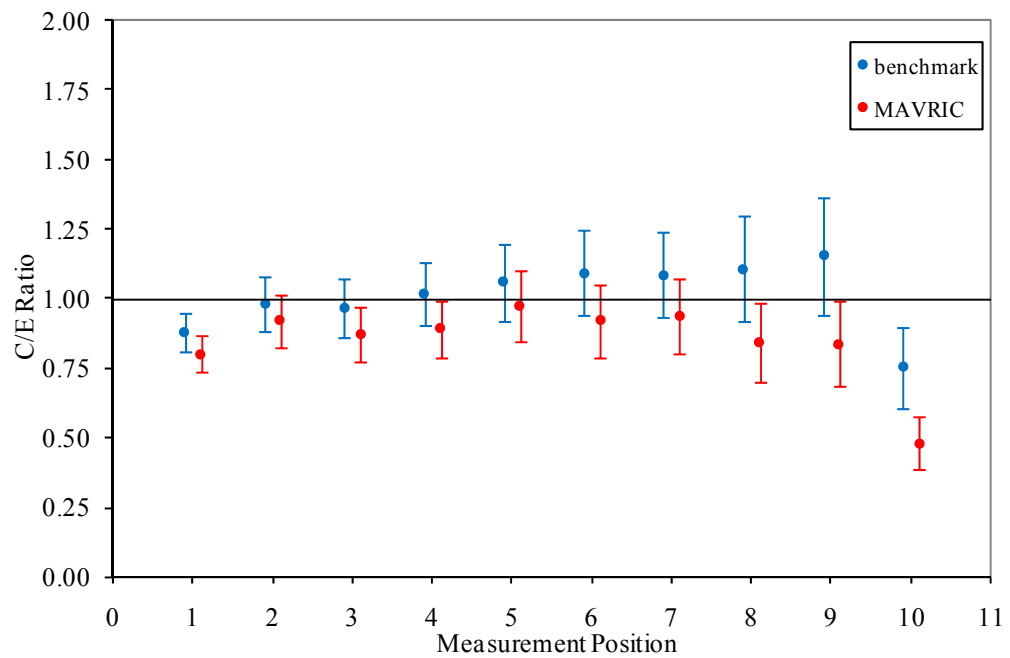


Fig. 3.20 Neutron count rate C/E for the 2-inch Bonner sphere (with cadmium) and the covered source. (Benchmark is computed function from Ref. 8.)

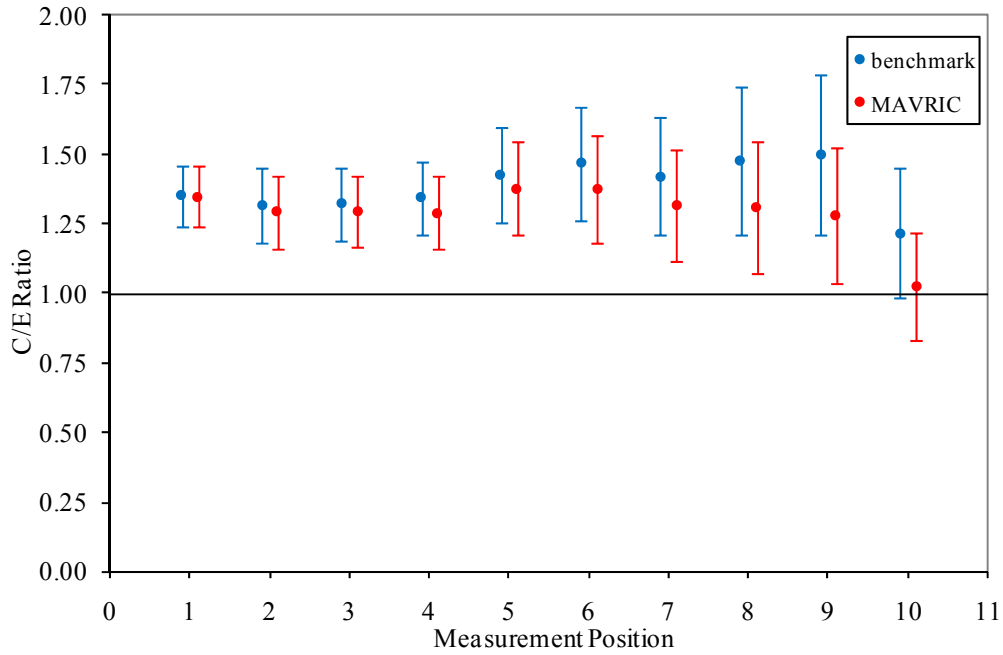


Fig. 3.21 Neutron count rate C/E for the 3-inch Bonner sphere (with cadmium) and the uncovered source. (Benchmark is computed function from Ref. 8.)

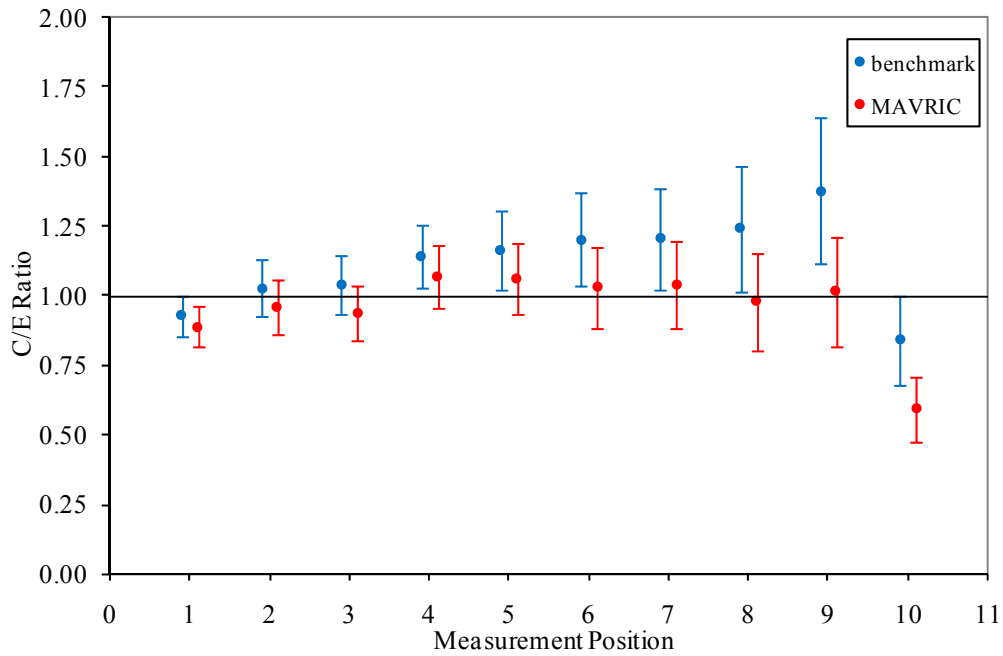


Fig. 3.22 Neutron count rate C/E for the 3-inch Bonner sphere (with cadmium) and the covered source. (Benchmark is computed function from Ref. 8.)

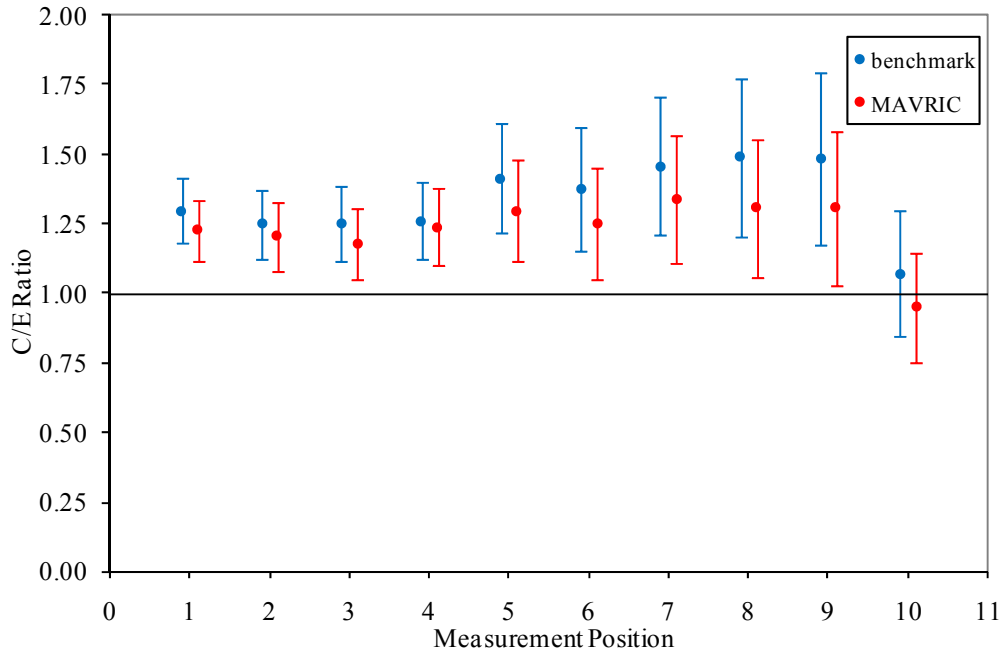


Fig. 3.23 Neutron count rate C/E for the 5-inch Bonner sphere (with cadmium) and the uncovered source. (Benchmark is computed function from Ref. 8.)

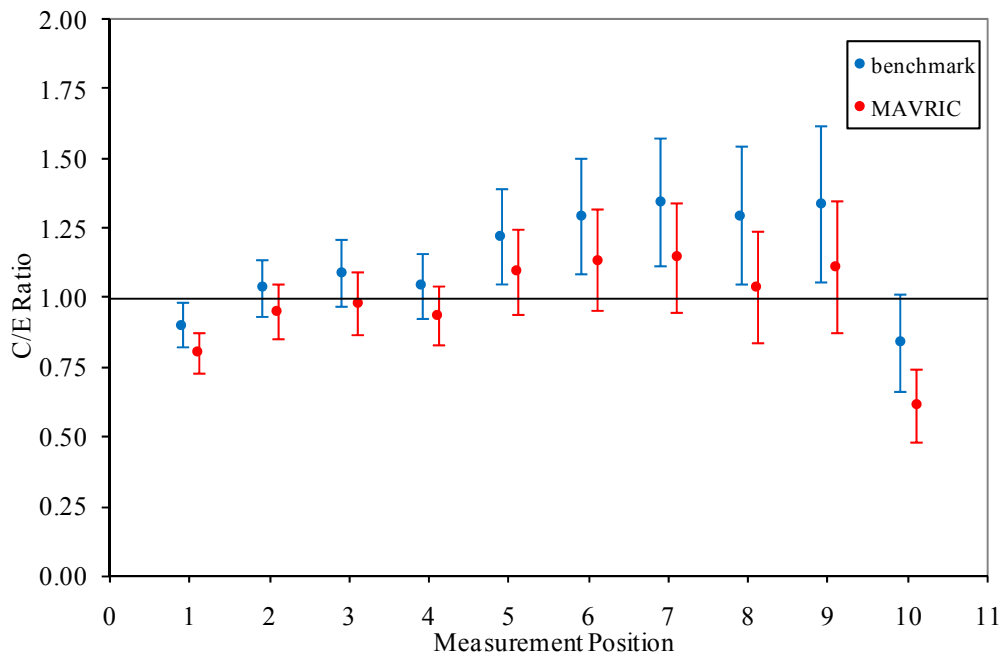


Fig. 3.24 Neutron count rate C/E for the 5-inch Bonner sphere (with cadmium) and the covered source. (Benchmark is computed function from Ref. 8.)

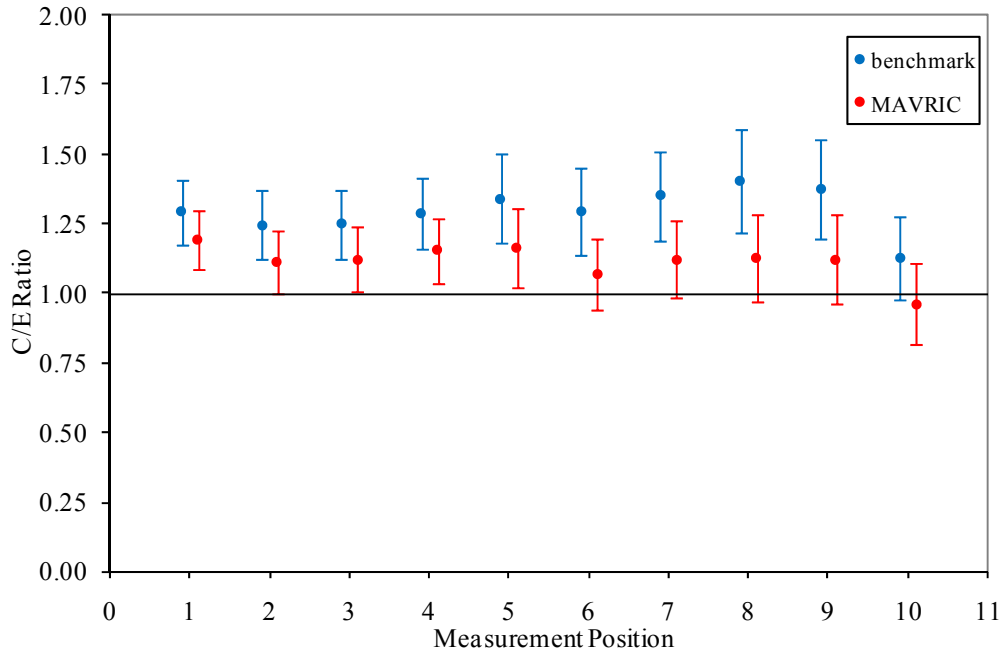


Fig. 3.25 Neutron count rate C/E for the 5-inch Bonner sphere (no cadmium) and the uncovered source. (Benchmark is computed function from Ref. 8.)

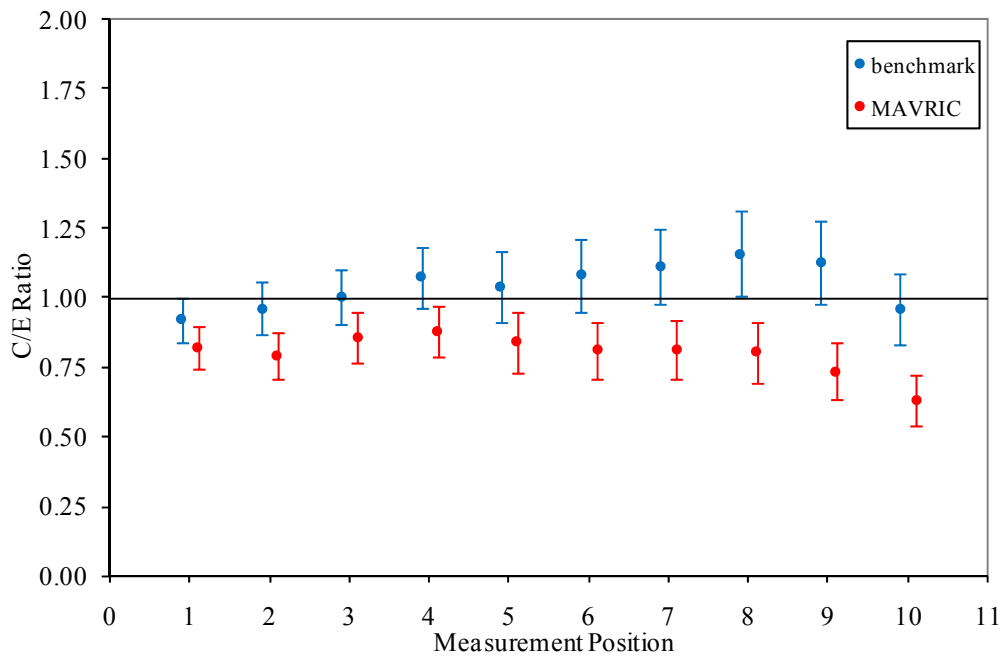


Fig. 3.26 Neutron count rate C/E for the 5-inch Bonner sphere (no cadmium) and the covered source. (Benchmark is computed function from Ref. 8.)

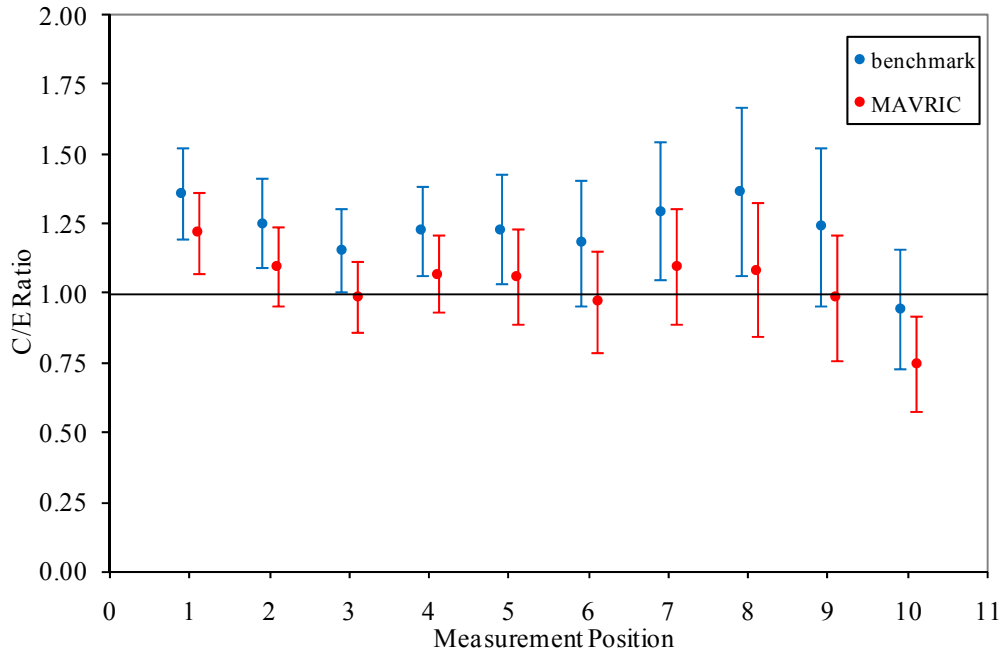


Fig. 3.27 Neutron count rate C/E for the 8-inch Bonner sphere (with cadmium) and the uncovered source. (Benchmark is computer function from Ref. 8.)

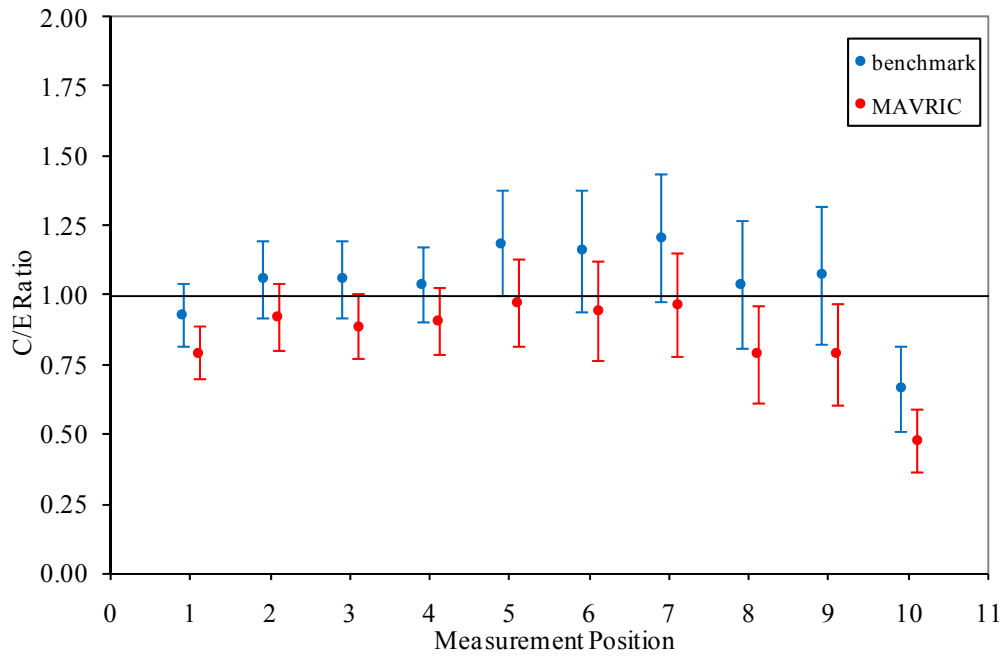


Fig. 3.28 Neutron count rate C/E for the 8-inch Bonner sphere (with cadmium) and the covered source. (Benchmark is computer function from Ref. 8.)

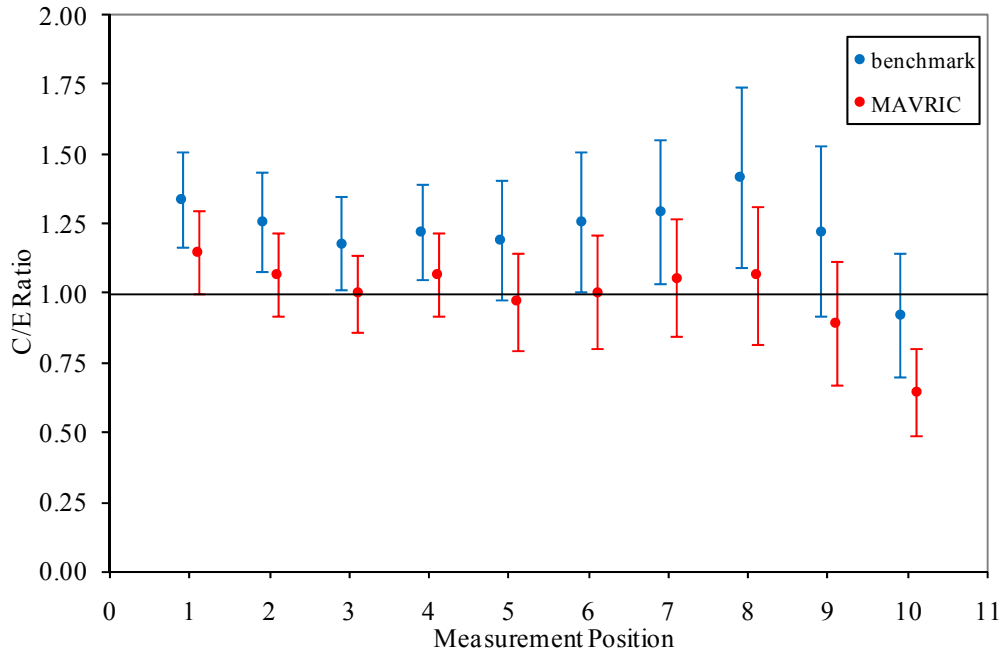


Fig. 3.29 Neutron count rate C/E for the 10-inch Bonner sphere (with cadmium) and the uncovered source. (Benchmark is computer function from Ref. 8.)

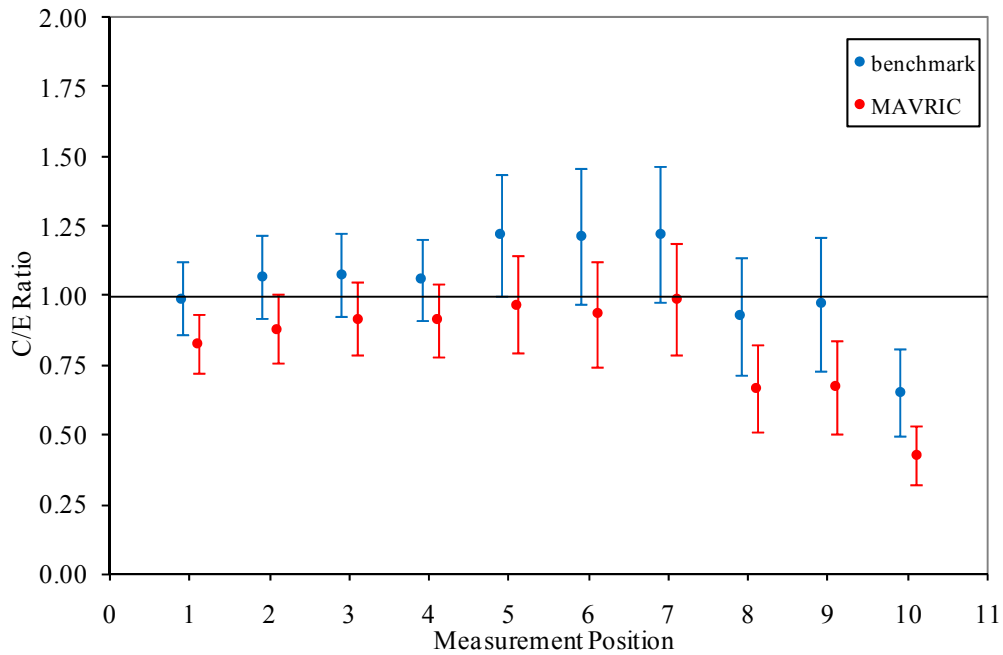


Fig. 3.30 Neutron count rate C/E for the 10-inch Bonner sphere (with cadmium) and the covered source. (Benchmark is computer function from Ref. 8.)

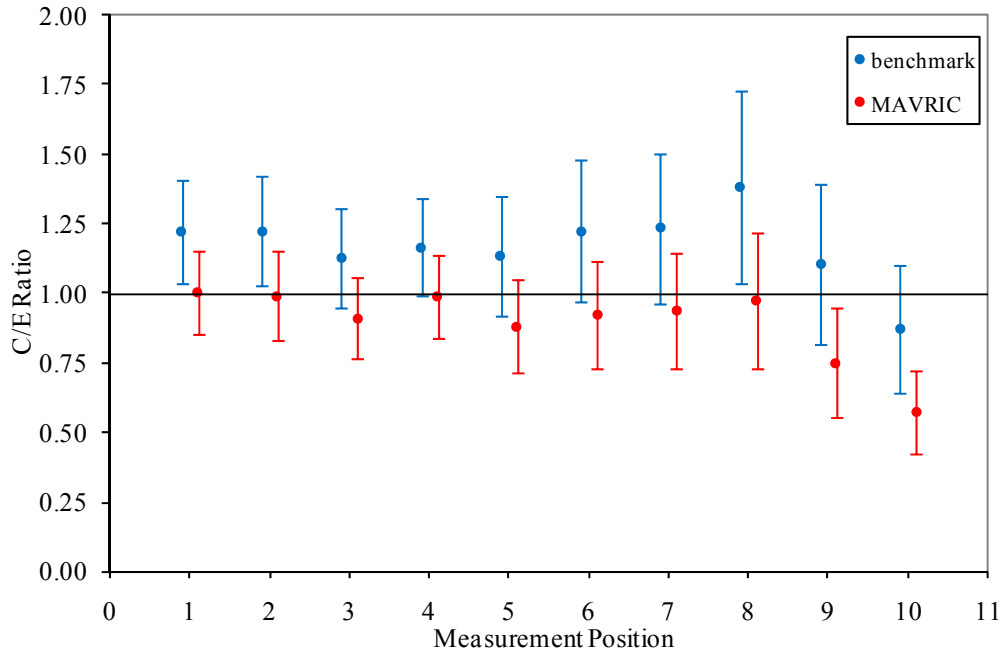


Fig. 3.31 Neutron count rate C/E for the 12-inch Bonner sphere (with cadmium) and the uncovered source. (Benchmark is computer function from Ref. 8.)

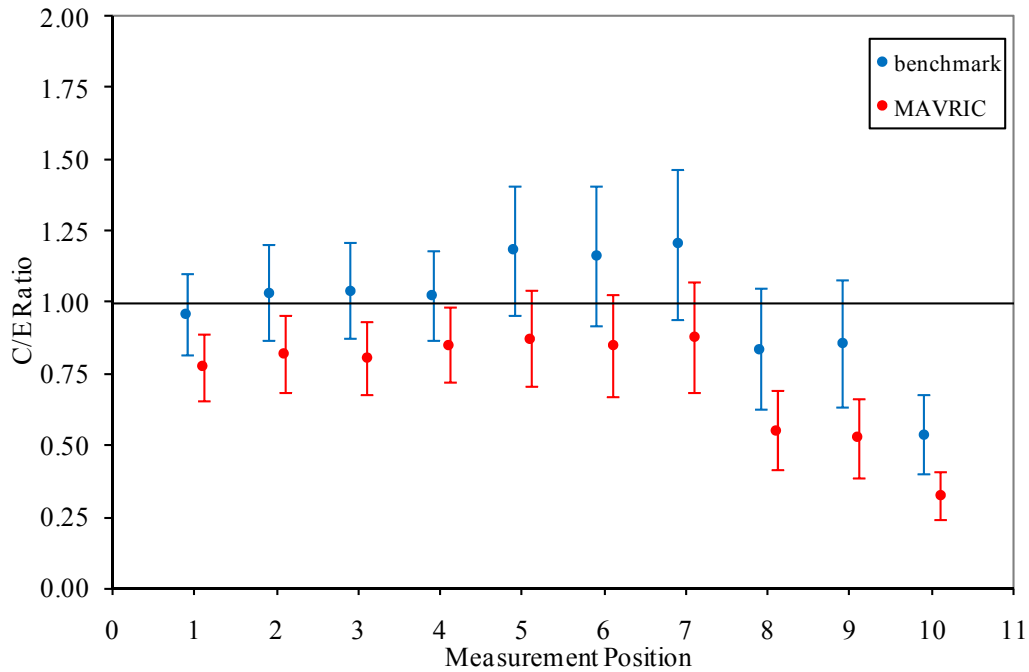


Fig. 3.32 Neutron count rate C/E for the 12-inch Bonner sphere (with cadmium) and the covered source. (Benchmark is computed function from Ref. 8.)

The MAVRIC count rates are all a bit lower than the benchmark MCNP count rates (due to lower detector response functions) but follow the MCNP C/E well for both the covered and uncovered sources for all seven detectors.

3.2.2 Neutron and photon leakage spectra from ^{252}Cf source at centers of six iron spheres of different diameters

3.2.2.1 Benchmark overview

Neutron and photon leakage spectra were measured from a ^{252}Cf source through iron spheres of various diameters in Russia during the 1980s. These data and instructions for benchmark calculations were presented in 2007 in an Organization for Economic Cooperation and Development report.⁹

Thirteen sets of experimental data are presented in the report—one for the bare source and one for each of six different diameters of iron shielding (20 cm, 30 cm, 40 cm, 50 cm, 60 cm, and 70 cm). Note that no photon measurement was made for the 20 cm shield. Each data set was the difference of two measurements—one with and one without a cone shaped shield between the source and detector. The experimental geometry is shown in Fig. 3.33.

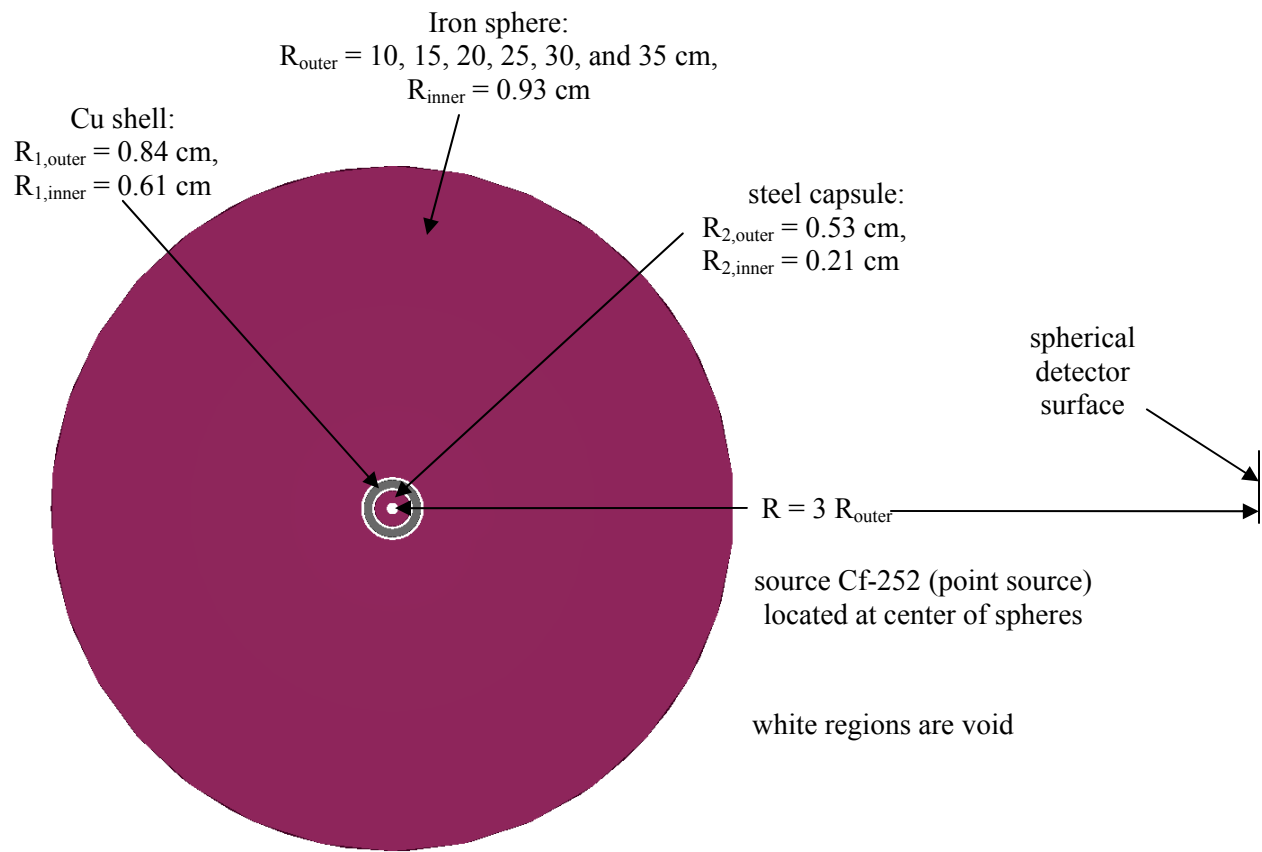


Fig. 3.33 Iron sphere experiments.

3.2.2.2 Monaco calculations

Monaco (SCALE 6) and the new ENDF/B-VI.8 fine-group shielding library were used to compute leakage spectra of both neutrons and photons according to the benchmark instructions.

For the Monaco neutron source, the experimentally measured neutron flux spectrum of the bare source was converted into a 200-group source specification. For the Monaco photon source, the experimentally measured photon flux spectrum of the bare source was converted into a 47-group source specification. Note that the “bare source” did include copper and steel canisters, so a small fraction of the measured photon flux could have come from secondary gammas from neutrons interacting in the source capsule. For every neutron emitted from the ^{252}Cf source, 3.82 photons were emitted. Monaco combined the sources into a single coupled neutron-photon source.

Benchmark results are listed in the above document in terms of $4\pi R^2\Phi(E)/Q$, where R is the radius of the detector (three times the radius of the shield, or 60 cm for the bare source) and Q is the neutron source strength. Experimental uncertainties ranged from 5% to 30%, so the experimental values are shown on the following plots as two lines, representing the values $\pm 1\sigma$.

Since the Monaco source was created from the bare source measurements, the Monaco simulation for these should match the experiment well, as shown in Figs. 3.34 and 3.35.

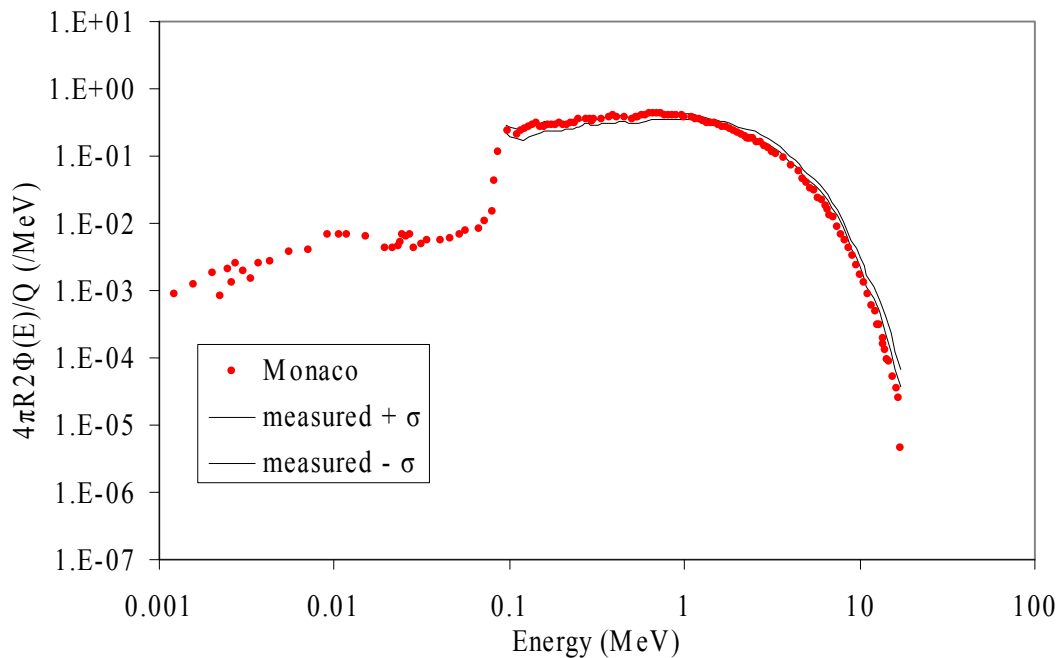


Fig. 3.34 Comparison of the neutron calculation to the measurement of the bare source.

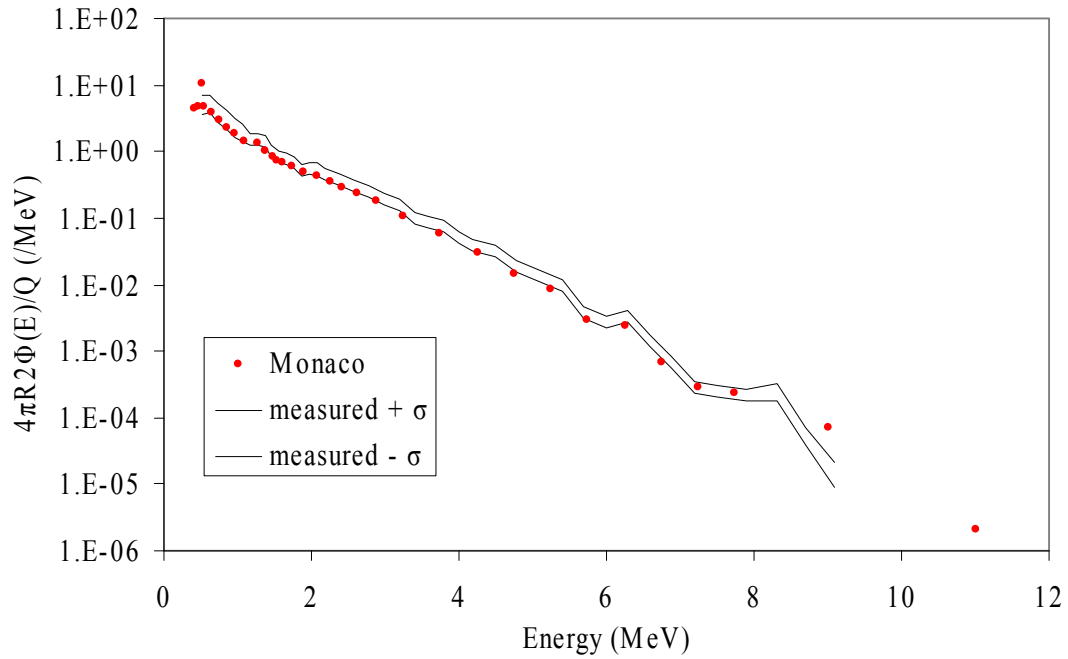


Fig. 3.35 Comparison of the photon calculation to the measurement of the bare source.

Neutron flux results for various shield thicknesses are shown in Figs. 3.36–3.41.

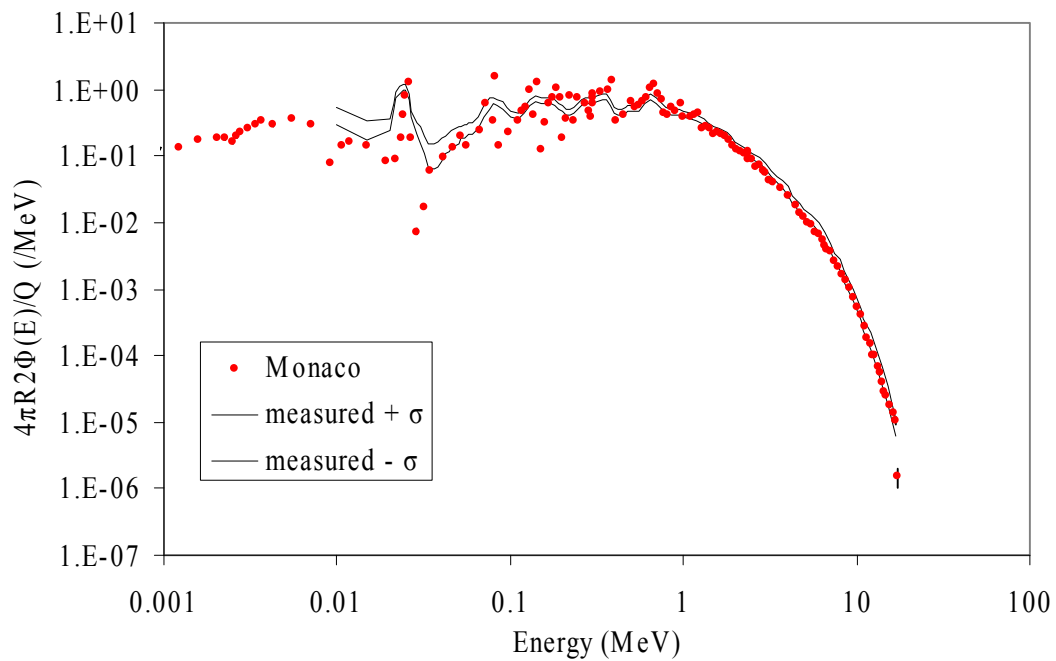


Fig. 3.36 Comparison of the neutron calculation to the measurement of the 20 cm shield.

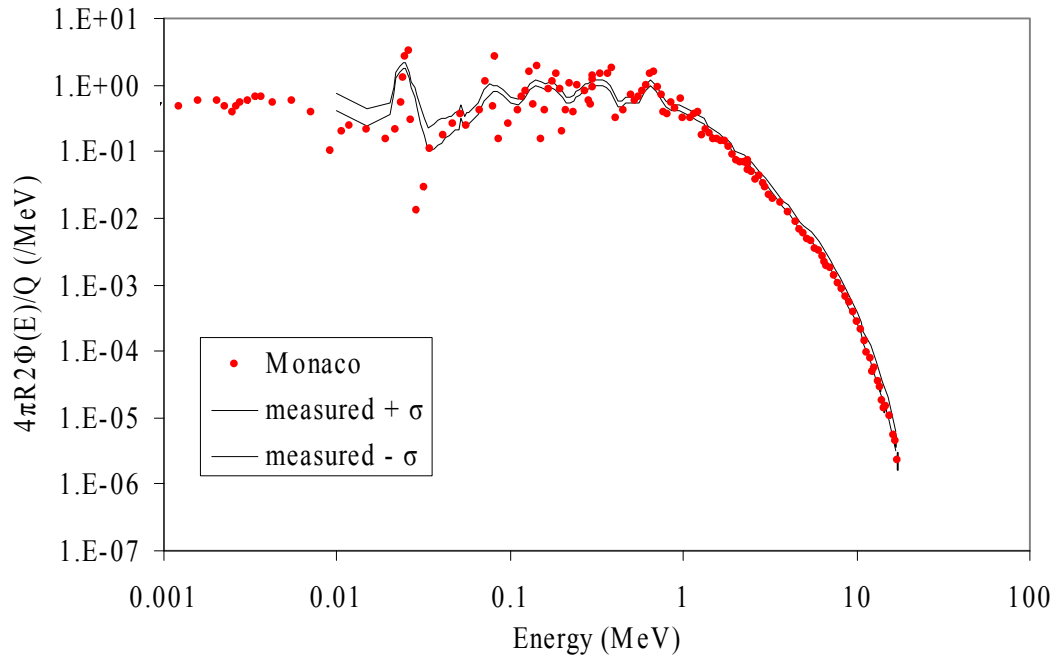


Fig. 3.37 Comparison of the neutron calculation to the measurement of the 30 cm shield.

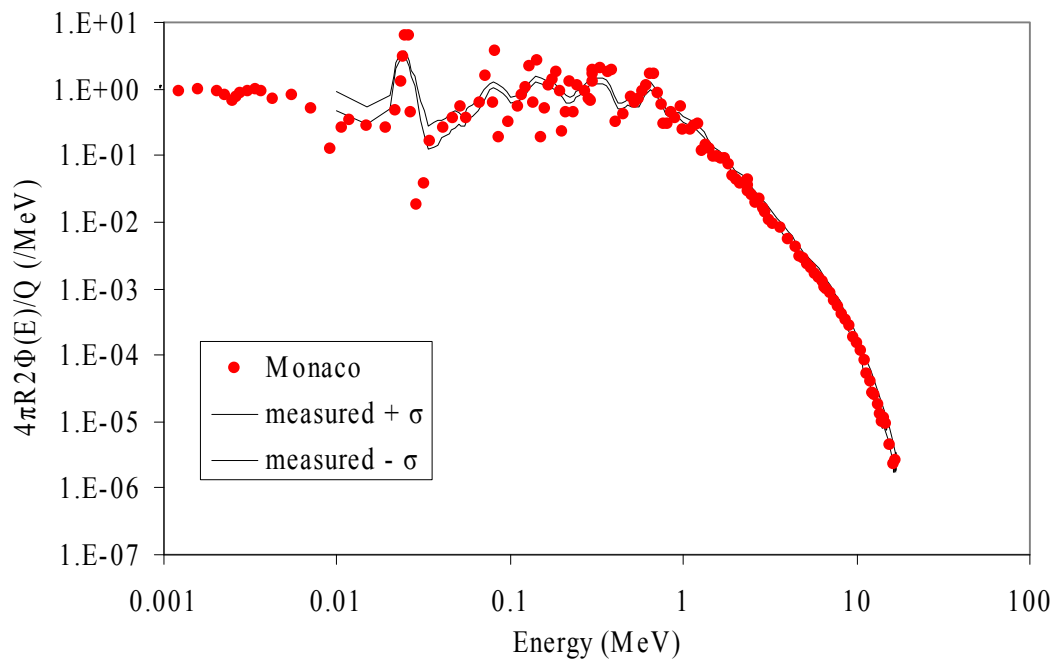


Fig. 3.38 Comparison of the neutron calculation to the measurement of the 40 cm shield.

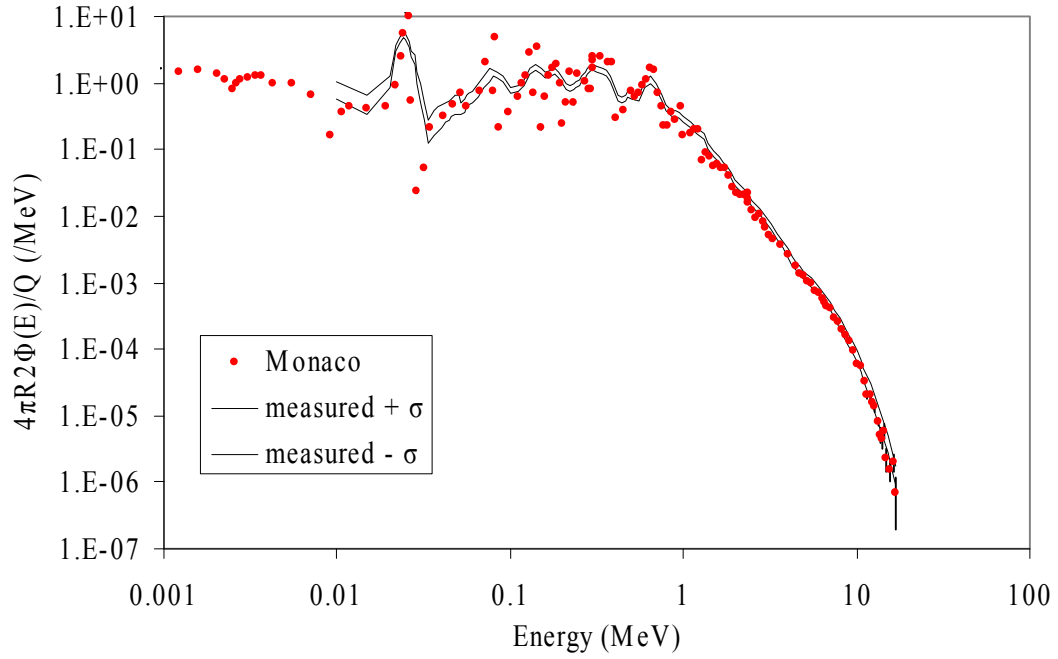


Fig. 3.39 Comparison of the neutron calculation to the measurement of the 50 cm shield.

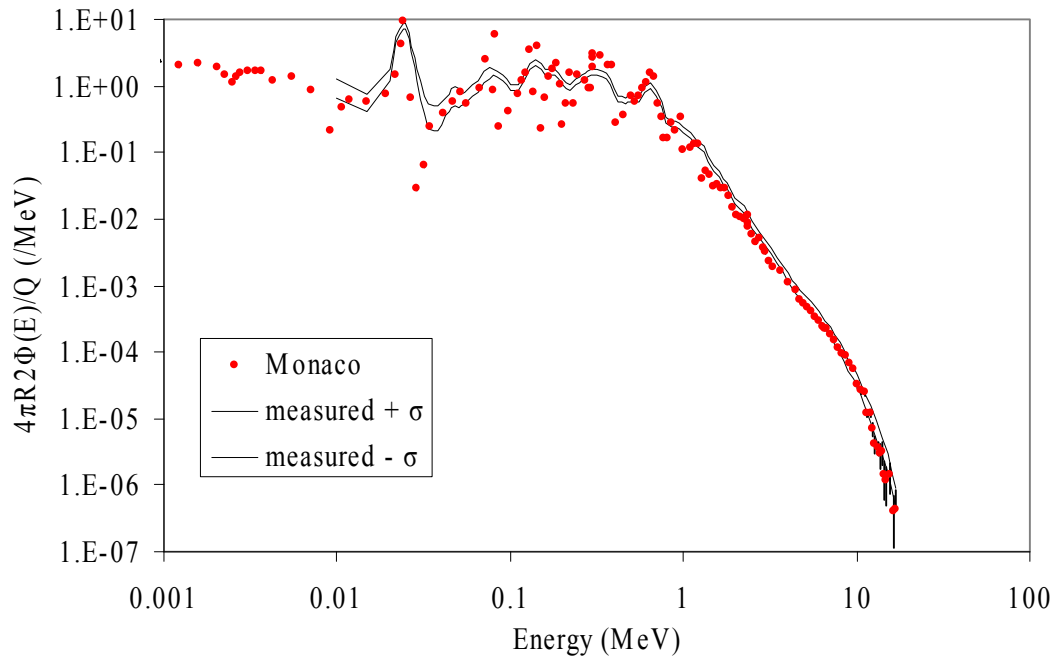


Fig. 3.40 Comparison of the neutron calculation to the measurement of the 60 cm shield.

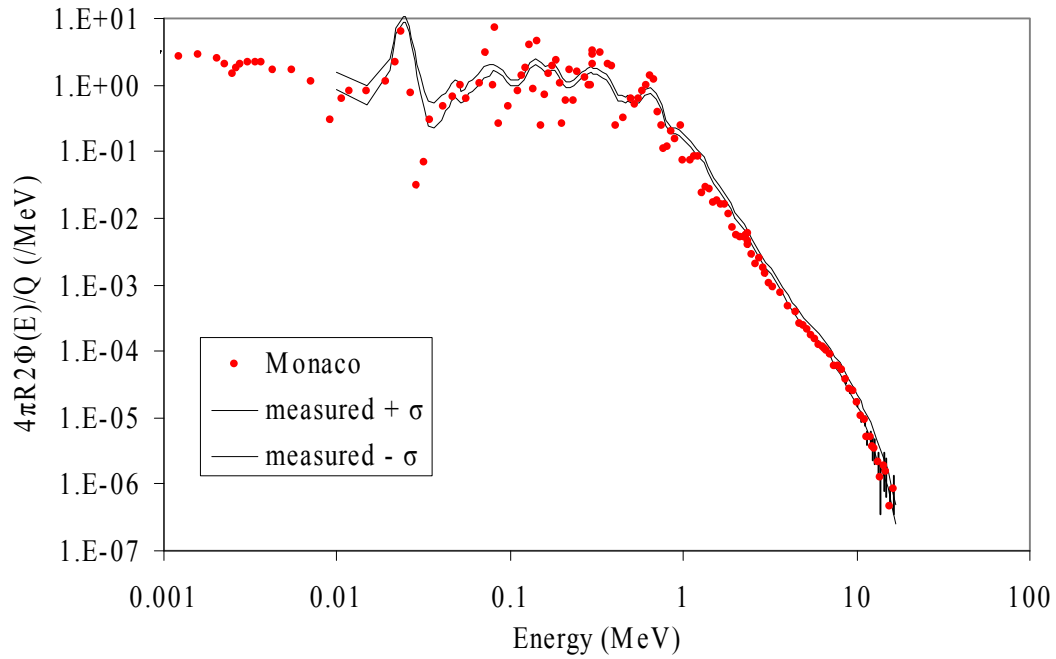


Fig. 3.41 Comparison of the neutron calculation to the measurement of the 70 cm shield.

Photon flux results for various shield thicknesses are given in Figs. 3.42–3.46.

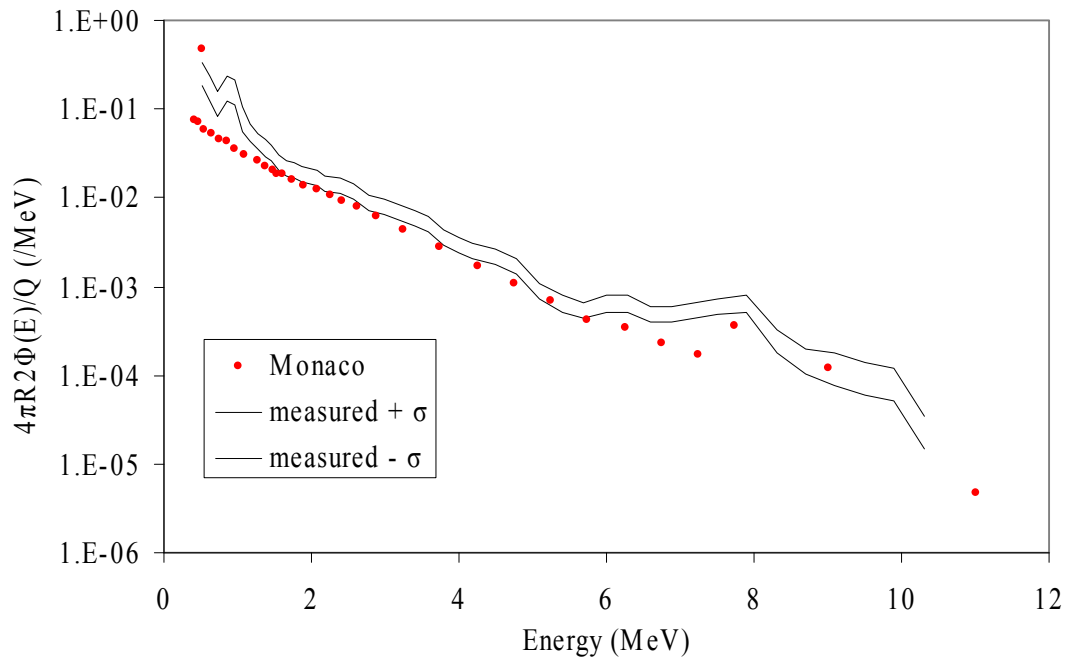


Fig. 3.42 Comparison of the photon calculation to the measurement of the 30 cm shield.

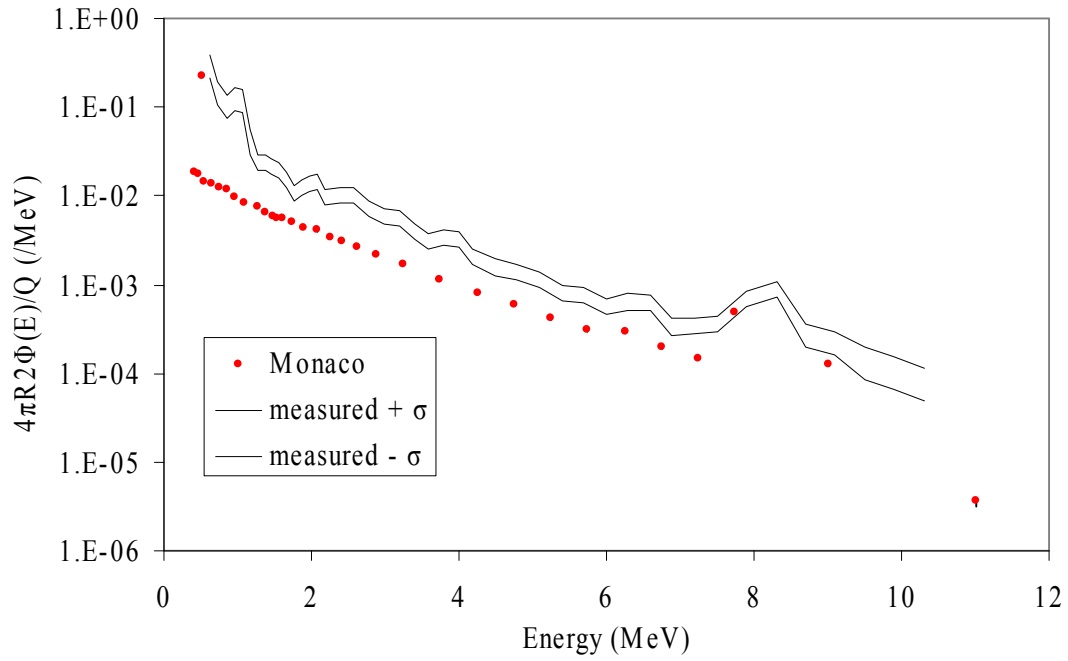


Fig. 3.43 Comparison of the photon calculation to the measurement of the 40 cm shield.

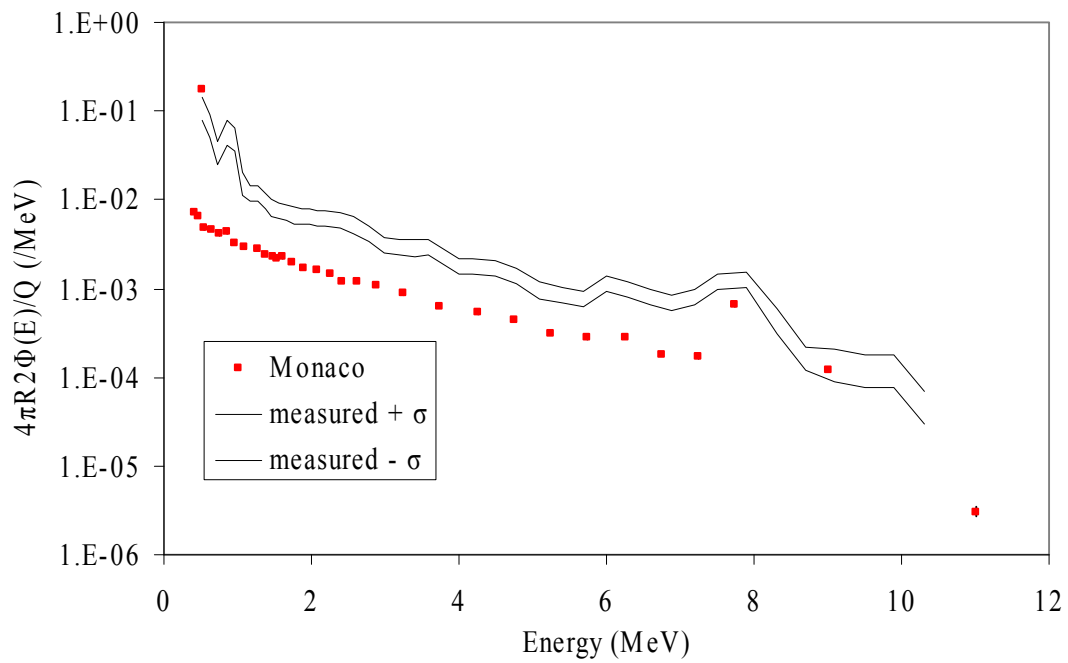


Fig. 3.44 Comparison of the photon calculation to the measurement of the 50 cm shield.

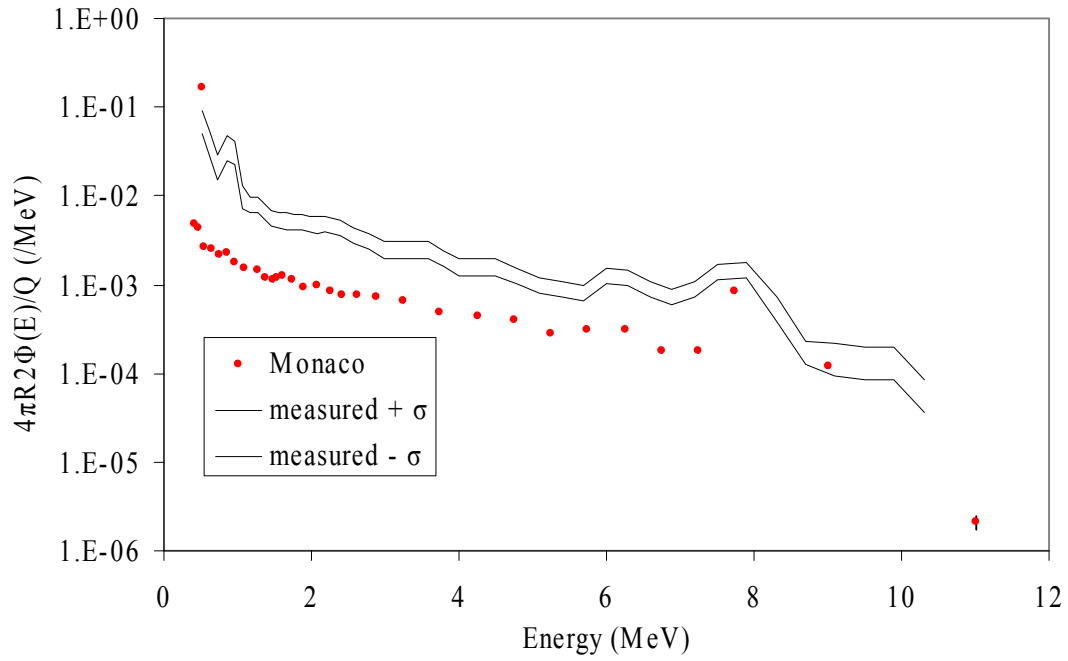


Fig. 3.45 Comparison of the photon calculation to the measurement of the 60 cm shield.

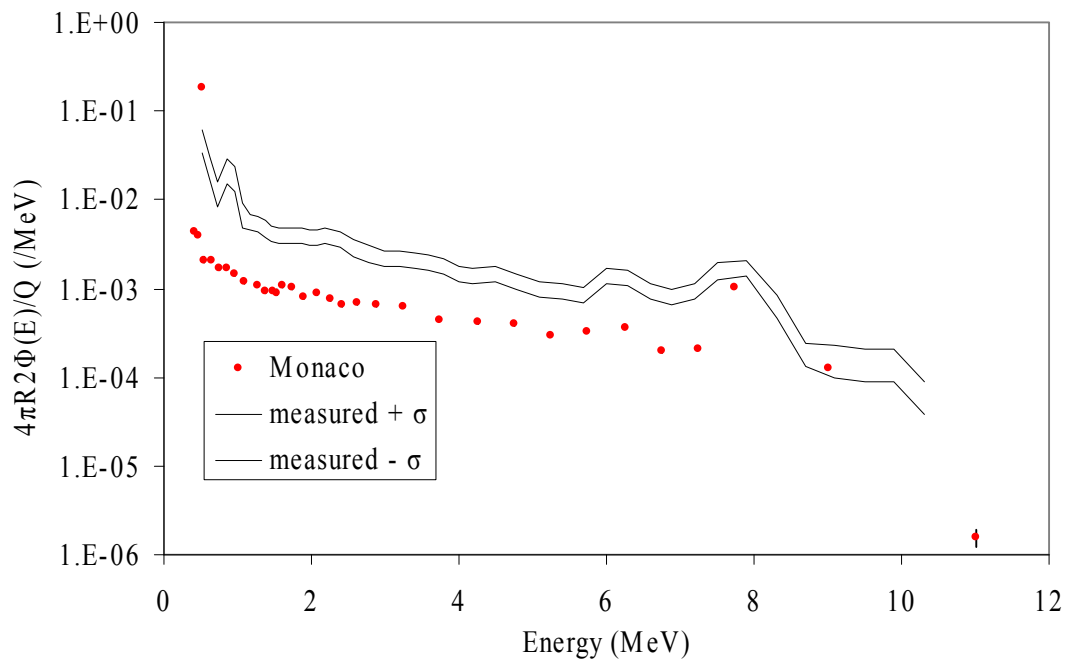


Fig. 3.46 Comparison of the photon calculation to the measurement of the 70 cm shield.

Photon fluxes are underpredicted by Monaco and MCNP5 as is depicted in Fig. 3.47.

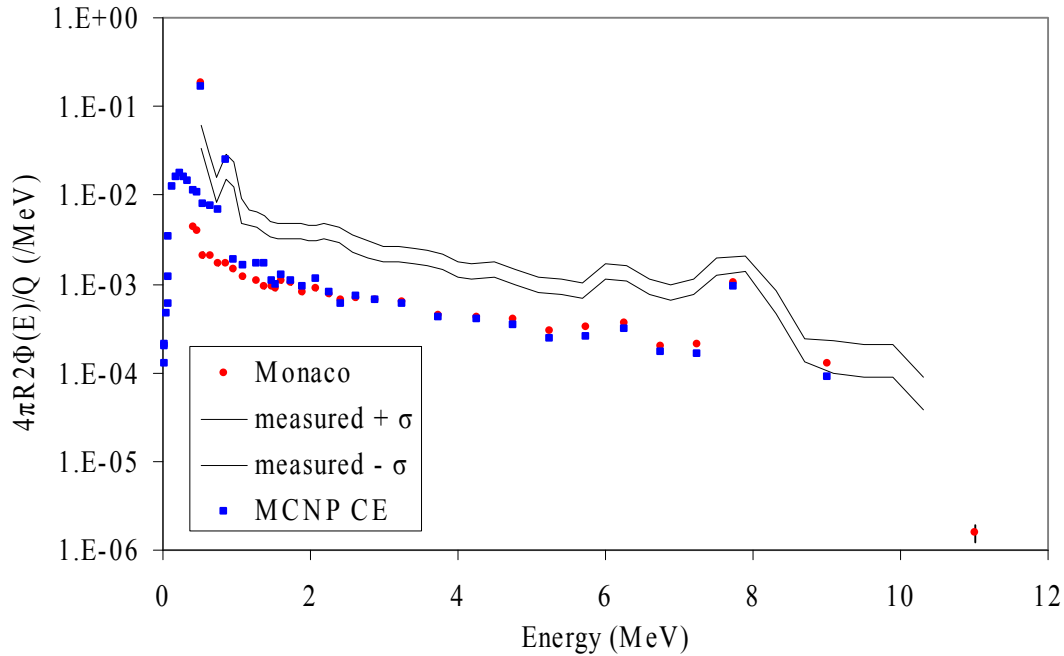


Fig. 3.47 Photon flux through the 70 cm shield as calculated by Monaco and MCNP5.

MCNP results in the benchmark study were similar to those shown in Fig. 3.47 (see Fig. 20 of Ref. 9).

3.2.3 Comparison of measured and calculated neutron transmission through heavy water for a ^{252}Cf source placed in the center of a 30 cm diameter sphere

3.2.3.1 Experiment overview

The transmission of ^{252}Cf neutrons through a sphere filled with heavy water was measured in Prague in the mid 1990s (Ref. 10). For each experiment, two measurements were made: one with an iron/polyethylene shield and one without the shield. The purpose of the shield was to block all direct particle transmission from the sphere to the detector. The difference in these two measurements accounts for scatter from the floor, walls, and ceiling (which is about a 5% effect for energies above 10 keV). A great amount of detail is given for the materials and geometry of the source holder, insertion tube, and detectors in Ref. 10. Two different assemblies holding the californium source were measured.

3.2.3.2 Monaco calculations

The Monaco SGGP geometry model consists of two nested spheres for the source and the heavy water. For the experiments where the iron/polyethylene shield is present, three borated polyethylene cylinders and one iron cylinder are placed between the sphere and the detector position (75,0,0). The experiment sat 2 m above the floor of an experimental hall that measured $10 \times 13 \times 25$ m. Here, the origin corresponds to the source at the center of the heavy water sphere. Neither of the two source holder assemblies was modeled in any detail. The geometry model is shown in Fig. 3.48.

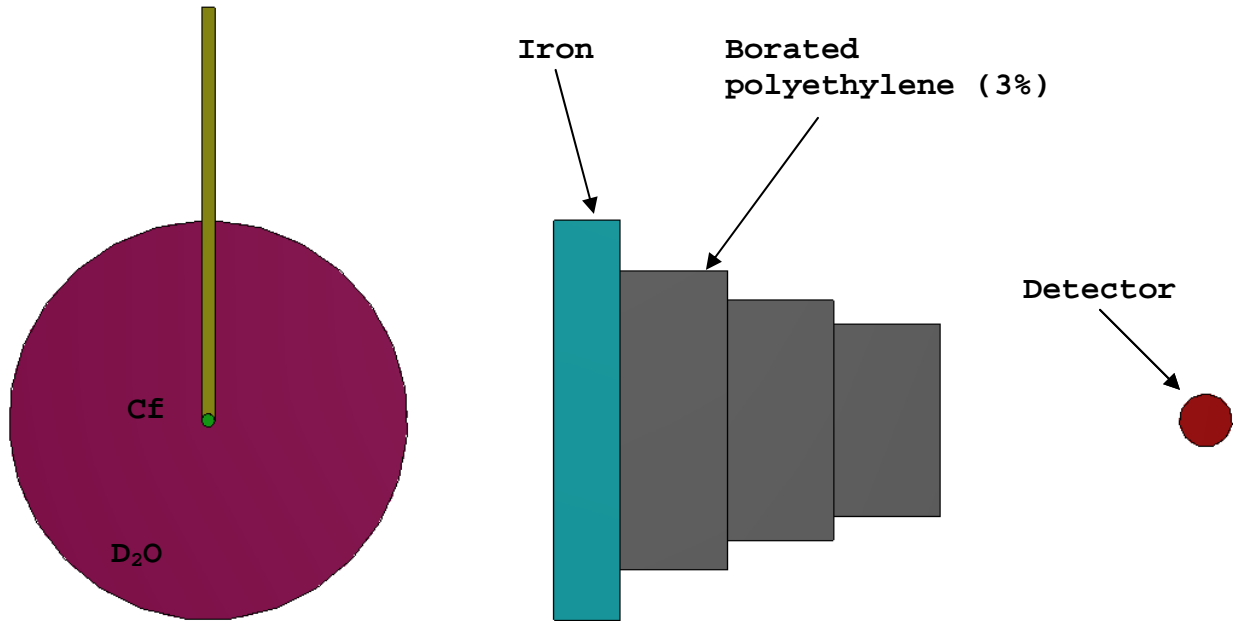


Fig. 3.48 Monaco model of ^{252}Cf source in heavy water experiment.

A second Monaco input file was created for the geometry without the 4 cylindrical shields in place.

For the source, the Watt spectrum with constants $\alpha=1.025$ MeV, $b=2.926/\text{MeV}$ was used.

$$p(E) = ce^{-E/\alpha} \sinh(\sqrt{bE}) . \quad (3.3)$$

The measurements listed in the paper were normalized such that the total flux at the detector (at $r=75$ cm) without the D_2O sphere or the shields would have been $1 \text{ n/cm}^2/\text{s}$. In Monaco, the source strength was set to a strength of $4\pi(75)^2 = 70686 \text{ n/s}$. No biasing was used, other than implicit capture.

A point detector tally at the detector location was used to calculate the energy dependent neutron flux.

Results for the ENDF/B-VI.8 library are depicted in Figs 3.49 and 3.50. Results for ENDF/B-VII.0 are shown in Figs. 3.51 and 3.52.

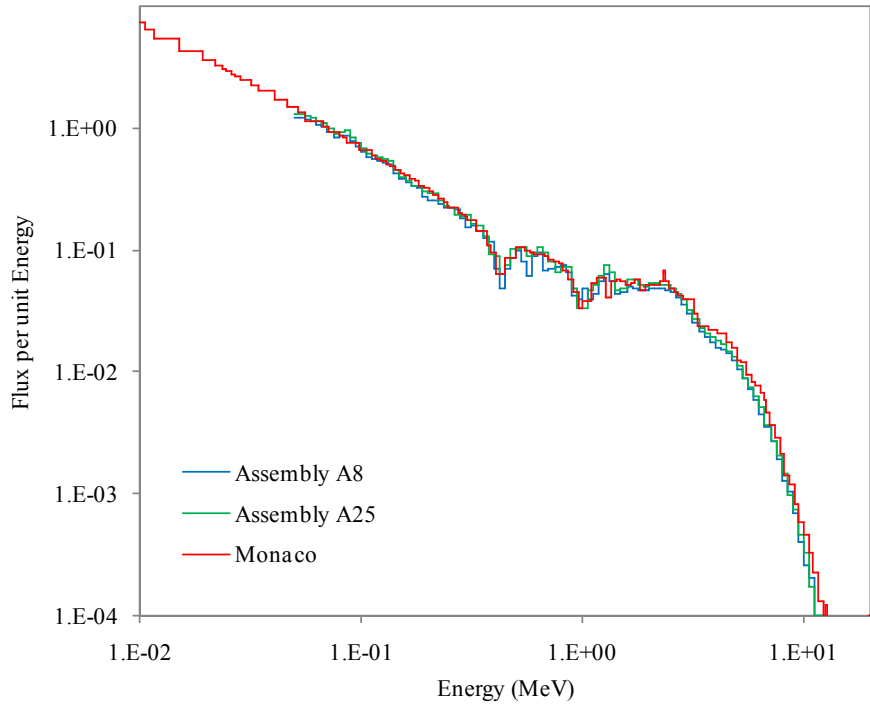


Fig. 3.49 Comparison of the Monaco (ENDF/B-VI.8) results and the measured data.

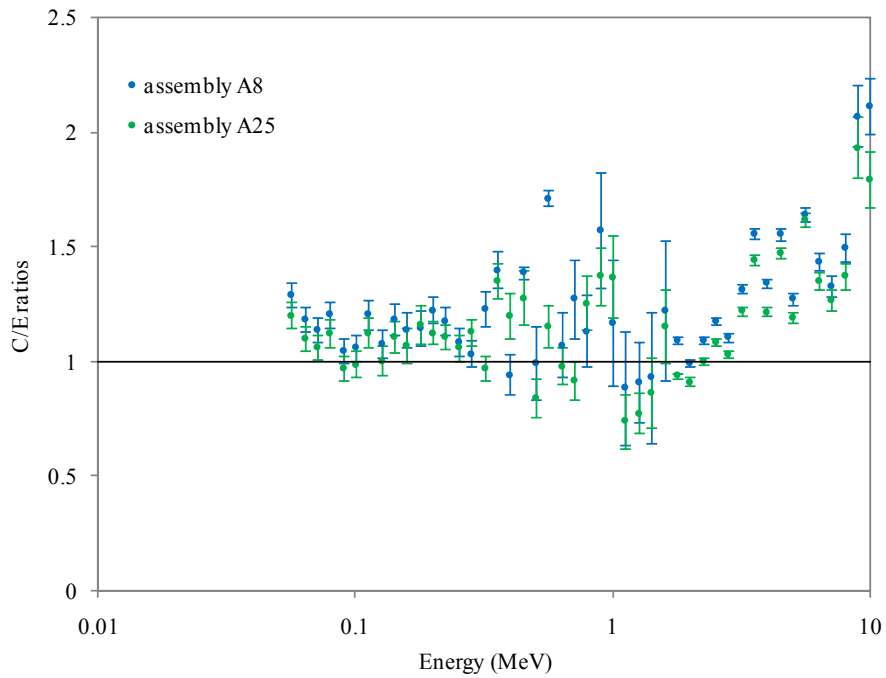


Fig. 3.50 Ratios of the Monaco (ENDF/B-VI.8 fine-group library) results and the measured data.

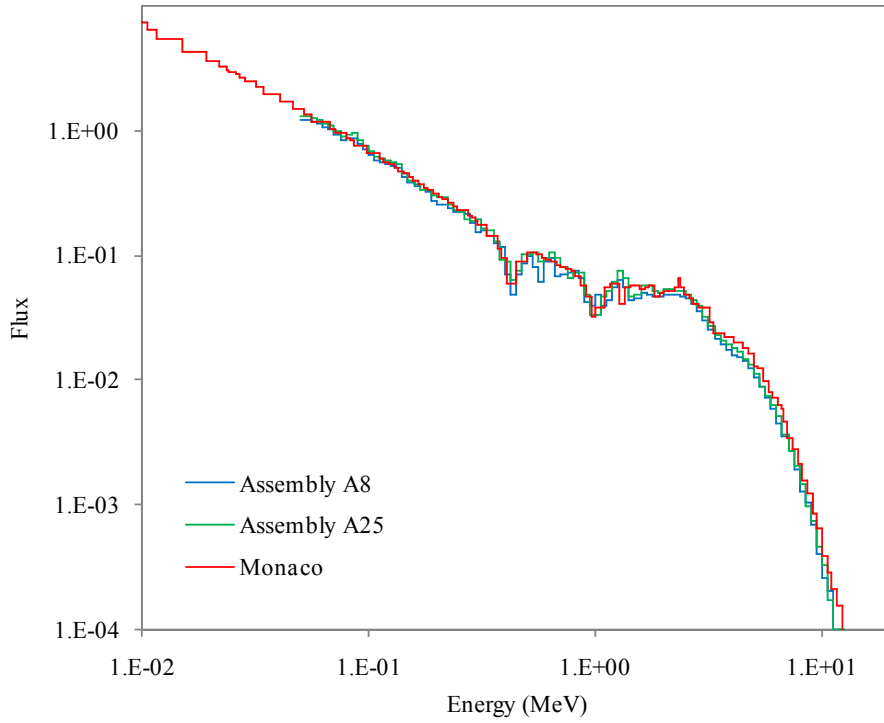


Fig. 3.51 Comparison of the Monaco (ENDF/B-VII.0) results and the measured data.

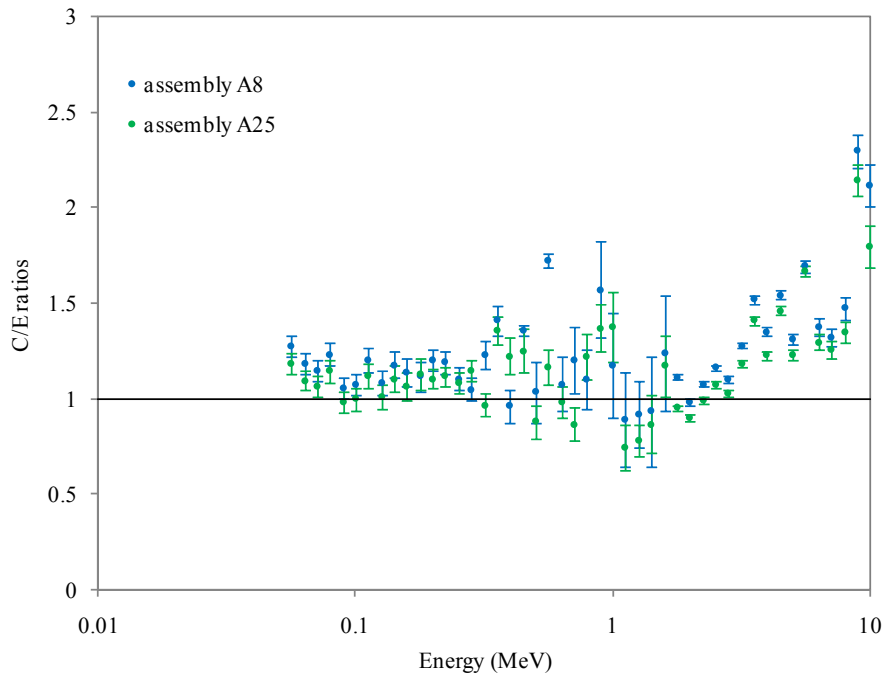


Fig. 3.52 Ratios of the Monaco (ENDF/B-VII.0 fine-group library) results and the measured data.

3.2.4 Comparison of measured and calculated neutron transmission through steel for a ^{252}Cf source

3.2.4.1 Experiment overview

In the early 1990s, several experiments measuring the transmission of ^{252}Cf neutrons through a sphere of iron were performed to benchmark ENDF/B-VI cross-section data. Two sets of measurements were made—one by the Czechoslovakian National Research Institute and the other by the Skoda Company.¹¹

3.2.4.2 Monaco calculations

The Monaco model consists of just a point source and a spherical shell of iron. Two different tallies are used which should all give the same result: a region tally (for a thin spherical shell at radius=100 cm); a point detector tally at $(x,y,z)=(100,0,0)$. For the source, the Watt spectrum with constants $\alpha = 1.025$ MeV, $b = 2.926/\text{MeV}$ was used.

$$p(E) = ce^{-E/\alpha} \sinh(\sqrt{bE}) . \quad (3.4)$$

The measurements listed in the paper were normalized such that the total flux at the detector (at $r=100$ cm) without the iron shield would have been $1 \text{ n/cm}^2/\text{s}$. In Monaco, the source strength was set to a strength of $4\pi(100)^2 = 125664 \text{ n/s}$. No biasing was used, other than implicit capture. The geometry is shown in Fig. 1 of Ref. 11.

Results for ENDF/B-VI.8 are depicted in Figs. 3.53 and 3.54. Results for ENDF/B-VII.0 are shown in Figs. 3.55 and 3.56.

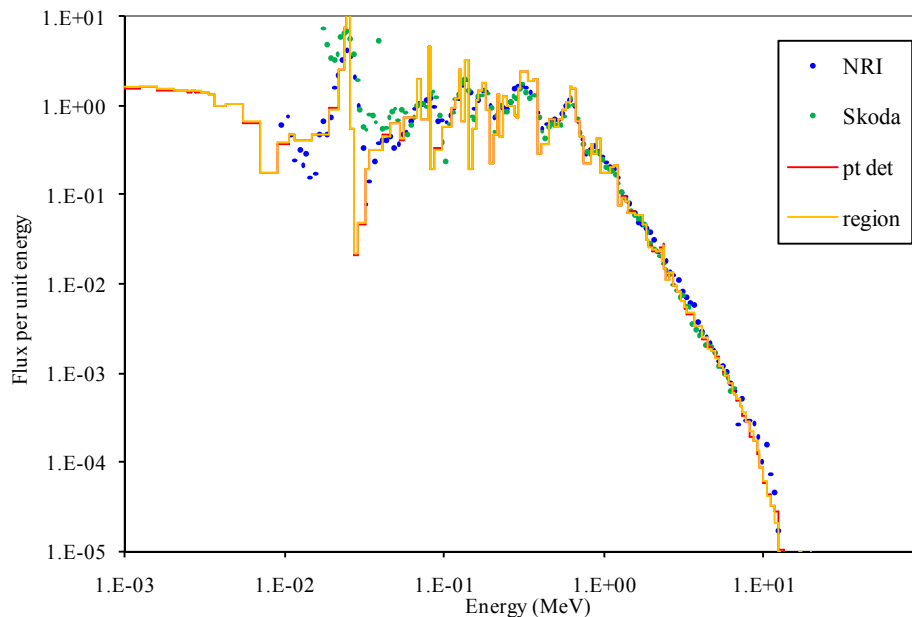


Fig. 3.53 Monaco output (ENDF/B-VI.8 fine-group library) for total flux at 10 cm using two different tallies compared to the two sets of measured data.

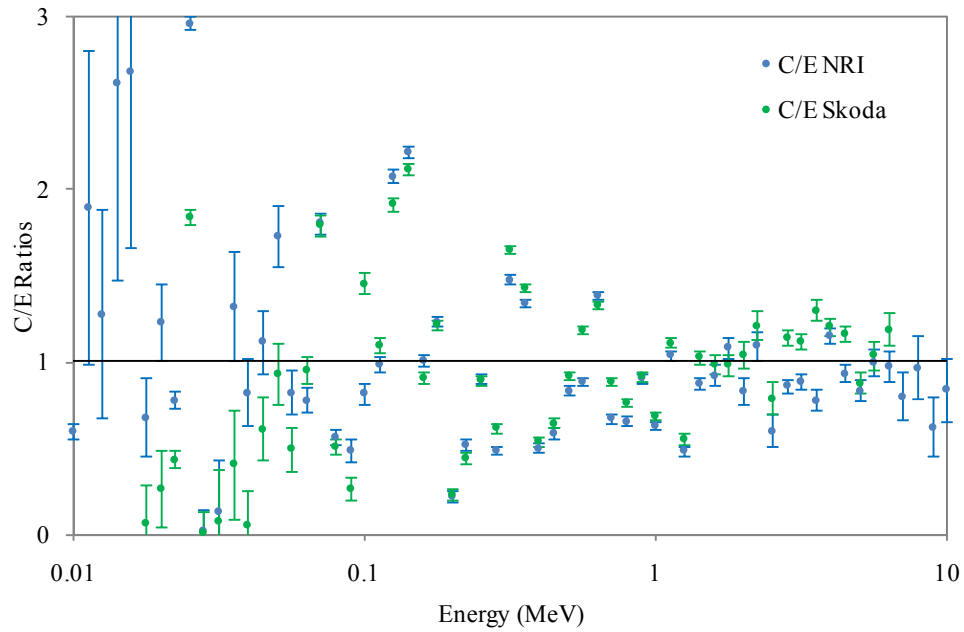


Fig. 3.54 Ratios of the Monaco (ENDF/B-VI.8 fine-group library) point detector tally to the measured fluxes.

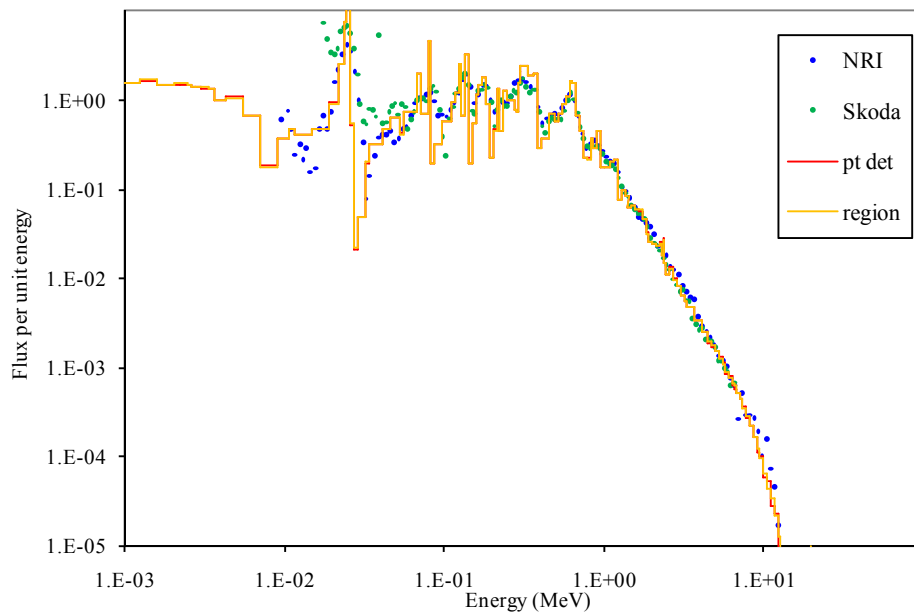


Fig. 3.55 Monaco output (ENDF/B-VII.0 fine-group library) for total flux at 10 cm using two different tallies compared to the two sets of measured data.

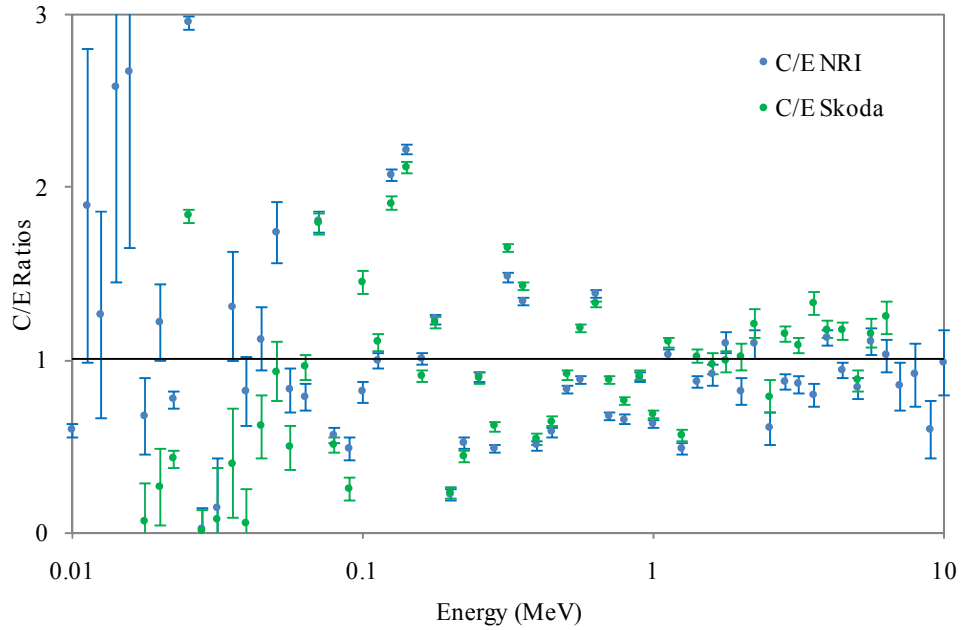


Fig. 3.56 Ratios of the Monaco (ENDF/B-VII.0 fine-group library) point detector tally to the measured fluxes.

3.2.5 Systematic evaluation of neutron shielding effects for materials

3.2.5.1 Experimental overview

Transmission of neutrons from a ^{252}Cf source through different thicknesses of five different materials was measured to determine their shielding effectiveness.¹² Combinations of steel and polyethylene were also measured to determine the change in shielding effectiveness on the order of the materials. The detector used was an Aloka moderator-type survey meter, made of polyethylene, which is supposed to mimic the human dose response. The data presented by Ueki et al.¹² was corrected for room scatter. An example of one experiment is shown in Fig. 3.57.

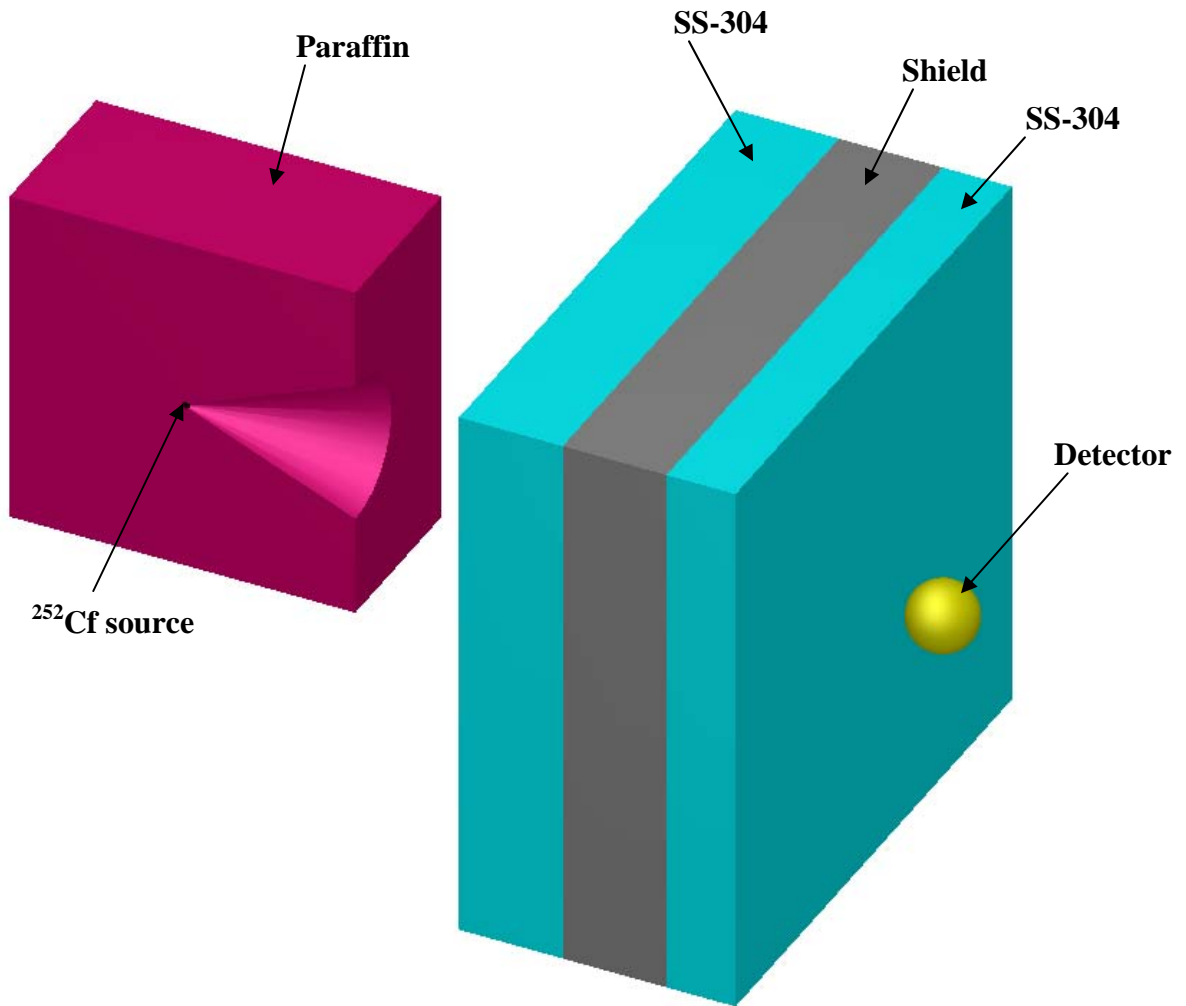


Fig. 3.57 Neutron shielding experiment example (half of paraffin removed to show source inside cone).

3.2.5.2 MCNP simulations

Polyethylene proved problematic for MCNP simulations. Reported results show good correlation with the findings of Ueki et al. for all materials except polyethylene.^{13–15}

3.2.5.3 MAVRIC calculations

For penetration through thick shields, the MAVRIC sequence and the CADIS methodology were used. For each experiment, an adjoint calculation using GTRUNC/Denovo was performed using the new ENDF/B-VII.0 broad-group library. An importance map and a biased source distribution were calculated by MAVRIC from the adjoint fluxes. The Monaco simulation used the new ENDF/B-VI.8 fine-group shielding library and the importance map, but not the biased source distribution, so that the ^{252}Cf spectral shape would be better preserved with the fine-group library. Adjoint calculations typically took 6–10 minutes and the Monaco calculations typically took 10–13 minutes each, and all had less than 4% statistical uncertainties.

3.2.5.4 Results

MAVRIC calculations match the type 1 experiments (single shield) within $\pm 20\%$, except for polyethylene. MAVRIC does not match the type 2 or type 3 experiments, probably due to the polyethylene component. Similar difficulties were observed with MCNP calculations.

Type 1 Experiment: Single material. Experiment geometries are shown in Fig. 1 of Ref. 12. Results are shown in Fig. 3.58.

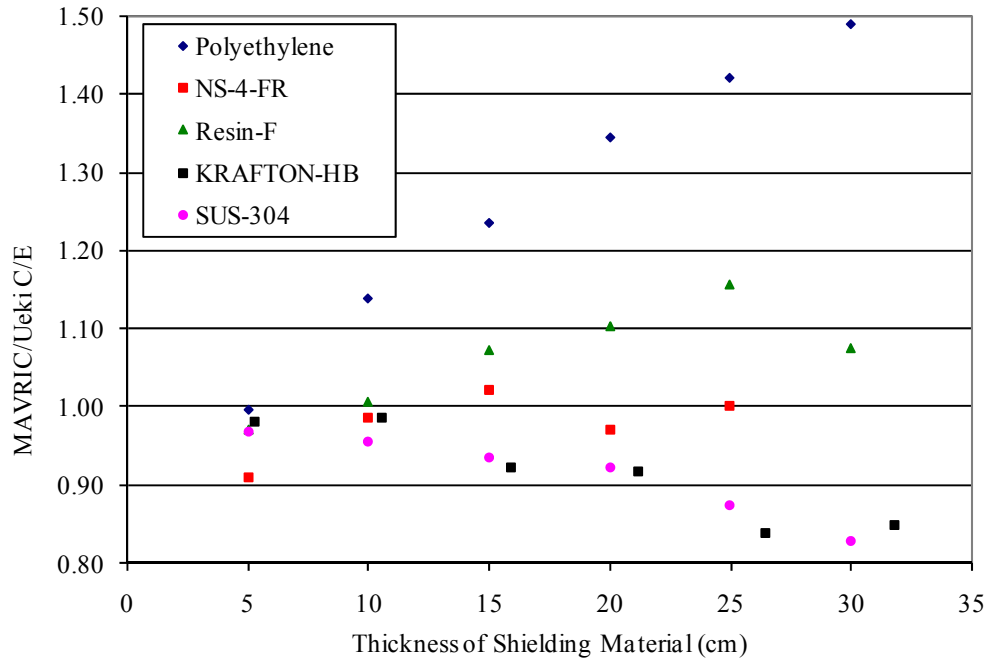


Fig. 3.58 Ratio of MAVRIC calculation of neutron detector dose rate to experimental measurement.

Type 2 Experiment: Stainless steel and polyethylene. Experiment geometries are shown in Ref. 12. Results are shown in Figs. 3.59 and . 3.60.

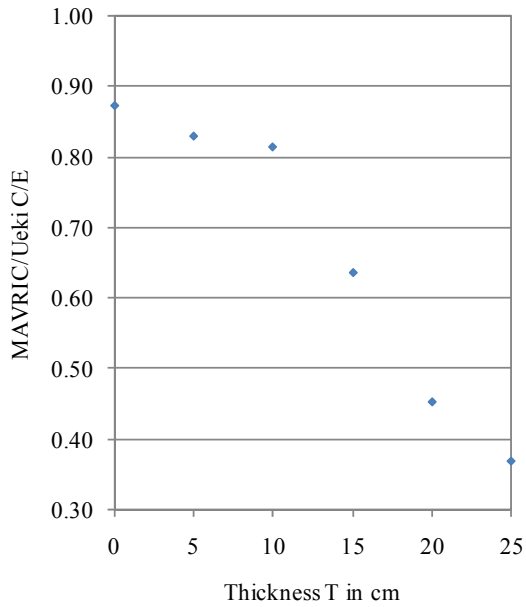


Fig. 3.59 Type 2a results—25 cm of stainless steel first, then polyethylene.

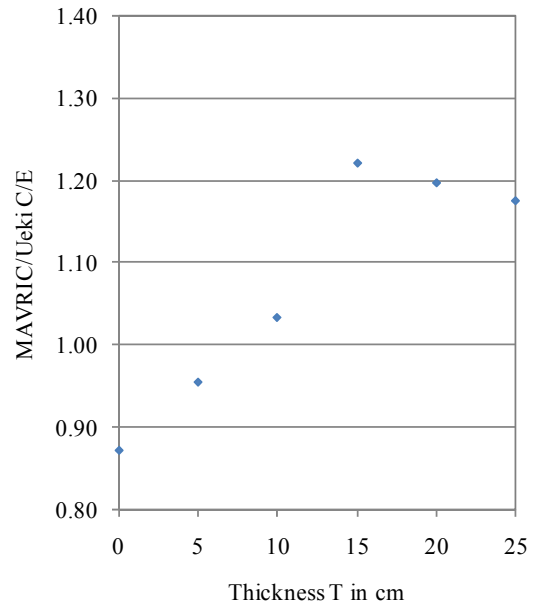


Fig. 3.60 Type 2b results—polyethylene, then 25 cm of stainless steel.

Type 3 Experiment: Polyethylene sandwiched in stainless steel. Experiment geometries are shown in Ref. 12. Results are depicted in Fig. 3.61.

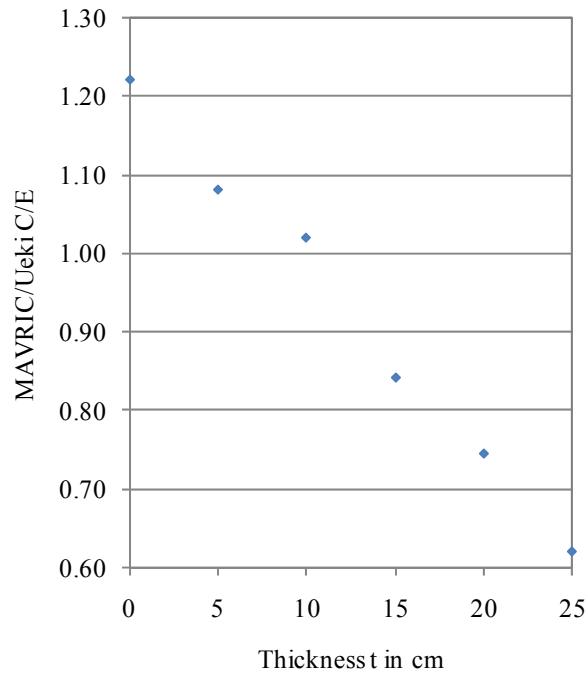


Fig. 3.61 Type 3 results for polyethylene fixed at a thickness of 15 cm.

4 SUMMARY

Coupled neutron-gamma libraries have been developed for SCALE based on ENDF/B-VI.8 and ENDF/B-VII.0 cross-section evaluations. The AMPX cross-section processing system was used for all library generation tasks for SCALE. ENDF/B-VI.8 and ENDF/B-VII.0 fine-group libraries were generated using 200 neutron and 47 gamma groups. The neutron group structure is identical to the 199-group VITAMIN-B6 structure except an additional neutron group has been added to extend the top energy boundary to 20 MeV. In addition to the fine-group libraries, a broad-group ENDF/B-VII.0 library has been generated using a 27 neutron and 19 gamma group structure. The broad-group library is primarily used to perform adjoint discrete ordinates calculations needed to prepare importance maps and a biased source distribution for biasing the forward Monte Carlo calculations. The SCALE shielding libraries have the following features.

- The multigroup neutron data were generated using a weighting function that has the form of a Maxwellian— $1/E$ —fission spectrum— $1/E$ above 10 MeV. This spectrum is consistent with the 238-group ENDF/B-VI library that was distributed with SCALE 5.1.
- Full-range Bondarenko factors are provided for all nuclides, thereby enabling faster neutron resonance self-shielding calculations using the narrow resonance approximation.
- Response functions consistent with previous SCALE libraries are maintained in the new shielding libraries.

As part of rigorous differential data testing activities, the AMPX code system was used to process all ENDF/B evaluations on three computing platforms: DEC Alpha Tru64, 32-bit Linux, and 64-bit Intel Mac. Because of the differences between compilers, experience has shown that different results can be obtained with different computing platforms. The use of the three platforms provided confirmatory checks of the cross-section processing calculations. In addition, independent verifications were performed between the AMPX results and results obtained with the NJOY code system for 1-D and 2-D processes. In general, the AMPX-NJOY comparisons show good agreement for the 1-D and 2-D processes. Although some differences have been observed between the independent processing systems, the overall agreement is good. The independent processing code comparisons provide additional verification checks for the differential cross-section data.

To complete the library testing effort, radiation transport calculations were performed with the SCALE shielding codes Monaco and MAVRIC using the coupled libraries to simulate several shielding benchmark calculations. Monaco/MAVRIC and the new ENDF/B-VI.8 and ENDF/B-VII.0 fine-group, coupled libraries matched experimental measurements well — in terms of transmission/attenuation values and spectral results. The ENDF/B-VII.0 broad-group library was not used in forward calculations but was used in creating importance maps for Monaco. Overall, the results obtained with MAVRIC/Monaco using the coupled libraries are good and demonstrate the effectiveness of the new SCALE methods and data capabilities for shielding applications.

5 REFERENCES

1. *SCALE: A Modular Code System for Performing Standardized Computer Analyses for Licensing Evaluation*, ORNL/TM-2005/39, Version 5.1, Vols. 1–III (November 2006). Available from Radiation Safety Information Computational Center at Oak Ridge National Laboratory as CCC-732.
2. National Nuclear Data Center (NNDC) at Brookhaven National Laboratory (BNL), Website <http://www.nndc.bnl.gov>
3. M. B. Chadwick et al., “ENDF/B-VII.0 Next Generation Evaluated Nuclear Data Library for Nuclear Science and Technology,” *Special Issue on Evaluated Nuclear Data File ENDF/B-VII.0 Nuclear Data Sheets* **107**(12), 2931–3059 (December 2006).
4. M. E. Dunn and N. M. Greene, “AMPX-2000: A Cross-Section Processing System for Generating Nuclear Data for Criticality Safety Applications,” *Trans. Am. Nucl. Soc.* **86**, 118–119 (2002).
5. *ENDF-102 Data Formats and Procedures for the Evaluated Nuclear Data File ENDF-6*, BNL-NCS-44945, Rev. 10/91 (ENDF/B-VI), Brookhaven National Laboratory (October 1991).
6. R. E. MacFarlane and D.W. Muir, *NJOY99.0 Code System for Producing Pointwise and Multigroup Neutron and Photon Cross Sections from ENDF/B Data*, PSR-480/NJOY99.0, Los Alamos National Laboratory, March 2000.
7. B. L. Broadhead et al., “Evaluation of Shielding Analysis Methods in Spent Fuel Cask Environments,” EPRI TR-104329, Electric Power Research Institute, Palo Alto, California, May 1995.
8. M. Nikolaev, N. Prokhorova, and T. Ivanova, “Neutron Fields in Three-Section Concrete Labyrinth from Cf-252 Source” (ALARM-CF-AIR-LAB-001), *International Handbook of Evaluated Criticality Safety Benchmark Experiments, Volume VIII — Criticality Alarm/Shielding Benchmarks*, NEA/NSC/DOC/(95)03, Organization for Economic Co-operation and Development — Nuclear Energy Agency (OECD-NEA) (September 2007).
9. G. Manturov, Y. Rozhikhin, and L. Trykov, “Neutron and Photon Leakage Spectra from Cf-252 Source at Centers of Six Iron Spheres of Different Diameters” (ALARM-CF-FE-SHIELD-001), *International Handbook of Evaluated Criticality Safety Benchmark Experiments, Volume VIII — Criticality Alarm/Shielding Benchmarks*, NEA/NSC/DOC/(95)03, Organization for Economic Co-operation and Development — Nuclear Energy Agency (OECD-NEA) (September 2007).
10. B. Jansky, Z. Turik, E. Novak, J. Kyncl, F. Cvachovec, and P. Tiller, “Comparison of Measured and Calculated Neutron Transmission Through Heavy Water for ^{252}Cf Source Placed in the Center of 30 cm Diameter Sphere,” *Annals of Nuclear Energy* **24**(15), 1189–1212 (1997).
11. E. Sajo, M. L. Williams, and M. Asgari, “Comparison of Measured and Calculated Neutron Transmission Through Steel for a ^{252}Cf Source,” *Annals of Nuclear Energy* **20**(9), 585–604 (1993).

12. K. Ueki, A. Ohashi, N. Nariyama, S. Nagayama, T. Fujita, K. Hattori, and Y. Anayama, "Systematic Evaluation of Neutron Shielding Effects for Materials," *Nucl. Sci. Eng.* **124**, 455–464 (1996).
13. D. A. Torres, R. D. Mosteller, and J. E. Sweezy, "Comparison of MCNP5 and Experimental Results on Neutron Shielding Effects for Materials," *ANS Annual Meeting*, Pittsburgh, PA, June 2004. *Trans. Am. Nucl. Soc.* **90**, 484–486 (2004).
14. D. A. Torres, B. Hehr, A. Sood, and R. D. Mosteller, "Comparison of MCNP5 Results with Experimental Measurements for Neutron-Shielding Materials," in *Proceedings of the American Nuclear Society's 14th Biennial Topical Meeting of the Radiation Protection and Shielding Division*, pp. 93–96, Carlsbad, New Mexico, April 3–6, 2006.
15. C. J. Solomon, A. Sood, and R. D. Mosteller, "A Study of A Polyethylene and Stainless Steel Composite Deep Shield Benchmark of MCNP," in *Proceedings of the American Nuclear Society's 14th Biennial Topical Meeting of the Radiation Protection and Shielding Division*, pp. 97–100, Carlsbad, New Mexico, April 3–6, 2006.

APPENDIX A

XML INPUT TEMPLATES

The input files used to run the AMPX program sequences are generated using an XML template. The XML templates used for the various tasks are reproduced here.

Input template to generate point-wise cross-section data

```

<!DOCTYPE InputData [
<!ENTITY polident_files "${RTNDR}/../neutron/writeData(tag)_polident">
<!ENTITY broaden_file "${RTNDR}/../neutron/writeData(tag)_broaden">
<!ENTITY weighting_file "${RTNDR}/../neutron/writeData(tag)_weight">

<!ENTITY home "input_neutron">
<!ENTITY case "&home;/writeData(tag)">
<!ENTITY batch "&home;/batch">

<!ENTITY ampx "/Users/dw8/ampx/mac/install/cmds/batcha">
]>

<InputData>
  <openFile name="&batch;"/>

  <writeFile name="&batch;">
<text>#!/bin/bash -x
</text>
</writeFile>

<loop restrict="+file3(yes) +neutron(yes)">
  <openFile name="&case;"/>
  <writeFile name="&case;">
<text>=shell
ln -sf writeData(tape) ft11f001      <!-- link ENDF tape in -->
end
=polident                            <!-- create point wise data -->
-1$$ 20000
0$$ 31 32 e 1$$ 1 t                  <!-- tab1 output on unit 31, file header info on unit 32
-->
2$$ writeData(endf) 11 2 6 e
4** a5 0.001 e                        <!-- generate grid with precision of epsilon=0.001 -->
6$$ a3 0 15000 t
end
=shell
cp ft31f001 &polident_files;
cp ft32f001 &polident_files;_ft32
end
=tgel      <!-- tgel to fix total cross section data -->
-1$$ 5000000
0$$ 31 33 e t  <!-- new file is on logical unit 33 -->
end
=broaden    <!-- broaden the data -->
limit=5000000
logpt=33 logdp=34      <!-- broadened data are on logical unit 34 -->
t= 0 300 600 900 1200 2400
end
=shell
cp ft34f001 &broaden_file;
end
=pickeze    <!-- pickeze -->
-1$$ 3000000
0$$ 34 35    <!-- pick T=300 from broadened file at unit=34 and write to unit 35 --
>
1$$ 1 0 0 1 0 e t
2$$ writeData(endf)

```

```

5** 300.0 t
end
=jergens          <!-- jergens  to generate desired flux -->
-1$$ all 3000000 e
0$$ 35 30 18 1$$ 2 t
3$$ 1 0 4 t
3$$ 1099 4 0 t
  2099 0 read 1.0 -1 0
  2099 0 save 0 0 0
  1099 2099 div 1.0 writeData(endf) 1
  1099 0 save 0 0 0
end
=shell
cp ft30f001 &weighting_file; <!-- save weighting spectrum -->
end
</text>

</writeFile>
<closeFile name="&case;"/>

  <writeFile name="&batch;">
<text>&ampx; writeData(tag)
</text>
  </writeFile>

</loop>

  <closeFile name="&batch;"/>
</InputData>

```

Input template to generate multigroup neutron and gamma cross-section data

```

<?xml version="1.0"?>
<!DOCTYPE InputData [

<!ENTITY polident_files "${RTNDIR}/../../../../neutron/writeData(tag)_polident">
<!ENTITY broaden_file "${RTNDIR}/../../../../neutron/writeData(tag)_broaden">
<!ENTITY weighting_file "${RTNDIR}/../../../../neutron/writeData(tag)_weight">
<!ENTITY x10_fast "${RTNDIR}/../neutron/writeData(tag)_fast">
<!ENTITY x10_yield "${RTNDIR}/../neutron/writeData(tag)_yield">
<!ENTITY group "${RTNDIR}/../groupStructure">

<!ENTITY mmel1 "32"> <!-- In y12 Lobatto quadrature angles for elastic scattering matrices
A<=180 -->
<!ENTITY mmel2 "8"> <!-- In y12 Lobatto quadrature angles for elastic scattering matrices
A>180 -->
<!ENTITY mmin1 "8"> <!-- In y12 Lobatto quadrature angles for discrete level inelastic
scattering matrices -->
<!ENTITY mmdf "8"> <!-- In y12 Number of Lobatto quadrature angles -->
<!ENTITY mmin2 "8"> <!-- In y12 Lobatto quadrature angles for discrete level inelastic
scattering matrices -->
<!ENTITY nl "5"> <!-- In y12 Number of legendre polynomilas to use -->

<!ENTITY igm "200"> <!-- number of neutron groups -->
<!ENTITY ipm "47"> <!-- number of gamma groups -->
<!ENTITY nlneutron "5"> <!-- The maximum order of Legendre fit to neutron scattering
processes -->
<!ENTITY nlyield "2"> <!-- The maximum order of Legendre fit to gamma-ray yield
processes -->
<!ENTITY nlgamma "5"> <!-- The maximum order of Legendre fit to gamma-ray interaction
scattering -->

<!ENTITY title "writeData(tag) writeData(endf) ENDFBV7 RELwriteData(rel) REVwriteData(rev)
MODwriteData(mod) AMPX writeData(date)">

<!ENTITY home "input_fast">
<!ENTITY case "&home;/writeData(tag)">

```

```

<!ENTITY batch "&home;/batch">

<!ENTITY ampx "~/ampx/mac/install/cmds/batcha">
]

<InputData>
  <openFile name="&batch;"/>

  <writeFile name="&batch;">
<text>#!/bin/bash -x
</text>a
</writeFile>

<loop restrict="+file3(yes) +neutron(yes) +neutron(yes)">
  <openFile name="&case;"/>
  <writeFile name="&case;">
<text>=shell
ln -sf writeData(tape) ft11f001
ln -sf &polident_files; ft31f001
ln -sf &broaden_file; ft34f001
ln -sf &weighting_file; ft30f001
ln -sf &group; ft47f001
</text>
<text>end
=y12 <!-- determine kinematic data -->
0$$ 32 11 0 0 <!-- kinematic data on unit 32, ENDF on 11. Generate no thermal neutron or
gamma data -->
1$$ writeData(endf)
2$$ 2 6 <!-- Endf file is BCD and ENDF version 6 -->
3$$ &mmel1; &mmel2; &mmin1; &mmdf; &mmin2; &nl; t
t
end
=pickeze <!-- pickeze -->
-1$$ 9000000
0$$ 34 35 <!-- pick T=300 from broadened file at unit=34 and write to unit 35 --
>
1$$ 1 0 0 1 0 e t
2$$ writeData(endf)
5** 300.0 t
end
</text>

<text>=x10
neutron <!-- x10 for yield -->
-1$$ 9000000
0$$ 1 30 35 32 <!-- Master on 1, weighting spectrum on 30, point data for T=300 on 35,
kinematic data in 32 -->
1$$ writeData(endf) &igm; 0 &ipm; &nlneutron; &nlyield; &nlgamma;
2$$ 99 2099 writeData(endf) writeData(endf) </text> <!-- flux data -->
<text restrict="file2(yes)">3** writeData(scattering)</text>
<text restrict="-file2(yes)">3** 0.0</text>
<text> 6$$ 99 2099 t
t
&title;
end
=rade <!-- use rade to check results -->
1$$ 1 e t
end
=shell
cp ft01f001 &x10_fast;
end
</text>

<text>=x10
yield
-1$$ 9000000
0$$ 71 30 35 32 <!-- Master on 71, weighting spectrum on 30, point data for T=300 on 35,
kinematic data in 32 -->
1$$ writeData(endf) &igm; 0 &ipm; &nlneutron; &nlyield; &nlgamma;

```

```

2$$ 99 2099 writeData(endf) writeData(endf) </text> <!-- flux data -->
<text restrict="+file2(yes)>3** writeData(scattering)</text>
<text restrict="-file2(yes)>3** 0.0</text>
<text> 6$$ 99 2099 t
t
&title;
end
=rade <!-- use rade to check results -->
1$$ 71 e t
end
=shell
cp ft71f001 &x10_yield;
end
</text>

</writeFile>
<closeFile name="&case;" />

<writeFile name="&batch;">
<text>&ampx; writeData(tag)
</text>
</writeFile>

</loop>

<closeFile name="&batch;" />

</InputData>

```

Input template to generate thermal cross-section data for moderators

```

<?xml version="1.0"?>
<!DOCTYPE InputData [
<!-- place where to put the kinematic data -->
<!ENTITY thermal_kinematics "${RTNDIR}/../thermal/writeData(tag)_kin">
<!-- place where to put the point-wise data -->
<!ENTITY thermal_point "${RTNDIR}/../thermal/writeData(tag)_point">
<!-- place for the master library -->
<!ENTITY thermal_master "${RTNDIR}/../thermal/writeData(tag)_master">
<!-- title to use for the library -->
<!ENTITY title "writeData(tag) writeData(endf) ENDFB V6 RELwriteData(rel) REVwriteData(rev)
MODwriteData(mod) AMPX writeData(date)">
<!ENTITY group "${RTNDIR}/../groupStructure">

<!ENTITY home "input_thermal">
<!ENTITY case "&home;/writeData(tag)">
<!ENTITY batch "&home;/batch">

<!ENTITY ampX "~/ampx/mac/install/cmds/batcha">
]>

<InputData>
<openFile name="&batch;" />

<writeFile name="&batch;">
<text>#!/bin/bash -x
</text>
</writeFile>

<loop restrict="file7(yes)"> <!-- only for evaluations that have file 7, i.e. have
thermal data -->
<openFile name="&case;" />
<writeFile name="&case;">
<text>=shell
ln -sf writeData(tape) ft11f001

```

```

ln -sf &group; ft47f001
end
=y12
0$$ 37 11 38 0 <!-- kinematics data will be on 37, ENDF is on 11, output for point-wise
data is 38 -->
1$$ writeData(endf) <!-- material to process -->
2$$ 2 6 <!-- endf format is BCD and ENDF version is 6 -->
3$$ 32 8 8 8 8 5 t <!-- Number of lobatto quadrutor: 32 for A <= 180, 8 otherwise;
Order of legendre fit is 5 -->
t
end
=shell <!-- save the kinematics data and the point-wise data -->
cp ft37f001 &thermal_kinematics;
cp ft38f001 &thermal_point;
end
=jergens <!-- generate weighting function -->
0$$ 11 30 18 <!-- external is endf , output is on unit 30 -->
1$$ 1 t <!-- Generate one function -->
3$$ 1099 0 2 t <!-- mt value of weighting function is 1099, and we generate Maxwellian -
1/E - fission spectrum -->
end
=x10
neutron <!-- calculate neutron interaction -->
0$$ 4 30 38 37 <!-- final on 4, jergens output on 30, y12 point-wise on 38, y12
kinematics output on 37 -->
1$$ writeData(endf) 200 34 <!-- new id, 200 neutron groups from that thermal
groups -->
0 <!-- no gamma groups -->
5 2 0 <!-- order of legendre polynomials -->
2$$ 99 1099 writeData(endf) writeData(endf) <!-- id of weighing function, kinematic data
and point-wise data -->
3** 0 t <!-- Potential Scattering Cross Section - 0 for all thermal runs since no file
2 -->
t
&title; <!-- title of the library -->
end
=shell
cp ft04f001 &thermal_master; <!-- copy master -->
end
=rade <!-- use rade to check results -->
1$$ 4 e t
end
=paleale <!-- use paleale to print results in ASCII -->
0$$ 4 e 2$$ 1 0 e 5$$ f 200 t
end
</text>

</writeFile>
<closeFile name="&case;"/>

<writeFile name="&batch;">
<text>&ampx; writeData(tag)
</text>
</writeFile>

</loop>

<closeFile name="&batch;"/>

</InputData>

```

Input template to generate thermal cross-section data for nonmoderators

```
<?xml version="1.0"?>
<!DOCTYPE InputData [
<!ENTITY weighting_file "${RTNDIR}/../neutron/writeData(tag)_weight">
<!ENTITY flange6 "${RTNDIR}/../neutron/writeData(tag)_flange6">
<!ENTITY group "${RTNDIR}/../groupStructure">

<!ENTITY igm "200">      <!-- number of neutron groups -->
<!ENTITY neg "34">      <!-- number of thermal groups -->

<!ENTITY home "input_bon">
<!ENTITY case "&home;/writeData(tag)">
<!ENTITY batch "&home;/batch">

<!ENTITY ampX "/home/dw8/ampx/build/install/cmds/batcha">
]>

<InputData>
  <openFile name="&batch;" />

  <writeFile name="&batch;">
<text>#!/bin/bash -x
</text>a
</writeFile>

<loop restrict="+file3(yes) +neutron(yes)">
  <openFile name="&case;" />
  <writeFile name="&case;">
<text>=shell
ln -sf &weighting_file; ft30f001
ln -sf &group; ft47f001
end
</text>

<text>=flange6 <!-- run flange6 -->
nl=3 za=writeData(za) awr=writeData(awr) </text>
<text restrict="file2(yes)">free=writeData(scattering) </text><text restrict="-
file2(yes)">free=0.0 </text>
<text>
mat=0 master=41 igm=200 neg=&neg;
t=300 t=600 t=900 t=1200 t=2100
end
=shell
cp ft41f001 &flange6;
end
</text>

</writeFile>
<closeFile name="&case;" />

  <writeFile name="&batch;">
<text>&amp;amp;px; writeData(tag)
</text>
</writeFile>

</loop>

<closeFile name="&batch;" />

</InputData>
```

Input template used to generate full-range Bondarenko data

```
<?xml version="1.0"?>
<!DOCTYPE InputData [
<!ENTITY polident_files "${RTNDIR}/../neutron/writeData(tag)_polident">
<!ENTITY weighting_file "${RTNDIR}/../neutron/writeData(tag)_weight">
<!ENTITY prude "${RTNDIR}/../neutron/writeData(tag)_prude">
<!ENTITY fabulous "${RTNDIR}/../neutron/writeData(tag)_fabulous">
<!ENTITY group "${RTNDIR}/../groupStructure">

<!ENTITY igm "200">      <!-- number of neutron groups -->
<!ENTITY neg "34">      <!-- number of thermal groups -->

<!ENTITY home "input_bon">
<!ENTITY case "&home;/writeData(tag)">
<!ENTITY batch "&home;/batch">

<!ENTITY ampx "~/ampx/mac/install/cmds/batcha">
]>

<InputData>
  <openFile name="&batch;" />

  <writeFile name="&batch;">
<text>#!/bin/bash -x
</text>a
</writeFile>

<loop restrict="+file3(yes) +neutron(yes)">
  <openFile name="&case;" />
  <writeFile name="&case;">
<text>=shell
ln -sf writeData(tape) ft11f001
ln -sf &polident_files; ft31f001
ln -sf &weighting_file; ft30f001
ln -sf &group; ft47f001
end
</text>

<!-- run prude if unresolved -->
<text restrict="unresolved(yes)">=prude
0$$ 36      <!-- output will be on unit 36 -->
1$$ 1 t      <!-- and we process one material -->
2$$ writeData(endf) 9 3 11 2 t <!-- process 9 sigma values, 3 temperatures. Endf file is on
11 and BCD -->
3** 1+8 1+6 1+5 1+4 1000 100 10 1 1-6 <!-- the 9 sigma values -->
4** 300.0 900.0 2000.0 e      <!-- the 3 temperatures -->
5** 0 1 e t
end
=shell
cp ft36f001 &prude;
end
</text>

<text>=tgel
-1$$ 9000000
0$$ 31 32 e t
end
</text>

<text>=fabulous <!-- generate full range bondarenko factors -->
Title Card for FABULOUS case <!-- title for master -->
-1$$ 2500000
0$$ 2 32 30 </text> <!-- master output=2, point data = 37, flux = 30 -->
<!-- unit of unresolved data if present is 36, 0 otherwise -->
<text restrict="unresolved(yes)">36 </text>
```

```

<text>e
1$$ writeData(endf) writeData(endf) 3 9 &igm; <!-- id on master, endf material to process,
number of temps, number of sigs -->
2$$ 99 2099 <!-- where to find the weighting function -->
5** writeData(awr) 0.0001 t <!-- mass ratio and to what precision to calculate -->
8** 300.0 900.0 2000.0 <!-- the 3 temperatures -->
9** 1+8 1+6 1+5 1+4 1000 100 10 1 1-6 <!-- the 9 sigma values -->
t
end
=shell
cp ft02f001 &fabulous;
end
</text>

</writeFile>
<closeFile name="&case;"/>

<writeFile name="&batch;">
<text>&ampx; writeData(tag)
</text>
</writeFile>

</loop>

<closeFile name="&batch;"/>

</InputData>

```

Input template used to process gamma cross-section data

```

<?xml version="1.0"?>
<!DOCTYPE InputData [
<!-- place where to put the kinematic data -->
<!ENTITY gamma_kinematics "${RTNDIR}/../gamma/writeData(tag)_kin">
<!-- place where to put the point-wise data -->
<!ENTITY gamma_point "${RTNDIR}/../gamma/writeData(tag)_point">
<!-- place for the master library -->
<!ENTITY gamma_master "${RTNDIR}/../gamma/writeData(tag)_master">
<!-- title to use for the library -->
<!ENTITY title "writeData(tag) writeData(endf) ENDFB V6 RELwriteData(rel) REVwriteData(rev)
MODwriteData(mod) AMPX writeData(date)">

<!ENTITY home "input_gamma">
<!ENTITY case "&home;/writeData(tag)">
<!ENTITY batch "&home;/batch">

<!ENTITY ampX "~/ampx/mac/install/cmds/batcha">
]>

<InputData>
<openFile name="&batch;"/>

<writeFile name="&batch;">
<text>#!/bin/bash -x
</text>
</writeFile>

<loop restrict="-neutron(yes)">
<openFile name="&case;"/>
<writeFile name="&case;">
<text>=shell
ln -sf writeData(tape) ft11f001
end
=y12

```

```

0$$ 32 11 31 0 <!-- kinematics data will be on 32, ENDF is on 11, output for point-wise
data is 31 -->
1$$ writeData(endf) <!-- material to process -->
2$$ 2 6 <!-- endf format is BCD and ENDF version is 6 -->
3$$ 32 8 8 8 8 5 t <!-- Number of lobatto quadrutor: 32 for A <= 180, 8 otherwise;
Order of legendre fit is 5 -->
t
end
=shell <!-- save the kinematics data and the point-wise data -->
cp ft32f001 &gamma_kinematics;
cp ft31f001 &gamma_point;
end
=jergens <!-- generate weighting function -->
0$$ 0 30 18 <!-- no external data needed, output is on unit 30 -->
1$$ 1 <!-- Generate one function -->
2** 1.0e3 3.0e7 t <!-- generate weighting function from 1e-3 to 3e7 -->
3$$ 1599 0 11 t <!-- mt value of weighting function is 1599, and we generate 1/E with
"rolloff" gamma weighting -->
end
=x10
gamma <!-- calculate gamma-ray interaction -->
0$$ 1 30 31 32 <!-- final on 1, jergens output on 30, y12 point-wise on 31 y12 kinematics
output on 32 -->
1$$ writeData(endf) 0 0 <!-- new id, no neutron or thermal groups -->
47 <!-- 47 gamma groups -->
0 0 5 <!-- order of legendre polynomials -->
2$$ 99 1599 writeData(endf) writeData(endf) <!-- id of weighing function, kinematic data
and point-wise data -->
3** 0.0 t <!-- Potential Scattering Cross Section -->
7** 2.0E+7 1.4E+7 1.2E+7 1.E+7 8.E+6 <!-- group
structure -->
7.5E+6 7.E+6 6.5E+6 6.E+6 5.5E+6
5.0E+6 4.5E+6 4.E+6 3.5E+6 3.E+6
2.75E+6 2.5E+6 2.35E+6 2.15E+6 2.E+6
1.8E+6 1.66E+6 1.57E+6 1.5E+6 1.44E+6
1.33E+6 1.2E+6 1.E+6 9.0E+5 8.0E+5
7.0E+5 6.0E+5 5.12E+5 5.1E+5 4.5E+5
4.0E+5 3.0E+5 2.6E+5 2.0E+5 1.5E+5
1.0E+5 7.5E+4 7.0E+4 6.0E+4 4.5E+4
3.0E+4 2.0E+4 1.0E+4 e
t
&title; <!-- title of the library -->
end
=shell
cp ft01f001 &gamma_master; <!-- copy master -->
end
=rade <!-- use rade to check results -->
1$$ 1 e t
end
=paleale <!-- use paleale to print results in ASCII -->
0$$ 1 e 2$$ 0 1 e 4$$ 502 504 e 5$$ f 47 t
end
</text>

</writeFile>
<closeFile name="&case;" />

<writeFile name="&batch;">
<text>&ampx; writeData(tag)
</text>
</writeFile>

</loop>

<closeFile name="&batch;" />

</InputData>

```

Input template to generate the AMPX master for nonmoderator evaluations

```

<?xml version="1.0"?>

<!DOCTYPE InputData [
<!ENTITY fast "${RTNDIR}/../neutron/writeData(tag)_fast">
<!ENTITY yield "${RTNDIR}/../neutron/writeData(tag)_yield">
<!ENTITY fabulous "${RTNDIR}/../neutron/writeData(tag)_fabulous">
<!ENTITY flange6 "${RTNDIR}/../neutron/writeData(tag)_flange6">
<!ENTITY gamma "${RTNDIR}/../gamma/writeData(taggamma)_master">
<!ENTITY title "writeData(tag) writeData(endf) ENDFB6 RELwriteData(rel) REVwriteData(rev)
MODwriteData(mod) AMPX writeData(date)">

<!ENTITY neutron_final "${RTNDIR}/../master/writeData(tag)_neutron">

<!ENTITY home "input_stitch">
<!ENTITY case "&home;/writeData(tag)">
<!ENTITY batch "&home;/batch">

<!ENTITY ampx "~/ampx/mac/install/cmds/batcha">
]>

<InputData>
  <openFile name="&batch;"/>

  <writeFile name="&batch;">
<text>#!/bin/bash -x
</text>
</writeFile>

<loop restrict="+file3(yes) +neutron(yes) -file7(yes)"> <!-- restrict to non-moderator
data -->
  <openFile name="&case;"/>
  <writeFile name="&case;">
<text>=shell
ln -sf &fast; ft01f001          <!-- fast neutron data -->
ln -sf &yield; ft02f001         <!-- gamma yield data -->
ln -sf &fabulous; ft03f001      <!-- bondarenko data -->
ln -sf &flange6; ft04f001       <!-- thermal scattering data -->
</text>
<text restrict="gamma">ln -sf &gamma; ft05f001    <!-- add gamma evaluation if present -->
</text>
<text>end
</text>

<!-- run simonize to combine data -->
<text>=simonize
Identifier=writeData(changedza) master=20 source=endf    <!-- change to -->
title= &title;
id45=writeData(scaleid) id46=0 </text>

<!-- add gamma values if available -->
<text restrict="gamma"> id47=writeData(scaleidgamma) </text>
<text restrict="-gamma"> id47=0 </text>

<text restrict="AWP0(yes) file12(yes) file13(yes)"> id48=writeData(scaleid) </text>
<text restrict="-AWP0(yes) -file12(yes) -file13(yes)"> id48=0 </text>

<!-- make sure simonize has at least one neutron flag to move over id data -->
<text>
neutron=1 id19=writeData(endf)          <!-- fast neutron data - always present -->
</text>
<text> yield=2 id19=writeData(endf) <!-- yield data if present -->

```

```

</text>
<text restrict="nis(0) nis(1)"> BONDARENKO=3 id19=writeData(endf) <!-- bondarenko data if
present -->
</text>
<text>2dn=4 id19=writeData(za) <!-- thermal scattering data - always present -->
</text>
<text restrict="gamma">gamma=5 id19=writeData(endfgamma) <!-- add the gamma data if present
-->
</text>
<text>end
</text>

<!-- copy final result -->
<text>
=rade
l$$ 20 e t
end
=shell
cp ft20f001 &neutron_final;
end
</text>

</writeFile>
<closeFile name="&case;" />

<writeFile name="&batch;">
<text>&ampx; writeData(tag)
</text>
</writeFile>

</loop>

<closeFile name="&batch;" />
</InputData>

```

Input template to generate the AMPX master for moderator evaluations

```

<?xml version="1.0"?>
<!DOCTYPE InputData [
<!ENTITY fast "${RTNDIR}/../neutron/writeData(tag)_fast">
<!ENTITY yield "${RTNDIR}/../neutron/writeData(tag)_yield">
<!ENTITY fabulous "${RTNDIR}/../neutron/writeData(tag)_fabulous">
<!ENTITY flange6 "${RTNDIR}/../neutron/writeData(tag)_flange6">
<!ENTITY gamma "${RTNDIR}/../gamma/writeData(taggamma)_master">
<!ENTITY title "writeData(tag) writeData(endf) ENDFB6 RELwriteData(rel) REVwriteData(rev)
MODwriteData(mod) AMPX writeData(date)">

<!ENTITY neutron_final "${RTNDIR}/../master/writeData(tag)_neutron">

<!ENTITY home "input_stitch">
<!ENTITY case "&home;/writeData(tag)">
<!ENTITY batch "&home;/batch">

<!ENTITY ampx "~/ampx/mac/install/cmds/batcha">
]>

<InputData>
<openFile name="&batch;" />

<writeFile name="&batch;">
<text>#!/bin/bash -x

```

```

</text>
</writeFile>

<loop restrict="+file3(yes) +neutron(yes) -file7(yes)"> <!-- restrict to non-moderator
data -->
  <openFile name="&case;"/>
  <writeFile name="&case;">
  <text>=shell
  ln -sf &fast; ft01f001          <!-- fast neutron data -->
  ln -sf &yield; ft02f001         <!-- gamma yield data -->
  ln -sf &fabulous; ft03f001     <!-- bondarenko data -->
  ln -sf &flange6; ft04f001     <!-- thermal scattering data -->
  </text>
  <text restrict="gamma">ln -sf &gamma; ft05f001 <!-- add gamma evaluation if present -->
  </text>
  <text>end
  </text>

  <!-- run simonize to combine data -->
  <text>=simonize
  Identifier=writeData(changedza) master=20 source=endf <!-- change to -->
  title= &title;
  id45=writeData(scaleid) id46=0 </text>

  <!-- add gamma values if available -->
  <text restrict="gamma"> id47=writeData(scaleidgamma) </text>
  <text restrict="-gamma"> id47=0 </text>

  <text restrict="AWP0(yes) file12(yes) file13(yes)"> id48=writeData(scaleid) </text>
  <text restrict="-AWP0(yes) -file12(yes) -file13(yes)"> id48=0 </text>

  <!-- make sure simonize has at least one neutron flag to move over id data -->
  <text>
  neutron=1 id19=writeData(endf) <!-- fast neutron data - always present -->
  </text>
  <text> yield=2 id19=writeData(endf) <!-- yield data if present -->
  </text>
  <text restrict="nis(0) nis(1)"> BONDARENKO=3 id19=writeData(endf) <!-- bondarenko data if
  present -->
  </text>
  <text>2dn=4 id19=writeData(za) <!-- thermal scattering data - always present -->
  </text>
  <text restrict="gamma">gamma=5 id19=writeData(endfgamma) <!-- add the gamma data if present
  -->
  </text>
  <text>end
  </text>

  <!-- copy final result -->
  <text>
  =rade
  l$$ 20 e t
  end
  =shell
  cp ft20f001 &neutron_final;
  end
  </text>

  </writeFile>
  <closeFile name="&case;"/>

  <writeFile name="&batch;">
  <text>&ampx; writeData(tag)
  </text>
  </writeFile>

</loop>

```

```
<closeFile name="&batch;" />  
</InputData>
```


APPENDIX B

EVALUATIONS INCLUDED IN ENDF/B-VI.8 LIBRARY

Evaluations included in the multigroup library for ENDF/B-VI.8 are listed in Table B.1.

Table B.1 Evaluations and IDs used for the ENDF/B-VI.8 library

Nuclide	ID	Photon yield data	Full range self-shielding factors	Corresponding photon data
h-1	1801	yes	yes	h
h-2	1802	yes	yes	h
h-3	1003		yes	h
he-3	2003		yes	he
he-4	2004		yes	he
li-6	3006	yes	yes	li
li-7	3007	yes	yes	li
be-9	4009	yes	yes	be
b-10	5010	yes	yes	b
b-11	5011	yes	yes	b
c	6000	yes	yes	c
n-14	7014	yes	yes	n
n-15	7015	yes	yes	n
o-16	8016	yes	yes	o
o-17	8017		yes	o
f-19	9019	yes	yes	f
na-23	11023	yes	yes	na
mg	12000	yes	yes	mg
al-27	13027	yes	yes	al
si 1	4000	yes	yes	si
si-28	14028	yes	yes	si
si-29	14029	yes	yes	si
si-30	14030	yes	yes	si
p-31	15031	yes	yes	p
s	16000	yes		s
s-32	16032	yes	yes	s
cl	17000	yes	yes	cl
cl-35	17035	yes	yes	cl
cl-37	17037	yes	yes	cl
k	19000	yes	yes	k
ca	20000	yes	yes	ca
sc-45	21045	yes	yes	sc
ti	22000	yes	yes	ti
v	23000	yes		v
cr-50	24050	yes	yes	cr
cr-52	24052	yes	yes	cr
cr-53	24053	yes	yes	cr
cr-54	24054	yes	yes	cr
mn-55	25055	yes	yes	mn
fe-54	26054	yes	yes	fe
fe-56	26056	yes	yes	fe
fe-57	26057	yes	yes	fe
fe-58	26058	yes	yes	fe

Table B.1 Evaluations and IDs used for the ENDF/B-VI.8 library (continued)

Nuclide	ID	Photon yield data	Full range self-shielding factors	Corresponding photon data
co-59	27059	yes	yes	co
ni-58	28058	yes	yes	ni
ni-60	28060	yes	yes	ni
ni-61	28061	yes	yes	ni
ni-62	28062	yes	yes	ni
ni-64	28064	yes	yes	ni
cu-63	29063	yes	yes	cu
cu-65	29065	yes	yes	cu
ga	31000	yes	yes	ga
ge-72	32072		yes	ge
ge-73	32073		yes	ge
ge-74	32074		yes	ge
ge-76	32076		yes	ge
as-75	33075		yes	as
se-74	34074		yes	se
se-76	34076		yes	se
se-77	34077		yes	se
se-78	34078		yes	se
se-80	34080		yes	se
se-82	34082		yes	se
br-79	35079		yes	br
br-81	35081		yes	br
kr-78	36078		yes	kr
kr-80	36080		yes	kr
kr-82	36082		yes	kr
kr-83	36083		yes	kr
kr-84	36084		yes	kr
kr-85	36085		yes	kr
kr-86	36086		yes	kr
rb-85	37085		yes	rb
rb-86	37086		yes	rb
rb-87	37087		yes	rb
sr-84	38084		yes	sr
sr-86	38086		yes	sr
sr-87	38087		yes	sr
sr-88	38088		yes	sr
sr-89	38089		yes	sr
sr-90	38090		yes	sr
y-89	39089	yes	yes	y
y-90	39090		yes	y
y-91	39091		yes	y
zr	40000			zr
zr-90	40090		yes	zr
zr-91	40091		yes	zr
zr-92	40092		yes	zr
zr-93	40093		yes	zr
zr-94	40094		yes	zr
zr-95	40095		yes	zr
zr-96	40096		yes	zr
nb-93	41093	yes	yes	nb

Table B.1 Evaluations and IDs used for the ENDF/B-VI.8 library (continued)

Nuclide	ID	Photon yield data	Full range self-shielding factors	Corresponding photon data
nb-94	41094		yes	nb
nb-95	41095		yes	nb
mo	42000	yes		mo
mo-94	42094		yes	mo
mo-95	42095		yes	mo
mo-96	42096		yes	mo
mo-97	42097		yes	mo
mo-99	42099		yes	mo
tc-99	43099		yes	tc
ru-96	44096		yes	ru
ru-98	44098		yes	ru
ru-99	44099		yes	ru
ru-100	44100		yes	ru
ru-101	44101		yes	ru
ru-102	44102		yes	ru
ru-103	44103		yes	ru
ru-104	44104		yes	ru
ru-105	44105		yes	ru
ru-106	44106		yes	ru
rh-103	45103		yes	rh
rh-105	45105		yes	rh
pd-102	46102	yes	yes	pd
pd-104	46104	yes	yes	pd
pd-105	46105	yes	yes	pd
pd-106	46106	yes	yes	pd
pd-107	46107		yes	pd
pd-108	46108	yes	yes	pd
pd-110	46110	yes	yes	pd
ag-107	47107		yes	ag
ag-109	47109		yes	ag
ag-111	47111		yes	ag
cd	48000		yes	cd
cd-106	48106		yes	cd
cd-108	48108		yes	cd
cd-110	48110		yes	cd
cd-111	48111		yes	cd
cd-112	48112		yes	cd
cd-113	48113		yes	cd
cd-114	48114		yes	cd
cd-115	48601		yes	cd
cd-116	48116		yes	cd
in	49000	yes		in
in-113	49113		yes	in
sn-112	50112		yes	sn
sn-114	50114		yes	sn
sn-115	50115		yes	sn
sn-116	50116		yes	sn
sn-117	50117		yes	sn
sn-118	50118		yes	sn
sn-119	50119		yes	sn
sn-120	50120		yes	sn

Table B.1 Evaluations and IDs used for the ENDF/B-VI.8 library (continued)

Nuclide	ID	Photon yield data	Full range self-shielding factors	Corresponding photon data
sn-122	50122		yes	sn
sn-123	50123		yes	sn
sn-124	50124		yes	sn
sn-125	50125		yes	sn
sn-126	50126		yes	sn
sb-121	51121		yes	sb
sb-123	51123		yes	sb
sb-124	51124		yes	sb
sb-125	51125		yes	sb
sb-126	51126		yes	sb
te-120	52120		yes	te
te-122	52122		yes	te
te-123	52123		yes	te
te-124	52124		yes	te
te-125	52125		yes	te
te-126	52126		yes	te
te-127	52601		yes	te
te-128	52128		yes	te
te-129	52611		yes	te
te-130	52130		yes	te
te-132	52132		yes	te
i-127	53127	yes	yes	i
i-129	53129		yes	i
i-130	53130		yes	i
i-131	53131		yes	i
i-135	53135		yes	i
xe-124	54124		yes	xe
xe-126	54126		yes	xe
xe-128	54128		yes	xe
xe-129	54129		yes	xe
xe-130	54130		yes	xe
xe-131	54131		yes	xe
xe-132	54132		yes	xe
xe-133	54133		yes	xe
xe-134	54134		yes	xe
xe-135	54135		yes	xe
xe-136	54136		yes	xe
cs-133	55133		yes	cs
cs-134	55134		yes	cs
cs-135	55135		yes	cs
cs-136	55136		yes	cs
cs-137	55137		yes	cs
ba-134	56134		yes	ba
ba-135	56135		yes	ba
ba-136	56136		yes	ba
ba-137	56137		yes	ba
ba-138	56138	yes	yes	ba
ba-140	56140		yes	ba
la-139	57139		yes	la
la-140	57140		yes	la
ce-140	58140		yes	ce

Table B.1 Evaluations and IDs used for the ENDF/B-VI.8 library (continued)

Nuclide	ID	Photon yield data	Full range self-shielding factors	Corresponding photon data
ce-141	58141		yes	ce
ce-142	58142		yes	ce
ce-143	58143		yes	ce
ce-144	58144		yes	ce
pr-141	59141		yes	pr
pr-142	59142		yes	pr
pr-143	59143		yes	pr
nd-142	60142		yes	nd
nd-143	60143		yes	nd
nd-144	60144		yes	nd
nd-145	60145		yes	nd
nd-146	60146		yes	nd
nd-147	60147		yes	nd
nd-148	60148		yes	nd
nd-150	60150		yes	nd
pm-147	61147		yes	pm
pm-148	61148		yes	pm
pm-148	61601		yes	pm
pm-149	61149		yes	pm
pm-151	61151		yes	pm
sm-144	62144		yes	sm
sm-147	62147		yes	sm
sm-148	62148		yes	sm
sm-149	62149		yes	sm
sm-150	62150		yes	sm
sm-151	62151		yes	sm
sm-152	62152		yes	sm
sm-153	62153		yes	sm
sm-154	62154		yes	sm
eu-151	63151	yes	yes	eu
eu-152	63152		yes	eu
eu-153	63153	yes	yes	eu
eu-154	63154		yes	eu
eu-155	63155		yes	eu
eu-156	63156		yes	eu
eu-157	63157		yes	eu
gd-152	64152		yes	gd
gd-154	64154		yes	gd
gd-155	64155		yes	gd
gd-156	64156		yes	gd
gd-157	64157		yes	gd
gd-158	64158		yes	gd
gd-160	64160		yes	gd
tb-159	65159		yes	tb
tb-160	65160		yes	tb
dy-160	66160		yes	dy
dy-161	66161		yes	dy
dy-162	66162		yes	dy
dy-163	66163		yes	dy
dy-164	66164		yes	dy
ho-165	67165	yes	yes	ho

Table B.1 Evaluations and IDs used for the ENDF/B-VI.8 library (continued)

Nuclide	ID	Photon yield data	Full range self-shielding factors	Corresponding photon data
er-166	68166		yes	er
er-167	68167		yes	er
lu-175	71175		yes	lu
lu-176	71176		yes	lu
hf	72000			hf
hf-174	72174		yes	hf
hf-176	72176		yes	hf
hf-177	72177		yes	hf
hf-178	72178		yes	hf
hf-179	72179		yes	hf
hf-180	72180		yes	hf
ta-181	73181	yes	yes	ta
ta-182	73182		yes	ta
w	74000	yes		w
w-182	74182	yes	yes	w
w-183	74183	yes	yes	w
w-184	74184	yes	yes	w
w-186	74186	yes	yes	w
re-185	75185		yes	re
re-187	75187		yes	re
ir-191	77191	yes	yes	ir
ir-193	77193	yes	yes	ir
au-197	79197	yes	yes	au
pb-206	82206	yes	yes	pb
pb-207	82207	yes	yes	pb
pb-208	82208	yes	yes	pb
bi-209	83209	yes	yes	bi
th-230	90230		yes	th
th-232	90232	yes	yes	th
pa-231	91231		yes	pa
pa-232	91232		yes	pa
pa-233	91233		yes	pa
u-232	92232		yes	u
u-233	92233	yes	yes	u
u-234	92234		yes	u
u-235	92235	yes	yes	u
u-236	92236		yes	u
u-237	92237	yes	yes	u
u-238	92238	yes	yes	u
np-236	93236		yes	np
np-237	93237	yes	yes	np
np-238	93238		yes	np
np-239	93239		yes	np
pu-236	94236		yes	pu
pu-237	94237		yes	pu
pu-238	94238		yes	pu
pu-239	94239	yes	yes	pu
pu-240	94240	yes	yes	pu
pu-241	94241	yes	yes	pu
pu-242	94242	yes	yes	pu
pu-243	94243	yes	yes	pu

Table B.1 Evaluations and IDs used for the ENDF/B-VI.8 library (continued)

Nuclide	ID	Photon yield data	Full range self-shielding factors	Corresponding photon data
pu-244	94244		yes	pu
am-241	95241	yes	yes	am
am-242	95242		yes	am
am-242	95601	yes	yes	am
am-243	95243	yes	yes	am
cm-241	96241		yes	cm
cm-242	96242	yes	yes	cm
cm-243	96243		yes	cm
cm-244	96244	yes	yes	cm
cm-245	96245		yes	cm
cm-246	96246		yes	cm
cm-247	96247	yes	yes	cm
cm-248	96248	yes	yes	cm
bk-249	97249		yes	bk
cf-249	98249		yes	cf
cf-250	98250	yes	yes	cf
cf-251	98251	yes	yes	cf
cf-252	98252	yes	yes	cf
cf-253	98253		yes	cf
es-253	99253		yes	es
h_h2o	1001		yes	h
para_h	1501		yes	h
ortho_h	1401		yes	h
h_zrh	1701		yes	h
d_d2o	1002		yes	h
para_d	1502		yes	h
ortho_d	1402		yes	h
be_metal	4309	yes	yes	be
beo	4509	yes	yes	be
graphite	6312	yes	yes	c
l_ch4	1101		yes	h
s_ch4	1201		yes	h
h_ch2	1901		yes	h
benzine	1601		yes	h
zr_zrh	40701			zr

APPENDIX C

EVALUATIONS INCLUDED IN ENDF/B-VII.0 LIBRARY

Evaluations included in the multigroup library for ENDF/B-VII.0 are listed in Table C.1.

Table C.1 Evaluations included in ENDF/B-VII.0 library

Nuclide	ID	Photon yield data	Full range self-shielding factors	Corresponding photon data
h-1	1801		yes	h
h-2	1802	yes	yes	h
h-3	1003		yes	h
he-3	2003		yes	he
he-4	2004		yes	he
li-6	3006	yes	yes	li
li-7	3007	yes	yes	li
be-7	4007		yes	be
be-9	4009	yes	yes	be
b-10	5010	yes	yes	b
b-11	5011	yes	yes	b
c 6	000	yes	yes	c
n-14	7014	yes	yes	n
n-15	7015	yes	yes	n
o-16	8016	yes	yes	o
o-17	8017		yes	o
f-19	9019	yes	yes	f
na-22	11022		yes	na
na-23	11023	yes	yes	na
mg-24	12024	yes	yes	mg
mg-25	12025	yes	yes	mg
mg-26	12026	yes	yes	mg
al-27	13027	yes	yes	al
si-28	14028	yes	yes	si
si-29	14029	yes	yes	si
si-30	14030	yes	yes	si
p-31	15031	yes	yes	p
s-32	16032	yes	yes	s
s-33	16033	yes	yes	s
s-34	16034	yes	yes	s
s-36	16036	yes	yes	s
cl-35	17035	yes	yes	cl
cl-37	17037	yes	yes	cl
ar-36	18036		yes	ar
ar-38	18038		yes	ar
ar-40	18040		yes	ar
k-39	19039	yes	yes	k
k-40	19040	yes	yes	k
k-41	19041	yes	yes	k
ca-40	20040	yes	yes	ca
ca-42	20042	yes	yes	ca
ca-43	20043	yes	yes	ca

Table C.1 Evaluations included in ENDF/B-VII.0 library (continued)

Nuclide	ID	Photon yield data	Full range self-shielding factors	Corresponding photon data
ca-44	20044	yes	yes	ca
ca-46	20046	yes	yes	ca
ca-48	20048	yes	yes	ca
sc-45	21045	yes	yes	sc
ti-46	22046	yes	yes	ti
ti-47	22047	yes	yes	ti
ti-48	22048	yes	yes	ti
ti-49	22049	yes	yes	ti
ti-50	22050	yes	yes	ti
v 2	3000	yes	no	v
cr-50	24050	yes	yes	cr
cr-52	24052	yes	yes	cr
cr-53	24053	yes	yes	cr
cr-54	24054	yes	yes	cr
mn-55	25055	yes	yes	mn
fe-54	26054	yes	yes	fe
fe-56	26056	yes	yes	fe
fe-57	26057	yes	yes	fe
fe-58	26058	yes	yes	fe
co-58	27058		yes	co
co-58	27601		yes	co
co-59	27059	yes	yes	co
ni-58	28058	yes	yes	ni
ni-59	28059	yes	yes	ni
ni-60	28060	yes	yes	ni
ni-61	28061	yes	yes	ni
ni-62	28062	yes	yes	ni
ni-64	28064	yes	yes	ni
cu-63	29063	yes	yes	cu
cu-65	29065	yes	yes	cu
zn 3	0000		no	zn
ga-69	31069		yes	ga
ga-71	31071		yes	ga
ge-70	32070	yes	yes	ge
ge-72	32072	yes	yes	ge
ge-73	32073	yes	yes	ge
ge-74	32074	yes	yes	ge
ge-76	32076	yes	yes	ge
as-74	33074	yes	yes	as
as-75	33075	yes	yes	as
se-74	34074		yes	se
se-76	34076		yes	se
se-77	34077		yes	se
se-78	34078		yes	se
se-79	34079		yes	se
se-80	34080		yes	se
se-82	34082		yes	se
br-79	35079		yes	br
br-81	35081		yes	br
kr-78	36078		yes	kr

Table C.1 Evaluations included in ENDF/B-VII.0 library (continued)

Nuclide	ID	Photon yield data	Full range self-shielding factors	Corresponding photon data
kr-80	36080		yes	kr
kr-82	36082		yes	kr
kr-83	36083		yes	kr
kr-84	36084		yes	kr
kr-85	36085	yes	yes	kr
kr-86	36086		yes	kr
rb-85	37085		yes	rb
rb-86	37086	yes	yes	rb
rb-87	37087		yes	rb
sr-84	38084	yes	yes	sr
sr-86	38086		yes	sr
sr-87	38087		yes	sr
sr-88	38088		yes	sr
sr-89	38089		yes	sr
sr-90	38090		yes	sr
y-89	39089	yes	yes	y
y-90	39090	yes	yes	y
y-91	39091		yes	y
zr-90	40090	yes	yes	zr
zr-91	40091	yes	yes	zr
zr-92	40092	yes	yes	zr
zr-93	40093		yes	zr
zr-94	40094	yes	yes	zr
zr-95	40095		yes	zr
zr-96	40096	yes	yes	zr
nb-93	41093	yes	yes	nb
nb-94	41094		yes	nb
nb-95	41095		yes	nb
mo-92	42092	yes	yes	mo
mo-94	42094	yes	yes	mo
mo-95	42095	yes	yes	mo
mo-96	42096	yes	yes	mo
mo-97	42097	yes	yes	mo
mo-98	42098	yes	yes	mo
mo-99	42099		yes	mo
mo-100	42100		yes	mo
tc-99	43099	yes	yes	tc
ru-96	44096		yes	ru
ru-98	44098		yes	ru
ru-99	44099		yes	ru
ru-100	44100		yes	ru
ru-101	44101	yes	yes	ru
ru-102	44102		yes	ru
ru-103	44103		yes	ru
ru-104	44104		yes	ru
ru-105	44105		yes	ru
ru-106	44106		yes	ru
rh-103	45103	yes	yes	rh
rh-105	45105		yes	rh
pd-102	46102	yes	yes	pd
pd-104	46104	yes	yes	pd

Table C.1 Evaluations included in ENDF/B-VII.0 library (continued)

Nuclide	ID	Photon yield data	Full range self-shielding factors	Corresponding photon data
pd-105	46105	yes	yes	pd
pd-106	46106	yes	yes	pd
pd-107	46107		yes	pd
pd-108	46108	yes	yes	pd
pd-110	46110	yes	yes	pd
ag-107	47107	yes	yes	ag
ag-109	47109	yes	yes	ag
ag-110	47601		yes	ag
ag-111	47111	yes	yes	ag
cd-106	48106	yes	yes	cd
cd-108	48108		yes	cd
cd-110	48110		yes	cd
cd-111	48111	yes	yes	cd
cd-112	48112		yes	cd
cd-113	48113		yes	cd
cd-114	48114		yes	cd
cd-115	48601	yes	yes	cd
cd-116	48116		yes	cd
in-113	49113		yes	in
in-115	49115		yes	in
sn-112	50112		yes	sn
sn-113	50113	yes	yes	sn
sn-114	50114		yes	sn
sn-115	50115		yes	sn
sn-116	50116		yes	sn
sn-117	50117		yes	sn
sn-118	50118		yes	sn
sn-119	50119		yes	sn
sn-120	50120		yes	sn
sn-122	50122		yes	sn
sn-123	50123		yes	sn
sn-124	50124		yes	sn
sn-125	50125	yes	yes	sn
sn-126	50126		yes	sn
sb-121	51121		yes	sb
sb-123	51123		yes	sb
sb-124	51124		yes	sb
sb-125	51125		yes	sb
sb-126	51126	yes	yes	sb
te-120	52120		yes	te
te-122	52122		yes	te
te-123	52123		yes	te
te-124	52124		yes	te
te-125	52125		yes	te
te-126	52126		yes	te
te-127	52601		yes	te
te-128	52128		yes	te
te-129	52611		yes	te
te-130	52130		yes	te
te-132	52132	yes	yes	te
i-127	53127	yes	yes	i

Table C.1 Evaluations included in ENDF/B-VII.0 library (continued)

Nuclide	ID	Photon yield data	Full range self-shielding factors	Corresponding photon data
i-129	53129		yes	i
i-130	53130	yes	yes	i
i-131	53131		yes	i
i-135	53135		yes	i
xe-123	54123		yes	xe
xe-124	54124		yes	xe
xe-126	54126		yes	xe
xe-128	54128		yes	xe
xe-129	54129		yes	xe
xe-130	54130		yes	xe
xe-131	54131	yes	yes	xe
xe-132	54132		yes	xe
xe-133	54133		yes	xe
xe-134	54134		yes	xe
xe-135	54135		yes	xe
xe-136	54136		yes	xe
cs-133	55133	yes	yes	cs
cs-134	55134		yes	cs
cs-135	55135		yes	cs
cs-136	55136		yes	cs
cs-137	55137		yes	cs
ba-130	56130		yes	ba
ba-132	56132		yes	ba
ba-133	56133	yes	yes	ba
ba-134	56134		yes	ba
ba-135	56135		yes	ba
ba-136	56136		yes	ba
ba-137	56137		yes	ba
ba-138	56138		yes	ba
ba-140	56140		yes	ba
la-138	57138		yes	la
la-139	57139		yes	la
la-140	57140	yes	yes	la
ce-136	58136	yes	yes	ce
ce-138	58138	yes	yes	ce
ce-139	58139	yes	yes	ce
ce-140	58140		yes	ce
ce-141	58141		yes	ce
ce-142	58142		yes	ce
ce-143	58143	yes	yes	ce
ce-144	58144		yes	ce
pr-141	59141	yes	yes	pr
pr-142	59142	yes	yes	pr
pr-143	59143		yes	pr
nd-142	60142	yes	yes	nd
nd-143	60143	yes	yes	nd
nd-144	60144	yes	yes	nd
nd-145	60145	yes	yes	nd
nd-146	60146	yes	yes	nd
nd-147	60147	yes	yes	nd
nd-148	60148	yes	yes	nd

Table C.1 Evaluations included in ENDF/B-VII.0 library (continued)

Nuclide	ID	Photon yield data	Full range self-shielding factors	Corresponding photon data
nd-150	60150	yes	yes	nd
pm-147	61147		yes	pm
pm-148	61148		yes	pm
pm-148	61601		yes	pm
pm-149	61149		yes	pm
pm-151	61151	yes	yes	pm
sm-144	62144	yes	yes	sm
sm-147	62147	yes	yes	sm
sm-148	62148	yes	yes	sm
sm-149	62149	yes	yes	sm
sm-150	62150	yes	yes	sm
sm-151	62151	yes	yes	sm
sm-152	62152	yes	yes	sm
sm-153	62153	yes	yes	sm
sm-154	62154	yes	yes	sm
eu-151	63151		yes	eu
eu-152	63152		yes	eu
eu-153	63153	yes	yes	eu
eu-154	63154		yes	eu
eu-155	63155		yes	eu
eu-156	63156		yes	eu
eu-157	63157	yes	yes	eu
gd-152	64152	yes	yes	gd
gd-153	64153	yes	yes	gd
gd-154	64154	yes	yes	gd
gd-155	64155	yes	yes	gd
gd-156	64156	yes	yes	gd
gd-157	64157	yes	yes	gd
gd-158	64158	yes	yes	gd
gd-160	64160	yes	yes	gd
tb-159	65159		yes	tb
tb-160	65160	yes	yes	tb
dy-156	66156	yes	yes	dy
dy-158	66158	yes	yes	dy
dy-160	66160	yes	yes	dy
dy-161	66161	yes	yes	dy
dy-162	66162	yes	yes	dy
dy-163	66163	yes	yes	dy
dy-164	66164	yes	yes	dy
ho-165	67165	yes	yes	ho
ho-166	67601	yes	yes	ho
er-162	68162	yes	yes	er
er-164	68164	yes	yes	er
er-166	68166	yes	yes	er
er-167	68167	yes	yes	er
er-168	68168	yes	yes	er
er-170	68170	yes	yes	er
lu-175	71175		yes	lu
lu-176	71176		yes	lu
hf-174	72174		yes	hf
hf-176	72176		yes	hf

Table C.1 Evaluations included in ENDF/B-VII.0 library (continued)

Nuclide	ID	Photon yield data	Full range self-shielding factors	Corresponding photon data
hf-177	72177		yes	hf
hf-178	72178		yes	hf
hf-179	72179		yes	hf
hf-180	72180		yes	hf
ta-181	73181	yes	yes	ta
ta-182	73182		yes	ta
w-182	74182	yes	yes	w
w-183	74183	yes	yes	w
w-184	74184	yes	yes	w
w-186	74186	yes	yes	w
re-185	75185		yes	re
re-187	75187		yes	re
ir-191	77191	yes	yes	ir
ir-193	77193	yes	yes	ir
au-197	79197	yes	yes	au
hg-196	80196	yes	yes	hg
hg-198	80198	yes	yes	hg
hg-199	80199	yes	yes	hg
hg-200	80200	yes	yes	hg
hg-201	80201	yes	yes	hg
hg-202	80202	yes	yes	hg
hg-204	80204	yes	yes	hg
pb-204	82204	yes	yes	pb
pb-206	82206	yes	yes	pb
pb-207	82207	yes	yes	pb
pb-208	82208	yes	yes	pb
bi-209	83209	yes	yes	bi
ra-223	88223		yes	ra
ra-224	88224		yes	ra
ra-225	88225		yes	ra
ra-226	88226		yes	ra
ac-225	89225		yes	ac
ac-226	89226		yes	ac
ac-227	89227		yes	ac
th-227	90227		yes	th
th-228	90228		yes	th
th-229	90229		yes	th
th-230	90230		yes	th
th-232	90232	yes	yes	th
th-233	90233		yes	th
th-234	90234		yes	th
pa-231	91231	yes	yes	pa
pa-232	91232		yes	pa
pa-233	91233	yes	yes	pa
u-232	92232	yes	yes	u
u-233	92233	yes	yes	u
u-234	92234	yes	yes	u
u-235	92235	yes	yes	u
u-236	92236	yes	yes	u
u-237	92237	yes	yes	u
u-238	92238	yes	yes	u

Table C.1 Evaluations included in ENDF/B-VII.0 library (continued)

Nuclide	ID	Photon yield data	Full range self-shielding factors	Corresponding photon data
u-239	92239	yes	yes	u
u-240	92240	yes	yes	u
u-241	92241	yes	yes	u
np-235	93235		yes	np
np-236	93236		yes	np
np-237	93237	yes	yes	np
np-238	93238		yes	np
np-239	93239		yes	np
pu-236	94236		yes	pu
pu-237	94237		yes	pu
pu-238	94238		yes	pu
pu-239	94239	yes	yes	pu
pu-240	94240	yes	yes	pu
pu-241	94241	yes	yes	pu
pu-242	94242	yes	yes	pu
pu-243	94243	yes	yes	pu
pu-244	94244		yes	pu
pu-246	94246		yes	pu
am-241	95241	yes	yes	am
am-242	95242		yes	am
am-242	95601		yes	am
am-243	95243	yes	yes	am
am-244	95244		yes	am
am-244	95611		yes	am
cm-241	96241		yes	cm
cm-242	96242	yes	yes	cm
cm-243	96243		yes	cm
cm-244	96244		yes	cm
cm-245	96245		yes	cm
cm-246	96246		yes	cm
cm-247	96247		yes	cm
cm-248	96248	yes	yes	cm
cm-249	96249		yes	cm
cm-250	96250		yes	cm
bk-249	97249		yes	bk
bk-250	97250		yes	bk
cf-249	98249		yes	cf
cf-250	98250	yes	yes	cf
cf-251	98251	yes	yes	cf
cf-252	98252	yes	yes	cf
cf-253	98253		yes	cf
cf-254	98254		yes	cf
es-253	99253		yes	es
es-254	99254		yes	es
es-255	99255		yes	es
fm-255	100255		yes	fm
al27	13701	yes	yes	al
fe56	26701	yes	yes	fe
be_metal	4309	yes	yes	be
be_beo	4509	yes	yes	be
d_d2o	1002		yes	h

Table C.1 Evaluations included in ENDF/B-VII.0 library (continued)

Nuclide	ID	Photon yield data	Full range self-shielding factors	Corresponding photon data
h_ch2	1901		yes	h
h_h2o	1001		yes	h
h_zrh	1701		yes	h
o_beo	8516	yes	yes	o
zr_zrh	40701	yes	yes	zr
benzine	1601		yes	h
graphite	6312	yes	yes	c
l_ch4	1101		yes	h
ortho_d	1402		yes	h
ortho_h	1401		yes	h
para_d	1502		yes	h
para_h	1501		yes	h
s_ch4	1201		yes	h



NUREG/
ORNL/TM-2008/047